Synthesis and Characterization of Hydrophobic-Hydrophilic Multiblock Copolymers for Proton Exchange Membrane and Segmented Copolymer Precursors for Reverse Osmosis Applications

Ishan Mehta

Thesis submitted to the faculty of the Virginia Polytechnic Institute and State University in partial fulfillment of the requirements for the degree of

Master of Science

in

Macromolecular Science and Engineering

S. Richard Turner, Chair

James E. McGrath

Judy Riffle

Sue Mecham

15th May, 2014

Blacksburg, VA

Keywords: Proton exchange membranes, hydrophobic-hydrophilic multiblock copolymers, reverse osmosis

Synthesis and Characterization of Hydrophobic-Hydrophilic Multiblock Copolymers for Proton Exchange Membrane and Segmented Copolymer Precursors for Reverse Osmosis Applications

Ishan Mehta

ABSTRACT

High performance engineering materials, poly(arylene ether)s, having very good mechanical properties, excellent oxidative and hydrolytic stability are promising candidates for alternative materials used in the field of Proton Exchange Membrane Fuel Cells (PEMFCs) and Reverse Osmosis (RO) applications. In particular, wholly aromatic sulfonated poly(arylene ether sulfone)s are of considerable interest in the field of PEMFCs & RO, due to their affordability, high T_g, and the ease of sulfonation.

Proton exchange membrane fuels cells (PEMFCs) are one of the primary alternate source of energy. A Proton exchange membrane (PEM) is one of the key component in a PEMFC and it needs to have good proton conductivity under partially humidified conditions. One of the strategies to increase proton conductivity under partially RH conditions is to synthesize hydrophobic-hydrophilic multiblock copolymers with high Ion exchange capacity (IEC) values to ensure sufficient ion channel size.

In this thesis two multiblock systems were synthesized incorporating trisulfonated hydrophilic oligomers and were characterized in the first two chapters of the thesis. The first multiblock system incorporated a non-fluorinated biphenol-based hydrophobic block. The second study was focused on synthesizing a fluorinated benzonitrile-based hydrophobic block. A fluorinated monomer was incorporated with the aim to improve phase separation which might lead to increased performance under partially humidified conditions.

The third study featured synthesis and characterization of a novel hydroquinone-based random copolymer system precursor, which after post-sulfonation, shall form mono-sulfonated polysulfone materials with potential applications in reverse osmosis. The ratio of the amount of hydroquinone incorporated in the copolymer were varied during the synthesis of the precursor to facilitate control over the post-sulfonation process. The simple and low cost process of post-sulfonating the random copolymer enables the precursor to be a promising material to be used in the reverse osmosis application.

DEDICATION

Dedicated to my family: Mr. Nilesh Mehta, Mrs. Nita Mehta and Isha.

The strongest pillars in my life. Thank you for your unconditional love, sacrifice and support with my studies. Thank you for being the best teachers who taught me to prove and improve through all my walks of life. I love you.

ACKNOWLEDGEMENT

I would like to thank the almighty god for giving me courage and determination to overcome all the difficulties in my life, and guidance for conducting my research study. For his support, words of encouragement and tutelage, I would like to thank Dr. James E. McGrath. He has constantly been my pillar of strength and been not only an advisor, but a teacher, a mentor, a parent and a guide. My committee members, Dr. S. Richard Turner, Dr. Judy Riffle and Dr. Sue Mecham have always taken out time to help me with this work. This research would not have been possible without the support and help of a few key people:

- Dr. Kwan-Soo Lee: For the extensive research done on ESQS100-BPS multiblock copolymers.
- Andrew Shaver and Ozma Lane: For preparing and characterizing the material samples.

This acknowledgement would also be incomplete without the mention of my sister for being my friend and confidante through the entire process.

Last but not the least, I would like to acknowledge all my friends, who is my family from away from. I would especially like to thank Riddhika Jain, Gaurav Soni, Sreyoshi Bhaduri, Tamoghna Roy, Abhishek Mukkopadhyay, Deba Pratim Saha and Prithwish Chakraborty who were always with me and motivated me.

Contents

List of Figures

List of Tables

Chapter 1 : Literature Review

1.1. Introduction

1.1.1. Fundamentals of proton exchange membranes (PEMs)

In recent times, with the increase in the consumption of fossil fuels and the resulting pollution, as well as decreasing reserves, it is imperative to develop clean and efficient alternate energy systems. Fuel cell technology is a viable alternative to the current fossil fuel based technology as it more energy efficient and does not produce carbon dioxide. Fuel cells produce electricity in a single step through an electrochemical process which leads to fewer losses and higher efficiency. Moreover, the byproduct water of the reaction is environmentally benign. Fuel cells are simpler than combustion engines as they lack moving parts. However, the current cost of fuel cells is too high and the long term durability needs improvement. Current research goals include the development of inexpensive electrolyte materials, and approaches to overcome the drawbacks of currently used materials. [1]

A fuel cell is a device which uses an electrochemical reaction to convert the chemical energy from a fuel directly into electricity.[2, 3] The electricity generated can be used to power electrical devices. The basic idea of the fuel cells was proposed, in the year 1838 by a German scientist named Christian Friedrich Schonbein and published in The London and Edinburgh Philosophical Magazine and Journal of Science.[4] In 1839, the first fuel cell was created by William Grove using Schonbein's proposal that generated electricity from the combination of hydrogen and oxygen gases. Grove termed his creation a "gaseous voltaic battery" and it had a very simple design, consisting of iron and copper electrodes, a porcelain diaphragm, an acidic copper sulfate solution as the electrolyte, and oxygen and hydrogen gases as the reactants.[4-6] Over

the years, many improvements and modifications were made in the fuel cell technology by the contributions of Ludwig Mond and Carl Langer (1889), who coined the term "fuel cell" for the first time; Walther Nernst (1889), who used a solid electrolyte for the first time in a fuel cell; and Francis T. Bacon (1932), who conceived the modern day fuel cell, which was practically feasible.[7] Francis T. Bacon created the alkaline fuel cell, which lead to the development of the modern day fuel cell. In 1959, Bacon developed a fuel cell, which consisted of forty module stacks and produced 6 kW of power, which was enough to power most construction equipment, including a forklift.

Until 1965, there were no applications where a fuel cell would be a commercially competitive power generation system. With the beginning of the space age, the first fuel cells were used on the spacecraft's for the Apollo and Gemini missions, both to provide power and supply clean drinking water for the astronomers. These fuel cells were proton exchange membrane fuel cells (PEMFCs), but based on Bacon's design of stacking modules to generate power and utilized a sulfonated polystyrene as a PEM.[4, 7]

1.1.2 Principles and Types of Fuel Cells

All fuel cells can be described in terms of their basic components: the anode, the electrolyte, and the cathode. Chemical reactions occur at the interfaces of the three different sections resulting in a net reaction where the fuel and oxidant are consumed to release energy and byproducts. A basic fuel cell design is shown in Figure 1.1.[8]

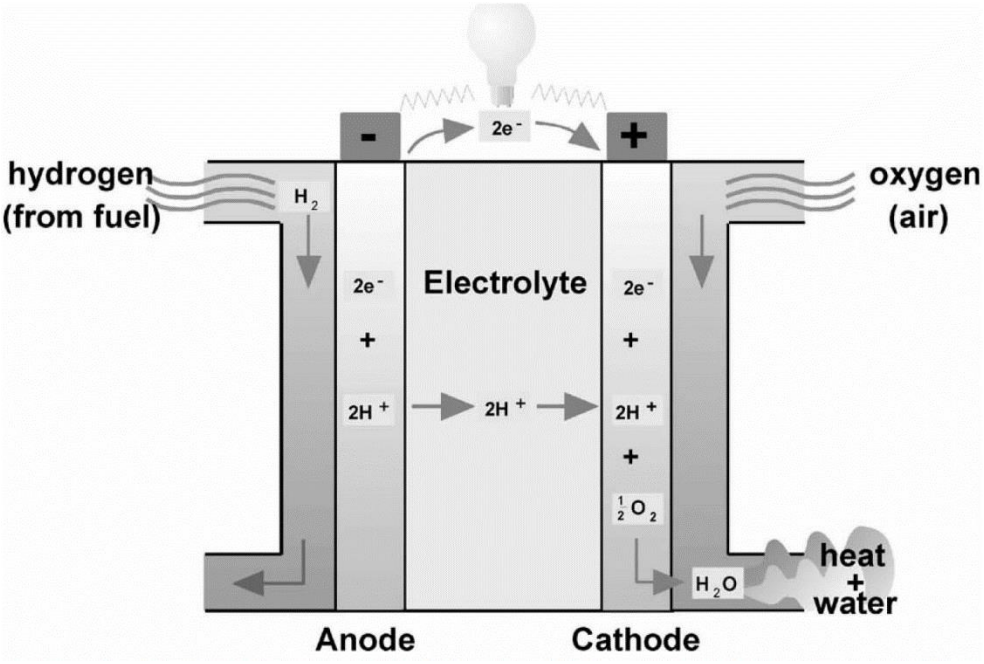

Figure 1.1: Schematic of a PEMFC. [8]

Similar to the first fuel cell design, a fuel cell consists of two electrodes- the anode and the cathode, an electrolyte. In a proton exchange membrane fuel cell (PEMFC), hydrogen is the fuel, oxygen is the oxidant, and water and some waste heat are produced. In a subcategory of PEMFCs termed direct methanol fuel cells (DMFCs), dilute methanol is used as the fuel. The basic electrochemical reactions are given in Figure 1.2 below:

PEMFC

Anode: $2H_2 \longrightarrow 4H^+ + 4e^-$

Cathode: $4H^+ + O_2 + 4e^- \longrightarrow 2H_2O$

Overall: $2H_2 + O_2 \longrightarrow 2H_2O$

DMFC

Anode: $CH_3OH + H_2O \longrightarrow CO_2 + 6H^+ + 6e^-$

Cathode: $3/2\ O_2 + 6H^+ + 6e^- \longrightarrow 3H_2O$

Overall: $CH_3OH + H_2O + 3/2\ O_2 \longrightarrow CO_2 + 3H_2O$

Figure 1.2: Electrochemical reactions for a PEMFC and DMFC. [2]

At the anode, hydrogen dissociates with the assistance of a platinum catalyst into a proton and an electron. The electrolyte is a substance specifically designed to have good proton conductivity but poor electron conductivity. The electrons travel through a wire creating the electric current. The protons travel through the electrolyte to the cathode. At the cathode, the protons are reunited with the electrons and the two react with oxygen to create water and in the case of a methanol-based fuel cell, carbon dioxide. Thus fuel cells can continue producing electricity as long as they are supplied with fuel. In a fuel cell, hydrogen is the most common fuel, but hydrocarbons such as natural gas and alcohols such as methanol are sometimes used. [2, 9]

Fuel cells, like primary batteries, generate power from electrochemical reactions. However, they can be used continuously as long as they have a supply of fuel. Hence we can say that fuel cells incorporate many advantages of both engines and batteries. Fuel cells also allow a simple scale-up between different levels of power generation, determined by the size and number of the

fuel cell stacks, and capacity, which is dependent on the fuel reservoir size.[10] Thus fuel cells can be used for a wide variety of applications, including stationary power sources, powering personal vehicles, or even as a portable energy source for charging electronics. The efficiency of a fuel cell from electrochemical reactions alone is over 40%, but may increase further if the waste heat generated is also recovered and used.[11]

Fuel cells are classified into five groups based on the electrolyte material. These groups are: alkaline fuel cell (AFC), polymer electrolyte membrane fuel cell (PEMFC), phosphoric acid fuel cell (PAFC), molten carbonate fuel cell (MCFC) and solid oxide fuel cell (SOFC). The operating temperature, materials and description the different types of fuel are presented in Table 1.1.[11]

Table 1.1: A comparison of different types of fuel cells.

	PEMFC	**AFC**	**PAFC**	**MCFC**	**SOFC**
Operating Temperature (^oC)	40-80	65-220	150-210	600-700	600-1000
Charge Carrier	H^+	OH^-	H^+	CO_3^{2-}	O^{2-}
Cathode Reaction	$1/2\ O_2 + 2H^+ + 2e^- \rightarrow H_2O$	$O_2 + 2H_2O + 4e^- \rightarrow 4OH^-$	$O_2 + 4H^+ + 4e^- \rightarrow 2H_2O$	$1/2\ O_2 + CO_2 + 2e^- \rightarrow CO_3^{2-}$	$1/2\ O_2 + 2e^- \rightarrow O^{2-}$

Anode Reaction	$H_2 \rightarrow 2H^+ + 2e^-$	$2H_2 + 4OH^- \rightarrow 4H_2O + 4e^-$	$2H_2 \rightarrow 4H^+ + 4e^-$	$H_2O + CO_3^{2-} \rightarrow H_2O + CO_3^{2-} + 2e^-$	$H_2 + O^{2-} \rightarrow H_2O + 2e^-$
Electrolyte	Hydrated polymeric ion exchange membrane	Potassium hydroxide in asbestos matrix	Liquid phosphoric acid in silicon carbide	Liquid molten carbonate in $LiAlO_2$	Ion conducting ceramics
Fuel	Hydrogen or methanol	Hydrogen or hydrazine	Hydrogen or alcohol	Hydrogen, hydrocarbons	Hydrogen, hydrocarbons
Oxidant	O_2/ air	O_2/ air	O_2/ air	CO_2/ O_2/ air	O_2/ air
Advantages	• Solid electrolyte reduces corrosion and electrolyte management problems • Low operating temperature • Quick start-up	• Faster cathode reaction • Wide range of electro-catalysts	• Tolerance to impurities in hydrogen	• Fuel flexibility • Low-cost catalyst	• All solid-state components • Fuel flexibility • Low-cost catalysts • No electrolyte flooding • Highest efficiency
Disadvantages	• Poisoning by trace contaminants in fuel • High-cost platinum catalyst • Difficulties in thermal and water management	• High purity hydrogen	• Show cathode reaction • Corrosive nature of phosphoric acid • High-cost platinum catalyst	• Corrosive electrolyte • High operating temperature • Long-term reliability of materials due to high temperature	• High operating temperature • High manufacturing cost • Long-term reliability of materials due to high temperature

From Table 1.1, we can see that the difference between types of fuel cell depends upon the electrolyte material. The operating temperatures of the different types of fuel cell vary and this leads to change in the type of fuel that can be used. As seen from the above table, every fuel cell type has certain advantages and disadvantages and is suited for specific type of applications. In the case of PEMFCs, the operating temperature is low, making PEMFCs suitable for powering personal vehicles, but creating the disadvantage of catalyst susceptibility to contamination by carbon monoxide impurities in the hydrogen fuel. The catalyst becomes more resistant to CO poisoning at higher temperatures, and so other fuel cell applications may tolerate greater levels of contamination. High temperature conditions leads to increase in output efficiency as seen in case of SOFC and MCFC and also increases the catalyst tolerance to impurities. But high operating temperatures also lead to limited applications as heat stress makes the system more susceptible to material failures.[8]

1.1.3 Basic criteria for a PEM

Hickner[9] describes an ideal PEM as having the following characteristics: proton conductivity, ion exchange capacity, hydrolytic and oxidative stability, and ease of fabrication into a membrane electrode assembly (MEA). Proton conductivity is one of the most important criteria for a PEM. Proton conductivity is related to the concentration of ion-conducting groups in the membrane material. This is related to the ion exchange capacity (IEC) of the polymer which is equivalent to ion-conducting groups in the polymer. The proton conductivity of the PEMs is determined by using electrochemical impedance spectroscopy which was developed at the Los Alamos National Laboratory (LANL). [12] The proton conductivity is measured in-plane rather than

normal to the plane, as it is very difficult to measure the latter due to high interfacial resistance.[13] Water uptake is the next criteria, which is dependent upon the ion-conducting group concentrations and is generally given in mass percentage. Water in a PEM is required as a medium for protons to transport through the membrane.[14] Hence, PEMs need to have a minimum amount of water uptake to get the proton transport efficiently. Proton conductivity also generally increases with water uptake. But a high increase in water uptake leads to swelling in the membrane, which reduces mechanical strength. Thus, there is a limit to how much water uptake may be tolerated in a membrane. For PEMFCs, ideally water uptake should be in the range of 20-30%.

As discussed above, the mechanical strength of the polymer is also very important. A fuel cell undergoes swelling-deswelling cycles during operation and it is important for the polymer to be tough and flexible so that it can retain its integrity in both the swelled and dry state. For the polymer to be tough and flexible, it should be of high molecular weight and have a chemical structure which can impart flexibility. For example, sulfonated poly(1,4-phenylene) and its derivatives form extremely rigid films which are not flexible because of the rod-like chains and hence cannot form good PEMs. Alternate PEM membranes have ether, sulfone or ketone bonds which impart flexibility. [15]

The fuel cell membranes also need hydrolytic and oxidative stability to survive the harsh conditions. Aliphatic components in a polymer are more susceptible to degradation by oxygen and water and cannot be used in fuel cells with an oxidizing environment. Thus membranes based on sulfonated polystyrene which has aliphatic carbon in its backbone can only be used in low temperature fuel cells where conditions are not as demanding.[16] Fully aromatic polymers, like

poly(benzimidazole)s are oxidatively more stable, and hence used in high power and high temperature fuel cells.

Polymers used in PEM are bonded with the electrodes, either using the decal method or the gas diffusion layer (GDL) method to form the membrane electrode assembly (MEA).[17] Thus, the polymers used as PEM should have good compatibility with the electrodes so as to have good long-term performance. Generally, the electrode layer contains Nafion as a catalyst binder. Thus partially fluorinated copolymers are being investigated as candidates for fuel cell as they show good adherence to Nafion. In the McGrath group, the focus is on developing alternative materials for proton exchange membranes.

1.2 Current Proton Exchange Membrane and Research into New Materials

The current state of the art PEM are perfluorosulfonic acid membranes such as Nafion®, which was developed by DuPont in the late 1960's. Its structure, which can be seen in Figure 1.3,[18] has a tetrafluoroethylene (Teflon) based backbone, which imparts a small amount of crystallinity, and contains pendant side chains of perfluorinated vinyl ethers terminated by perfluorosulfonic acid group. The pendant perfluorosulfonic acid groups are highly acidic in nature, which provides high proton conductivity under fully hydrated conditions, while the semicrystalline tetrafluoroethylene backbone imparts excellent chemical and electrochemical stability, as well as also good mechanical properties to the membrane.

However, some of the disadvantages of Nafion®, and other perfluorosulfonated PEMs include a reduction in conductivity performance under partially hydrated conditions, high material cost, low upper operation temperature, and high fuel permeability in case of DMFCs. [2, 19] The upper operation temperature results from difficulty in maintaining membrane water content at temperatures above 100°C. Temperatures above the glass transition temperature (110°C) for protonated Nafion can cause polymer chain rearrangement, which can lead to structural changes in the membrane and lower the membrane stability, performance, and lifetime.

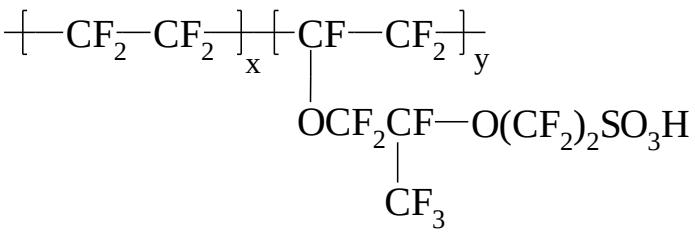

Figure 1.3: Chemical Structure of Nafion®

Therefore, the current research is focused on developing alternative proton exchange membranes which do not have the disadvantages of Nafion® and provide improved fuel cell performance with the cost kept low.[20, 21] The focus has generally been on developing alternate electrolyte systems such as poly(perfluorosulfonic acid) copolymers, sulfonated hydrocarbon polymers, phosphoric acid doped polybenzimidazole, polymer-inorganic composite membranes, hydrophobic-hydrophilic block copolymers having either aliphatic or aromatic backbone, and solid acid membranes. In the last few years, the McGrath group[22-24] has focused on developing hydrophilic-hydrophobic multiblock copolymers based on sulfonated poly(arylene ether sulfone)s for use as proton exchange membranes in PEMFCs.

1.3 Proton Exchange Membrane candidates and properties

1.3.1 Poly(perfluorosulfonic acid) Copolymers

As mentioned before, perfluorinated polymers like Nafion® are the most popular and the state of the art electrolytes for PEMFC and direct methanol fuel cell applications. Nafion was developed in the late 1960s by Walther Grot of DuPont and is commercially available today. In addition, because of the success of Nafion, other perfluorinated materials like Aquivision™ (developed by Dow Chemical but no longer produced), Neosepta-F (Tokuyama), Gore-Select (W. L. Gore and Associates, Inc.), Flemion® (Asahi glass company), and Asiplex® (Asahi Chemical Industry), have also been developed.

These membranes consist of a tetrafluoroethylene (TFE) backbone and a sulfonyl fluoride-containing vinyl ether with varying side chain lengths. In the case of Nafion, the comonomers are prepared by reacting a TFE-based monomer with sulfur trioxide and then with other monomers hexafluoropropyleneoxide (HFPO) to give the desired comonomer. This comonomer then undergoes a free radical polymerization reaction with TFE to give the sulfonyl-fluoride Nafion precursor. The synthetic scheme is shown in Figure 1.4.[10]

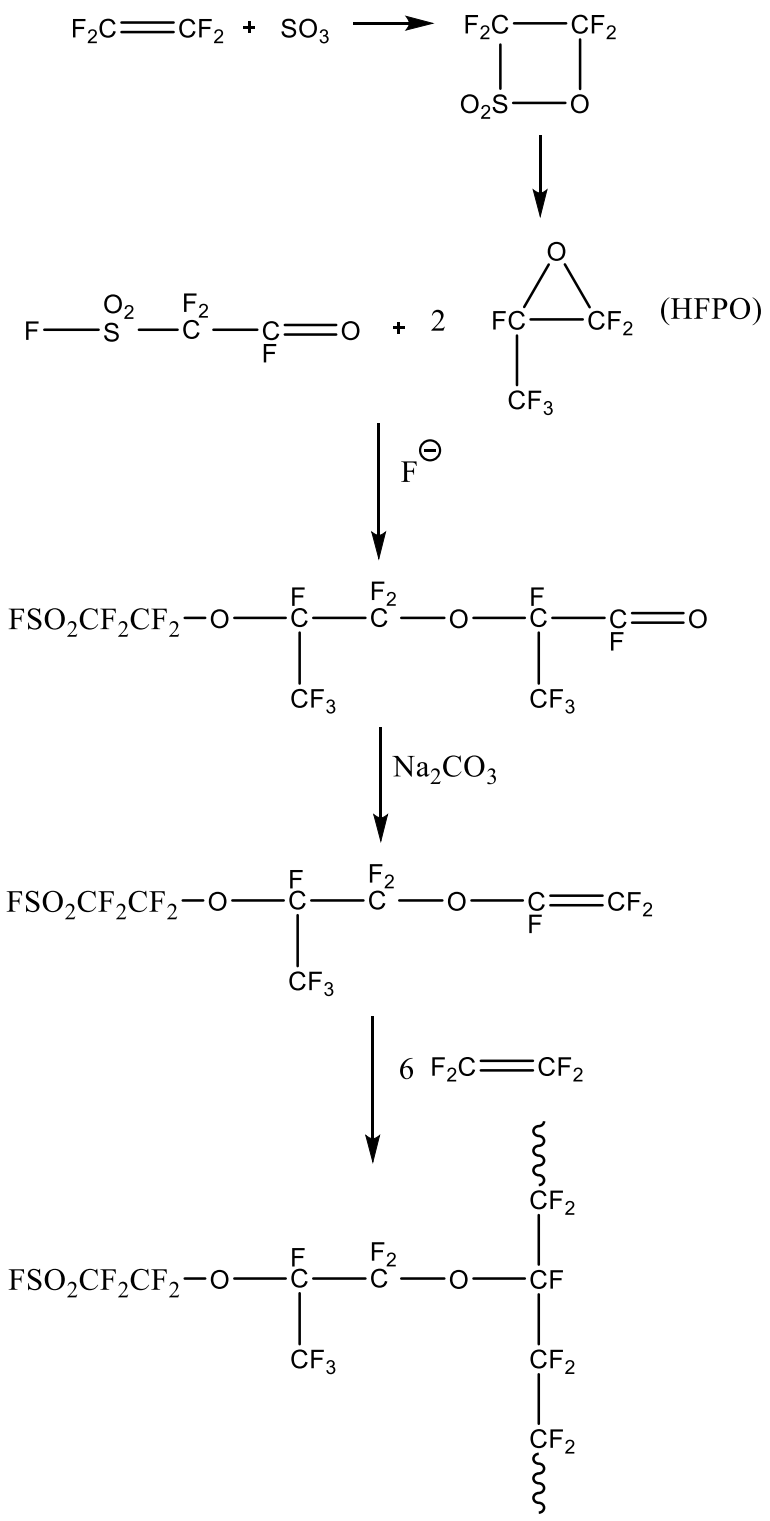

Figure 1.4: Synthetic schemes for the synthesis of Nafion

After this, the sulfonyl fluoride-containing polymer is extruded into sheets. The sulfonic acid groups in Nafion lead to strong intermolecular interactions which prevents melt processing, and hence the nonionic precursor is used for material fabrication. It is then treated with hot solutions of sodium or potassium hydroxide to convert the sulfonyl fluoride end group to sulfonic acid. This conversion gives the semi-crystalline Teflon-like structure, which imparts chemical resistivity and mechanical strength. But the extrusion of the sulfonyl fluoride-based precursors leads to microstructural orientation inside the polymer, which causes an increase in swelling and decrease of electrical conductivity of the ionomer form of Nafion. A new method was developed in the early 1980s, in which the ionomer was dispersed in water/alcohol mixtures at elevated temperature and pressure and then cast into films. These dispersions are commercially available and are used to uniformly cast thin membranes for fuel cell applications. The thickness of the membranes can be controlled with the concentration and volume of dispersion used.

The molecular weight of Nafion is very difficult to determine due to its poor solubility, and so in lieu of molecular weight measurements, it is common to use equivalent weight to describe sulfonic acid content. The equivalent weight (EW) of a Nafion membrane can easily be determined using an acid-base titration. The EW is use to determine the amount of sulfonic acid groups present in Nafion which is the value ‘m’. The relation between EW and m is given by the formula

$$EW = 100m + 446.$$

EW is also used to find the IEC of the polymer is given by the formula

$$IEC = 1000/EW.$$

The most common equivalent weight of Nafion found is around 1100g/mol. Nafion 112, 115, 117, and 212 all have equivalent weights of 1100 g/mol. [18, 25]

Even though Nafion is the state of the art membrane for PEMFCs, it still has some disadvantages such as limited operating temperature, reduced conductivity at low RH conditions and it is also very costly at more than $\$400/m^2$. Moreover, to reduce the risk of dehydration in the membrane, careful water management is required, which adds to the overall cost of manufacturing.[26]

1.3.2 Sulfonated Poly(arylene ether)s:

High performance engineering materials, having very good mechanical properties, excellent oxidative and hydrolytic stability, are promising candidates for alternative PEM materials. In particular, wholly aromatic high performance engineering thermoplastics are of considerable interest in the field of PEMFCs, particularly sulfonated poly(arylene ether)s, due to their affordability, high T_g, and the ease of sulfonation. Furthermore, their structures and properties can be easily modified by changing the functional linkages between the phenyl rings.[27] As shown in Figure 1.5, the change in the linking groups, which can be either an ether group, a ketone group, a sulfide group, or a sulfone group determines whether the polymer will be a poly(arylene ether), a poly(arylene ether ketone), a poly(arylene sulfide), or a poly(arylene sulfone).

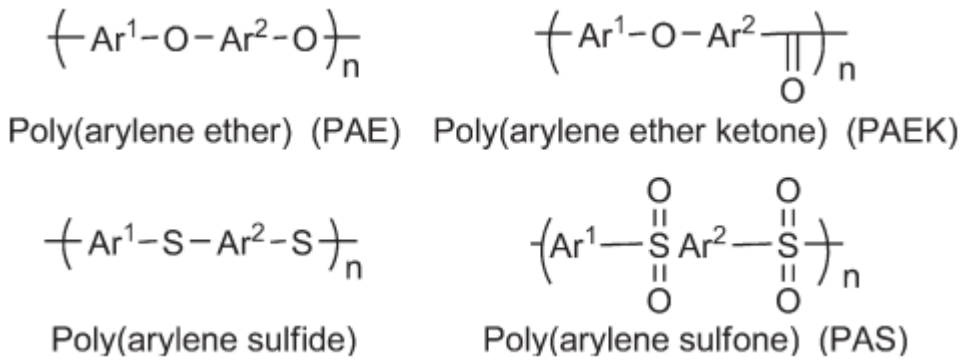

Figure 1.5: Typical repeat units of poly(arylene ether), poly(arylene ether ketone), poly(arylene sulfide), and poly(arylene sulfone). [27]

Although the first commercial wholly aromatic poly(arylene ether) was synthesized half a century ago by Hay et al using oxidative coupling polymerization,[28] the current method is nucleophilic aromatic substitution (S_NAr).[28, 29] Figure 1.6 shows the generalized mechanism for a S_NAr nucleophilic aromatic substitution. The S_NAr mechanism typically involves two steps: (1) nucleophilic attack, followed by (2) aromatic substitution between the activated aromatic ring and the phenol (or metal phenolates). In the first step, which is rate-determining, the carbon atom of the activated C-X bond is attacked by the nucleophile, which results in formation of resonance-stabilized Meisenheimer complex. The second step immediately follows, in which the leaving group 'X' departs.

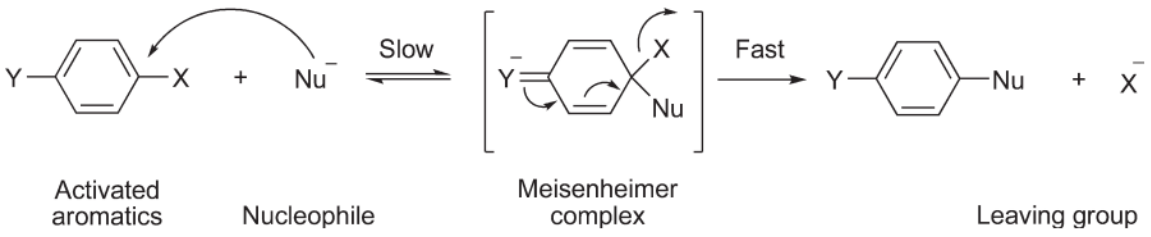

Figure 1.6: Mechanism of S_NAr nucleophilic aromatic substitution

Thus, the smaller the leaving group, the faster the reaction. Hence in case of halides, the order of reactivity was found to be F >> Cl > Br > I. The first step being the RDS, the electronegativity of the nucleophile is very important. As the electronegativity of the nucleophile increases, it leads to an increase in the rate of reaction.

Of the materials in the poly(arylene ether) family, poly(arylene ether sulfone)s (PAES) are interesting candidates for PEMs as they have a low permeability to methanol, as well as excellent thermal, hydrolytic and oxidative stability. Poly(arylene ether sulfone)s containing fluorine moieties are being widely investigated as a replacement for Nafion in PEMFCs.[30-33] PAES contains ether linkages which reduce the rotation barrier and rigidity in the polymer chain.[34, 35] The low barrier to rotation of the ether bond also leads to improved energy dispersion in the chain, which enhances both toughness and impact resistance. The C-O-C bond is also stabilized through resonance afforded by the sulfone group, which increases thermal and mechanical properties of the material illustrated in Figure 1.5.[29] However, the application of PAESs as alternative PEMs still depends upon compatibility with Nafion-containing electrode materials. One solution is the incorporation of fluorine moieties in the copolymer to increase compatibility at the electrode-electrolyte interface. Electrode-electrolyte compatibility is dependent on the development of a suitable electrode material or the optimization of their incorporation into an electrode formula, as Nafion-based electrodes are still used in evaluation.[36]

Some of the disadvantages of sulfonated poly(arylene ether sulfone) reported by Kreuer,[37] is that the PEMs based on these materials would have relatively smaller hydrophilic channels compared to perfluorosulfonic acid-based (PFSA) copolymers due to their more rigid aromatic structure. These smaller channels lead to an increase in the distance between sulfonic acid groups and hinder the migration of protons during transport. A greater level of sulfonation in a random

copolymer results in more frequent branching of the hydrophilic channels, increasing the number of dead-ends, hindering proton transport and efficiency. This observation seems valid only for statistically copolymerized poly(arylene ether sulfone)s (PAES) materials, while multiblock hydrophilic-hydrophobic copolymers have longer hydrophilic pathways which are more ordered. This will be discussed in greater detail in a later section when the performances of statistical and multiblock copolymers are compared.

1.3.2.1: Post-sulfonated polymer

The sulfonic acid group is easily the most widely used proton-conducting moiety for PEMs as it easily available, has high acidity and is very easy to introduce into the polymer backbone. Post-sulfonated copolymers (poly(arylene ether sulfone)s or poly(arylene ether ketone)s) are usually obtained by using concentrated sulfuric acid, fuming sulfuric acid, chlorosulfonic acid, or sulfur trioxide via the electrophilic substitution of proton with sulfonic acid group on the polymer's aromatic rings.[38-43] Post-sulfonation is a very common technique for introducing a sulfonic acid functional group on the polymer backbone as it is very inexpensive compared to synthesizing a sulfonated monomer and then forming a sulfonated copolymer. The post-sulfonation technique is also very flexible and reliable. For example, to achieve higher degrees of sulfonation, stronger sulfonating agents such as fuming sulfuric acid and chlorosulfonic acid can be used, while the use of mild sulfonating agent, such as concentrated sulfuric acid or SO_3 and triethyl phosphate complex, will result in partially sulfonated copolymers. [38, 40] An example of the post-sulfonated product is shown in Figure 1.7.

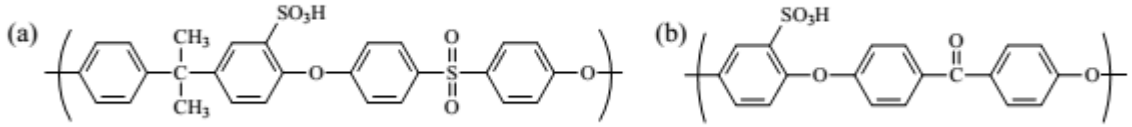

Figure 1.7: Examples of post-sulfonated poly(arylene ether sulfone)s and poly(arylene ether ketone)s.

The major disadvantages of the post-sulfonation process are lack of control of degree of sulfonation and polymer degradation. The use of strong sulfonating agents provides a higher degree of sulfonation, but also unwanted side reactions and degradation of the polymer chains. To reduce the polymer degradation, mild sulfonating agents are used, but they require a longer reaction time and result in a lower degree of sulfonation. Moreover, in the post-sulfonation process, the electrophilic substitution takes place onto the activated phenyl rings, rather than on the deactivated phenyl rings.[44] In the McGrath group, the post-sulfonation process using a mild sulfonating agent was investigated by Johnson,[38] in which post-sulfonation was performed on Udel polysulfone using 2:1 ratio of SO_3 and triethyl phosphate. The post-sulfonation resulted in the formation of mono sulfonated polysulfone with little or no degradation, but the procedure is somewhat lengthy, requires careful handling and preparation, and the results are limited to only one sulfonate per activated unit.[38]

1.3.2.2: Directly copolymerized PAES based on biphenol and DCDPS

The process of sulfonating 4,4'-dichlorodiphenyl sulfone (DCDPS) monomer was first developed by Ueda et al.,[43] which resulted in the formation of 3,3'-disulfonated 4,4'-dichlorodiphenyl sulfone (SDCDPS). This process was later refined by the McGrath group[44, 45] to produce SDCDPS, which was used with biphenol to produce directly copolymerized sulfonated poly(arylene ether sulfone) to overcome the disadvantages of the post-sulfonation process. The synthesis of SDCDPS is shown in Figure 1.8. This one step synthesis process was further optimized by the modifying the reactant mole ratio to improve the yield of the final product.[44] The final product was characterized with UV-VIS spectroscopy to assess the purity of SDCDPS.[44, 46]

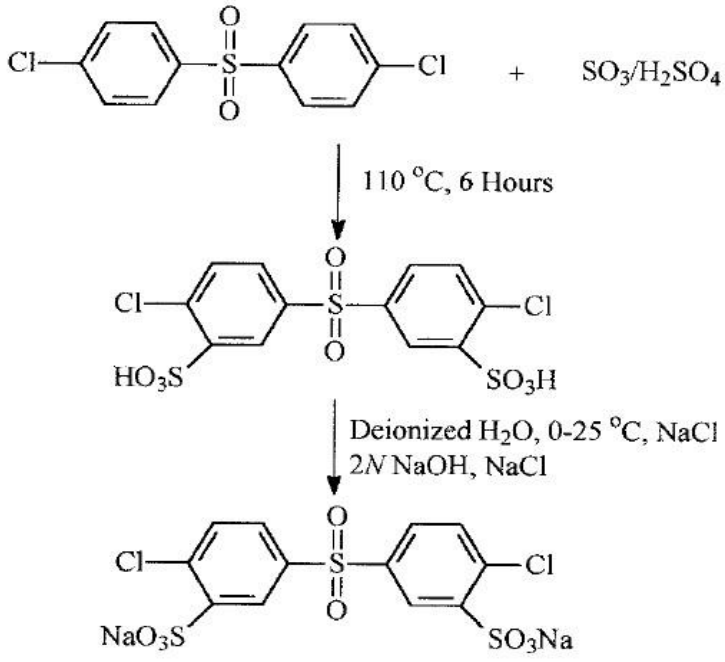

Figure 1.8: Initial synthetic procedure for producing 3,3'-disulfonated-4,4'-dichlorodiphenyl sulfone. [47]

Direct copolymerization to produce sulfonated poly(arylene ether sulfone)s offers several advantages over the post-sulfonation process. The degree of sulfonation and molecular weight of the polymer made can be easily tailored by controlling the stoichiometric ratios of the sulfonated and nonsulfonated monomers. Moreover, in the case of directly copolymerized polymers, there are two sulfonic acid groups attached to the deactivated phenyl ring which provides greater stability and acidity than in the case of post-sulfonation, where only a single sulfonic acid group is attached to the activated phenyl ring. The structures of sulfonated PAES formed from these processes are compared in Figure 1.9. The only major disadvantage of direct copolymerization technique is the increase in the synthetic steps.[44]

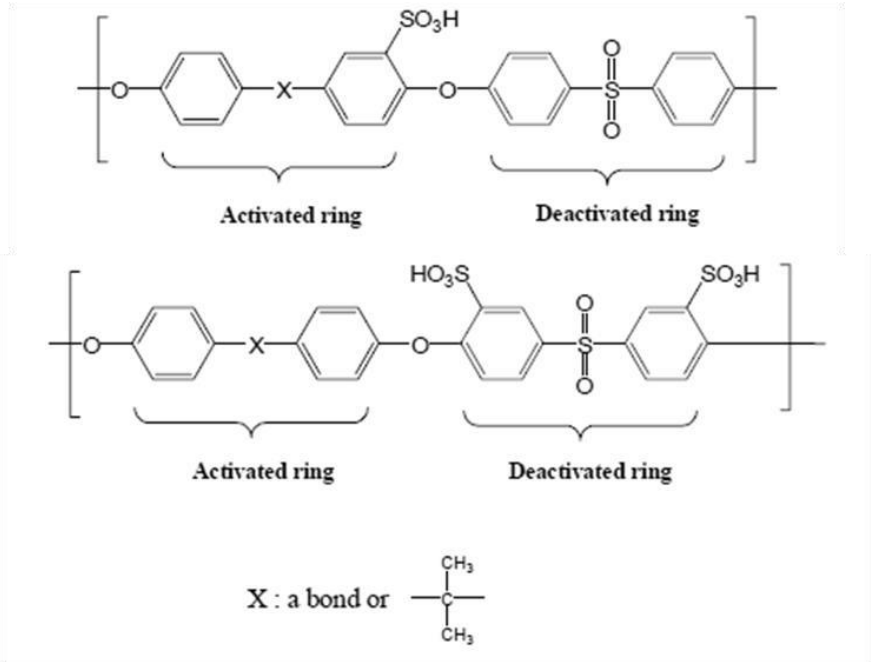

Figure 1.9: Comparison of structures of post-sulfonated (top) and directly copolymerized (bottom) poly(arylene ether sulfone) chains. [44]

The McGrath group works on the synthesis of sulfonated poly(arylene ether sulfone) known as BPS, which stands for **B**i**P**henyl**S**ulfone, and HQS, which stands for **H**ydro**Q**uinone**S**ulfone. BPS copolymer is synthesized using SDCDPS, DCDPS and biphenol via nucleophilic aromatic substitution reaction, as shown in Figure 1.10. The mole percent of SDCDPS also denotes the degree of sulfonation of the resulting copolymer. The nomenclature of the BPS copolymer is BPS-xx, where xx denotes the degree of sulfonation. For example, BPS-40 denotes a copolymer of SDCDPS, DCDPS and biphenol which incorporates 40% of the disulfonated SDCDPS monomer. The synthesis scheme for the BPS-xx copolymer is shown in Figure 1.10.

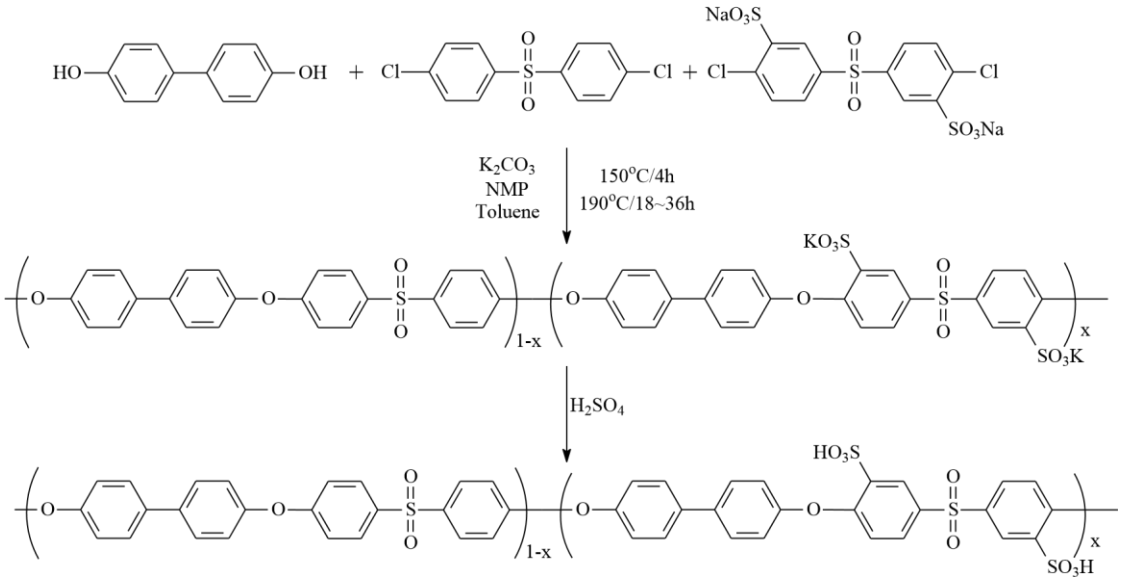

Figure 1.10: Synthetic scheme for the BPS-xx copolymer. [44]

As seen from the synthetic scheme, the copolymer is synthesized in the salt form and is converted to the acid form as shown in Figure 1.10. The number of repeating units of the polymer can be controlled using the stoichiometric ratio of the dihalide and biphenol

monomers, which is derived using the Carothers equation. The salt form of the copolymer is converted into acid form by boiling in 0.5M H_2SO_4 for 2 h, followed by washing and boiling in deionized water for 2 h. The characterization of the copolymer may be done in either salt or acid form. Whether the membrane is in acid or salt form is shown by the nomenclature. For example, a membrane in the salt form is denoted by BPS-xx, while a membrane in acid form is denoted by BPSH-xx, where H stands for acid form.[44, 48]

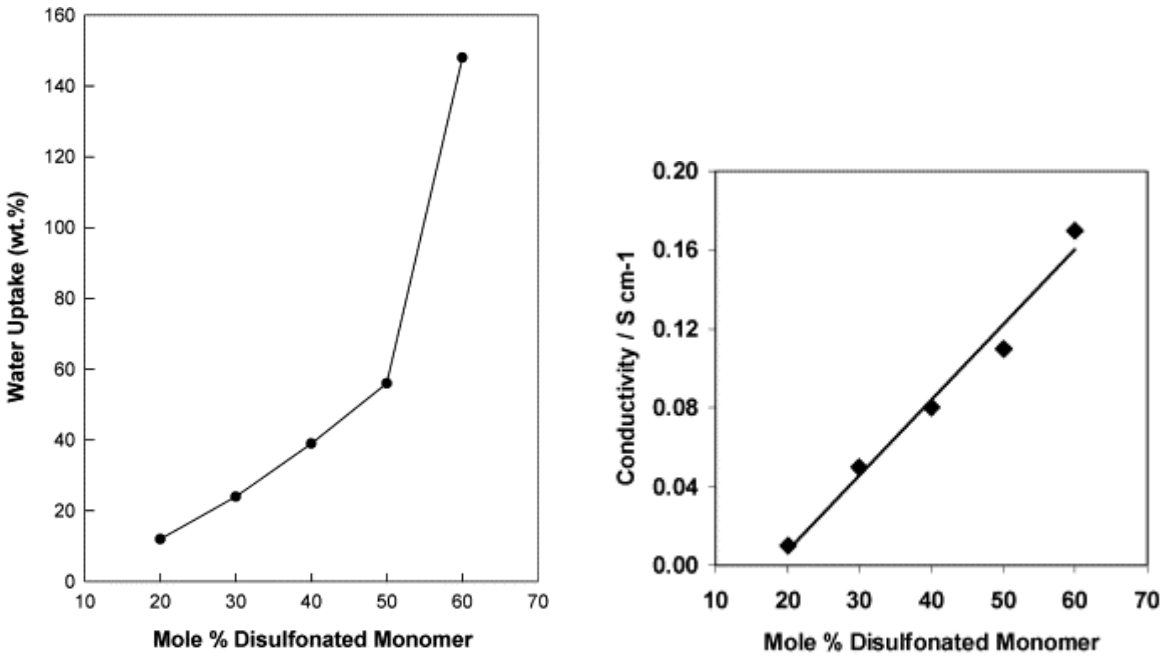

Figure 1.11: Mass water uptake and proton conductivity properties of BPSH polymer as a function of disulfonation, illustrating the impact of the percolation threshold on the former.[44]

The impact of sulfonation level on water uptake and conductivity is shown above in Figure 1.11. While we can summarize that the water uptake and conductivity both increase with disulfonated monomer content, there is a limit to the amount that can be incorporated in the polymer without a deleterious impact on polymer properties. When the amount of

SDCDPS exceeds 50%, the water uptake increases dramatically, leading to a loss of mechanical integrity and eventually resulting in a water soluble polymer. Thus even though the conductivity increases with the amount of disulfonated monomer, it is impractical to incorporate the disulfonated monomer beyond this point. This limit is called the percolation threshold, and it is a concern seen in all linear ionomer systems. One way to overcome this percolation threshold is by synthesizing multiblock copolymers in which the hydrophilic and hydrophobic phases of the multiblock copolymer are synthesized individually and then coupled together. Thus, multiblock copolymers incorporate the advantages of the random sulfonated copolymers while avoiding the disadvantages of low performance under partially humidified conditions.[47, 49-55] The McGrath group has done extensive research on the multiblock copolymers and its properties and comparison with the random copolymer will be discussed in the coming sections.

The degree of sulfonation also affects the glass transition of the copolymer as seen in Figure 1.12 below, where the influence of the degree of sulfonation on the glass transition temperature of BPS-xx copolymer is shown.

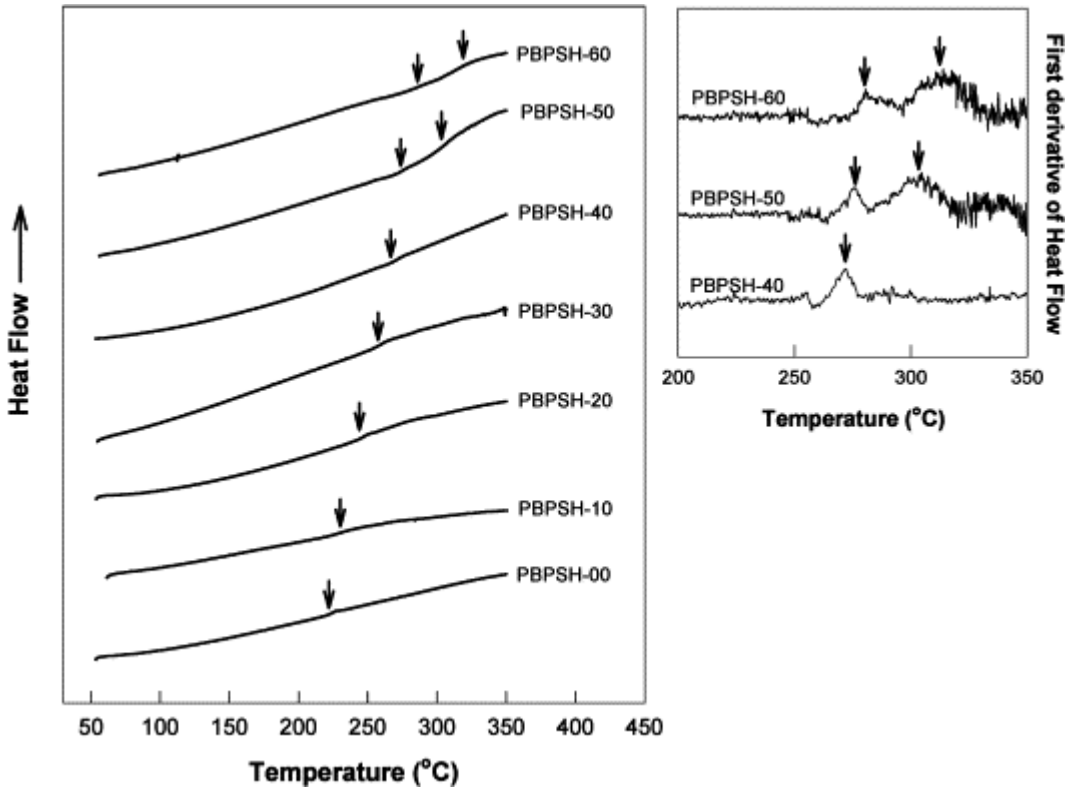

Figure 1.12: The influence of the degree of sulfonation on the glass transition temperature of a BPS-xx copolymer series. [44]

From Figure 1.12, we can interpret that the glass transition temperature of the copolymer also increases with the degree of sulfonation. This phenomenon can be described by the effect that the introduction of sulfonate groups leads to increased intermolecular interactions because of the pendant sulfonic acid groups. The introduction of the sulfonic acid groups increases the molecular bulk, resulting in hindered internal rotation and an increased glass transition temperature.[56]

Crosslinking is another way to get a highly conducting material. Materials with a very high degree of sulfonation can be crosslinked by incorporating a crosslinkable group. The advantages of crosslinking are that it leads to formation of a water-insoluble highly

sulfonated copolymer with high proton conductivity. Crosslinking also helps inhibit the water uptake due to the crosslinked network formation.[57, 58]

The effect of the molecular weight does not impact the proton conductivity or the water uptake significantly, as long as it exceeds the critical molecular weight of entanglement to produce tough, ductile and flexible copolymers.[47, 59] It has been reported that when the molecular weights of the copolymer exceeds 40 kg/mol, the copolymer produces films which can handle stress up to 1.4GPa before yielding.[59]

1.3.2.3 PAES comonomer variation and properties

The McGrath group has also worked on different statistical copolymers in which the biphenol is replaced by Bisphenol-A (BisA) and also a fluorine substituted version of bisphenol-A (6F-BisA). The substitution with the BisA based moieties might lead to an increase in the free volume of the copolymer which would give more mobility and area for the protons to travel, leading to increase in the conductivity.[60] Moreover, it might also lead to the formation of larger, more continuous hydrophilic ion-conducting channels compared to biphenol based BPS-xx.[44, 56] The incorporation of 6F-BisA might lead to decrease in water uptake and also improve adhesion to the Nafion-based electrodes. [46, 56]

Various other hydrophobic comonomers were also investigated with the intent of improving membrane properties. For example, a naphthalene-based dianhydride was used to couple with SDCDPS and DCDPS to form a statistical polyimide for use in DMFCs.[61, 62] Phosphine oxide-based copolymers were also synthesized with the intent of improving oxidative and hydrolytic stability, which demonstrated good mechanical properties and low methanol permeability.[63, 64] But, both the naphthalene-based polyimides and phosphine oxide incorporated

copolymer showed inferior proton conductivity compared to BPS-xx copolymer of comparable IEC.[64]

It is believed that the proton conductivity of the copolymer depends upon its IEC. Thus in order to increase the IEC of the polymer without increasing the amount of disulfonated monomer, another strategy was introduced in which the biphenol comonomer was substituted with lower molecular weight hydroquinone. This synthesis resulted in copolymer which has a higher IEC and improved conductivity.[65]

1.3.2.4 PAES Multiblock copolymers and properties

To improve fuel cell performance and to negate the disadvantages of the random copolymers, multiblock copolymers were proposed to be viable alternatives. Block copolymers are macromolecules made up of two or more usually multiphase blocks that are chemically conjoined in the same chain. Unlike random copolymers, in which the monomers are arranged statistically, in block copolymers, different chemical components exist in ordered sequences. Therefore, depending on the degree of order, multiblock copolymers have the potential to display interesting physico-chemical properties. Various morphological features of block copolymers can be obtained by tailoring the chemical composition, molecular weight, and/or volume fraction of the blocks.[66]

Hydrophobic/hydrophilic (amphiphilic) block copolymers can be obtained when one or more of the blocks is fully or partially modified with hydrophilic functional groups. Due to their unique properties, these materials can be utilized for a variety of purposes, including as stabilizers

in suspensions and emulsions, for pharmaceutical applications, and in the synthesis of advanced materials, adhesives, and coatings.[67, 68]

The development of hydrophobic-partially sulfonated ionic block copolymers as PEMs has been of great interest. These materials contain sequences of sulfonated and nonsulfonated segments which result in interesting structural and morphological features.[69, 70] Therefore, various block copolymer ionomers containing sulfonic acid groups have been synthesized. The research on the synthesis of sulfonated random PAES has given insight on understanding proton conductivity of the materials, its water uptake, mechanical and thermal properties, and how to tailor these properties by changing the comonomer amount of disulfonated monomer used.

The McGrath group developed the multiblock copolymers in order to overcome the limitations of the random copolymers by synthesizing hydrophilic and hydrophobic oligomers separately and then coupling them together to form multiblock copolymers.[21, 71, 72, 73-75] There are several advantages of the use of hydrophilic-hydrophobic multiblock copolymers compared to statistically copolymerized systems. The composition and the sequence length of the alternating hydrophobic-hydrophilic phases can be easily controlled. This control of the sequence length and composition leads to various types of morphology. For example, shorter sequence length gives rise to a short-range nano-phase separated morphologies while longer sequence length leads to formation of a lamellar morphology. Moreover, by changing the composition of the repeating sequence, the phase separation can be tailored which leads to well-defined ionic channel for proton transport. This leads to improved water retention even under partially humidified conditions which results in improved performance under these conditions, lower water uptake and increase in proton conductivity. By modifying the ratio of hydrophilic to hydrophobic oligomers, or by changing the sequence length of the hydrophobic and hydrophilic phase, we can easily tailor

the IEC of the final copolymer. Also, a higher IEC can be obtained by using 100% disulfonated monomer in the synthesis of the hydrophilic oligomers and these oligomers when coupled to the hydrophobic oligomers are prevented from being water soluble. Lastly, one of the most interesting behaviors of the multiblock copolymers is that they show anisotropic water swelling. The multiblock copolymers will swell primarily in the through-plane direction (z), while there will be very little swelling in in-plane direction (x&y), and the anisotropic swelling and proton conductivity performance under partially humidified condition improves with increase in the block length size.[74, 76-80]

The McGrath group has worked in the synthesis of multiblock copolymer consisting of 100% sulfonated oligomers which are synthesized by reaction of SDCDPS with biphenol or hydroquinone. Hydroquinone based multiblock copolymers show improved proton conductivity under partially humidified conditions because of higher IEC.[24, 81] Multiblock copolymers consisting of partially fluorinated hydrophobic blocks have also been investigated.[23, 24, 72, 82, 81, 83] Some of the advantages of using fluorinated moieties is that it helps in increasing hydrophobicity which leads to improved phase separation between the hydrophilic and hydrophobic phase. Presence of fluorine moieties will also lead to decrease in the water uptake and also increase adhesion to the Nafion-based electrodes.

Other than the McGrath group, many other research groups have also investigated multiblock copolymers for fuel cell applications.[50, 84-86] Some strategies have included developing multiblock membrane systems based on polyurethanes, sulfonated polyimides, polynaphthalimides, and containing tetraphenyl methane moieties.[86-89]

Other than the poly(arylene ether) based multiblock copolymer systems, many other multiblock copolymer systems have also been explored in the McGrath group. Benzimidazole-

based multiblock copolymers have also been researched and contain benzimidazole as the hydrophilic oligomer which is coupled with DCDPS based hydrophobic oligomer. DCDPS based hydrophobic oligomer were used to increase stronger and durable membranes even at high temperature. These systems were doped in phosphoric acid which acted as the medium for proton transfer from anode to cathode.[90-92] Polyimide based hydrophobic oligomers were coupled with BPSH100 with the intent of producing membranes with high proton conductivity and high glass transition temperature.[93]

1.4. Comparisons between random and block copolymer PEMs

As mentioned previously, block copolymers consist of ionic sequences which aggregate together to give ionic channels, thus facilitating proton transport. While in statistical copolymers, the ionic sequences are randomly distributed, resulting in poorly connected channels. Due to this, the proton transport is hindered. Well-defined ionic channels are very important for proton transport under partially humidified conditions. Moreover in case of the multiblock copolymers, we can also change the block lengths which helps in controlling the proton conductivity while in random copolymers, proton conductivity is more dependent on upon the humidity conditions. These advantages are reported in a few studies[94, 95] by comparing the diffusion coefficient and the proton conductivity of the multiblock copolymer to the random copolymer at various levels of humidity.

The performance of three types of proton exchange membrane were studied by Serpico et al.[96], in which proton conductivity of Nafion 117, sulfonated ethylene-styrene random copolymer(S-SE) and sulfonated ethylene-styrene block copolymer(S-SEBS) are compared. Figure 1.13 shows

the structure of the S-SE random copolymer. The proton conductivity vs humidity plot is shown in Figure 1.14 for the three proton exchange membranes.

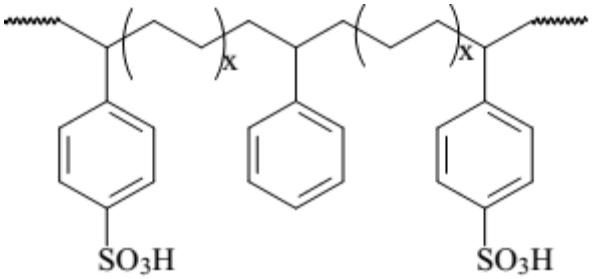

Figure 1.13: Structure of S-SEBS block copolymer.

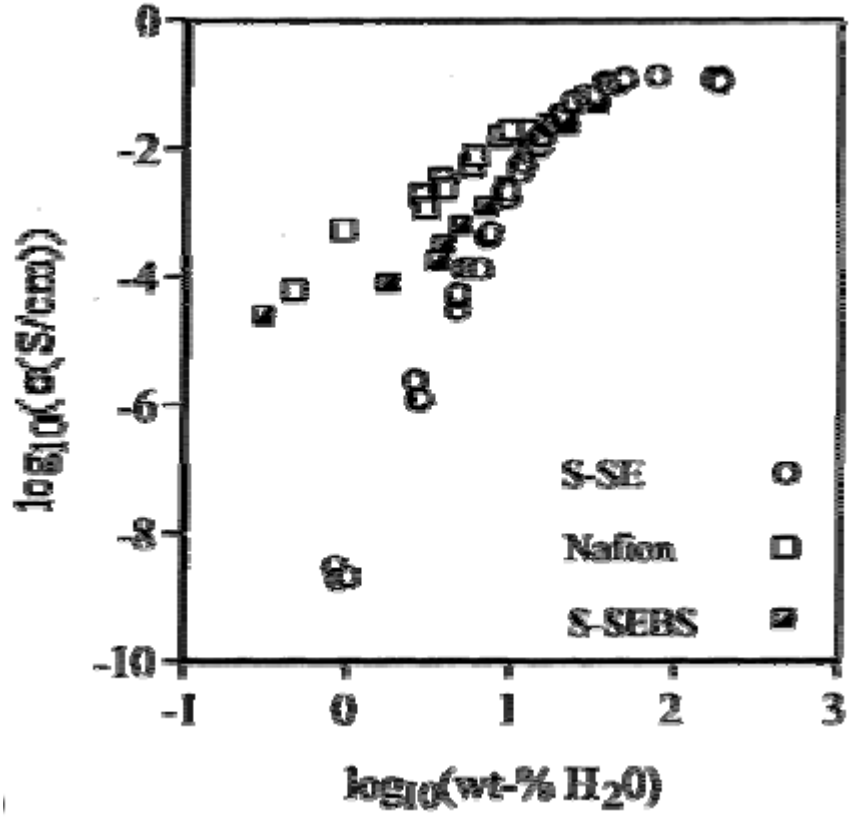

Figure 1.14: Proton conductivity vs. water content for S-SEBS, S-SE and Nafion PEMs. [96]

As seen from Figure 1.13 and Figure 1.14, all three PEMs showed almost similar proton conductivity at high levels of hydration. But as the humidity levels decrease, the S-SE random copolymer showed the most rapid decrease in proton conductivity, followed by S-SEBS block copolymer and Nafion 117. This plot shows that the ion-conducting channels in the S-SE random copolymer have poor connectivity, while those in the S-SEBS block copolymer are much more developed, resulting in a better performance.

A comparison of wholly aromatic random and multiblock copolymers was done by Roy *et al.*[70], who investigated the transport properties of sulfonated poly(arylene ether sulfone) and sulfonated poly(arylene ether ketone random copolymers and compared them to the highly fluorinated block copolymers synthesized by Yu and coworkers. The structure of the random and block copolymers are shown below in Figure 1.15.

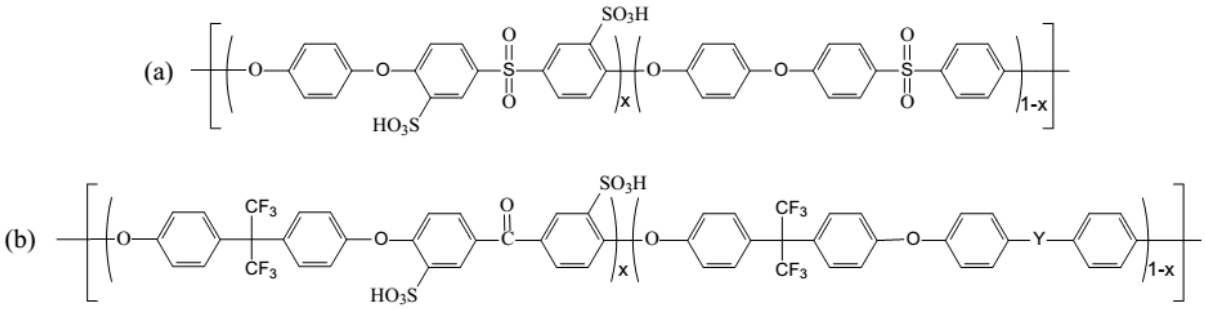

Figure 1.15: Structures of (a) poly(ether sulfone) and (b) poly(ether ketone) random copolymers.

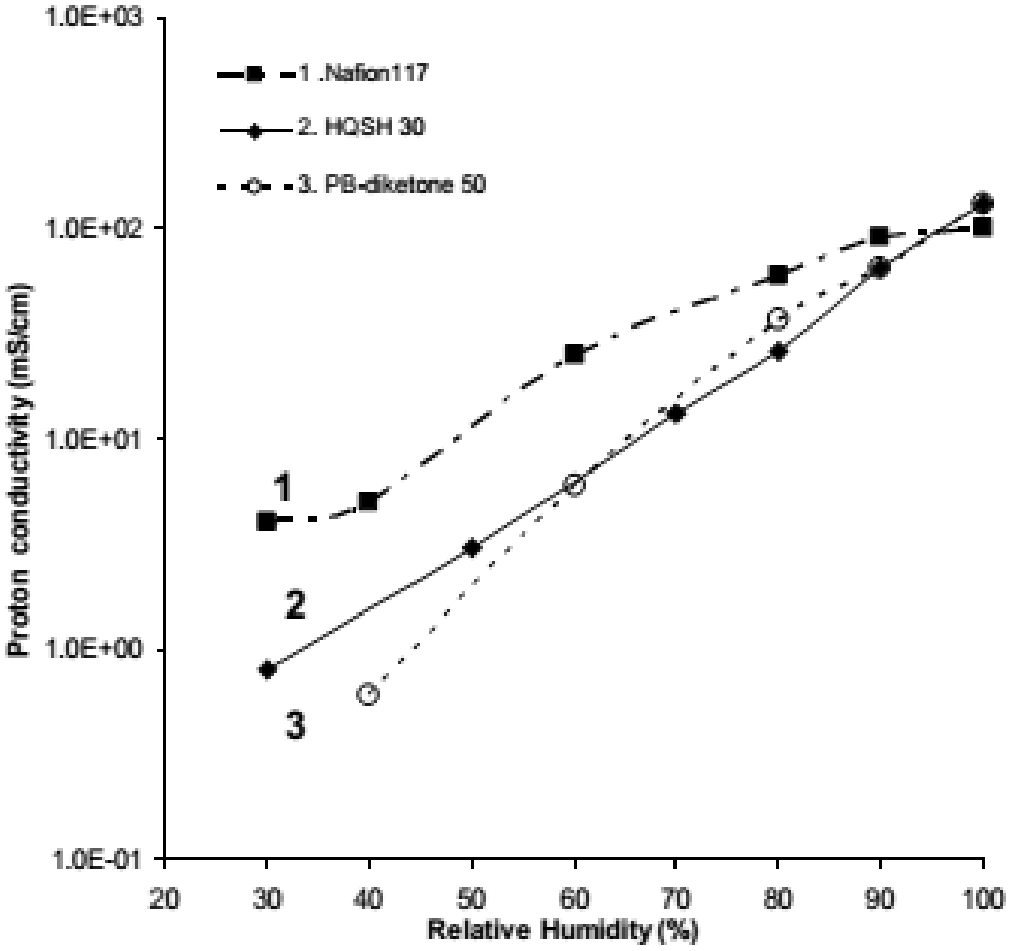

Figure 1.16: Proton conductivity vs. RH plots for Nafion 117, poly(ether sulfone) random copolymers (HQSH 30), and poly(ether ketone) random copolymers (PB-diketone 50). [70]

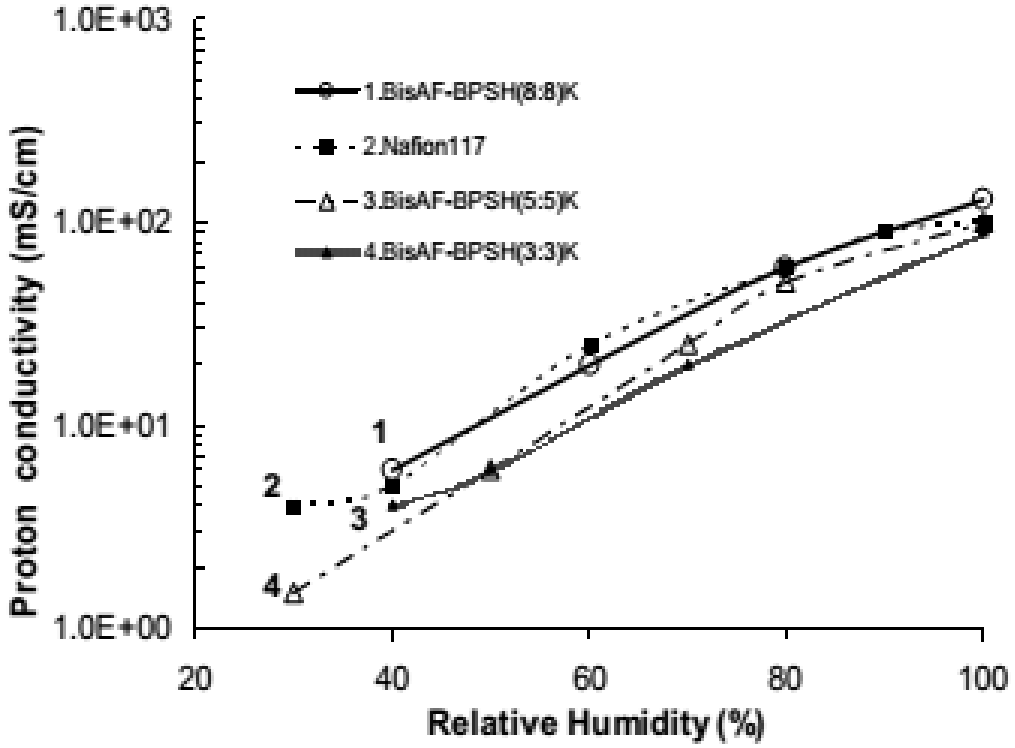

Figure 1.17: Proton conductivity vs. RH plots for Nafion 117 and BisAF-BPSH multiblock copolymers.

Figures 1.16 and 1.17 show the plots of proton conductivity vs. relative humidity (RH) for the random and block copolymers along with Nafion 117. From Figure 1.16, we can see that at high humidity levels, the proton conductivity of Nafion 117 and the random copolymers are similar. But as the humidity level decreases, the proton conductivity of both the random copolymers decreases rapidly compared to Nafion 117. However, the multiblock copolymers show a much smaller decrease in proton conductivity compared to Nafion 117, and at higher block lengths, the multiblock performance is comparable to Nafion 117 at all humidity levels. We also see that with the increase in the block length of the hydrophobic and hydrophilic sections of

the multiblock copolymer, the proton conductivity increases. From the results reported for BisSF-BPSH multiblock copolymers by Roy *et al*,[70] it is seen that the copolymer with the highest block length had the lowest IEC and water uptake compared to the other block copolymers tested. Still it showed the best proton conductivity of all the multiblock copolymers tested. A similar trend of sequence length affecting the proton conductivity was also reported by Yu et al,[97] in which proton conductivity vs RH performance was plotted for the BisSF-BPSH copolymers. The conductivity of the multiblock copolymer increased with block length, as illustrated in Figure 1.18.

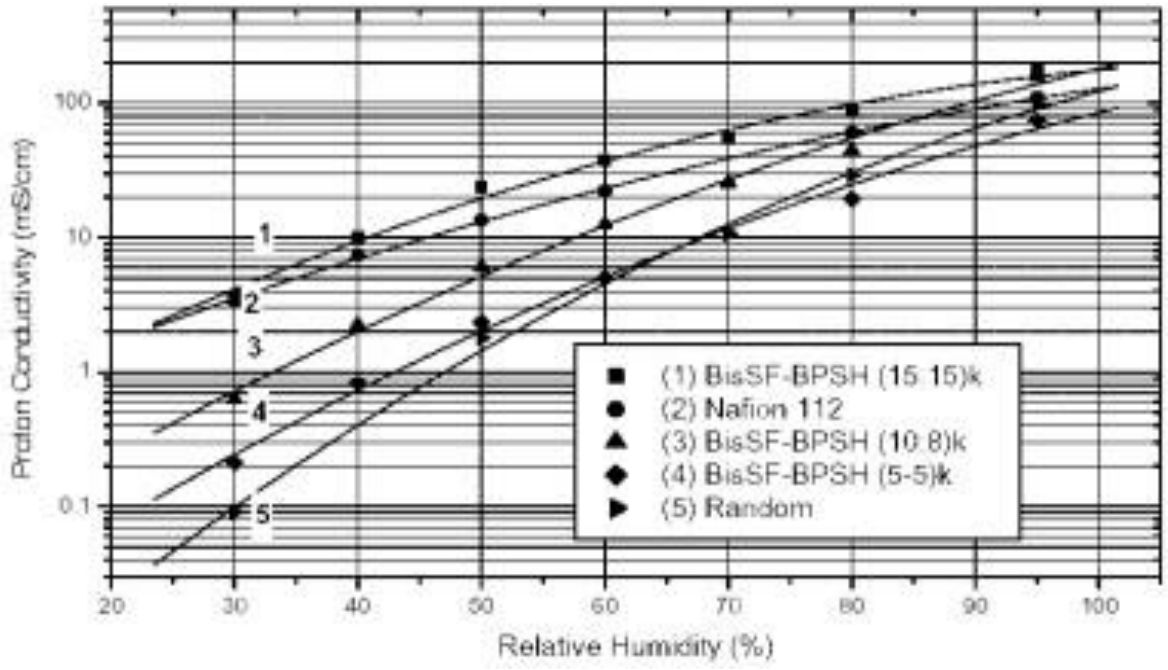

Figure 1.18: Proton conductivity vs. RH plots for BisSF-BPSH multiblock copolymers, Nafion 112 and BPSH-35 random copolymers. [78]

The presence of fluorine moieties also helps in increasing the phase separation, leading to formation of well-defined ionic channels.[98] This is illustrated by comparing the PI-BPSH multiblock copolymers containing polyimide hydrophobic blocks and the BisAF-BPSH multiblocks containing 6F-BisA based hydrophobic blocks. The BisAF-BPSH copolymers showed much better performance compared to polyimide based multiblock copolymers.

As discussed above, the well-defined morphology of the multiblock copolymers leads to improved performance of the multiblock copolymer. This theory is supported by AFM images of the random and multiblock copolymers. The tapping mode AFM images of the partially disulfonated random copolymer BPSH-xx is shown in Figure 1-19. The degree of sulfonation of the BPSH-xx ranges from 30 to 45 mol%.

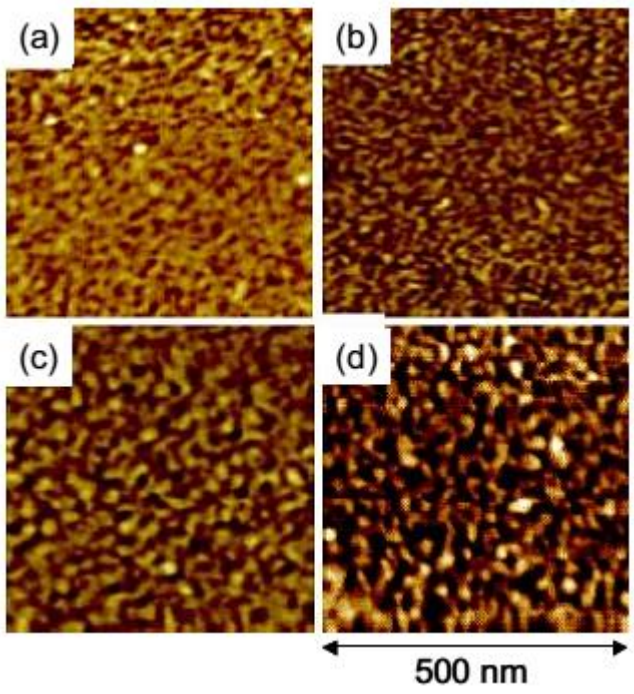

Figure 1.19: Tapping mode AFM images of BPSH-xx random copolymer membranes: (a).BPSH-30; (b).BPSH-35; (c).BPSH-40; (d).BPSH-45. [99]

In the AFM images, the darker region represents the hydrophilic domains, while the lighter region represents the hydrophobic region. From Figure 1.19, we can infer that the size of the hydrophilic domain increases as the degree of sulfonation increases, displaying increasing connectivity of the hydrophilic region. But overall, the morphology seems dispersed in the case of random copolymers.

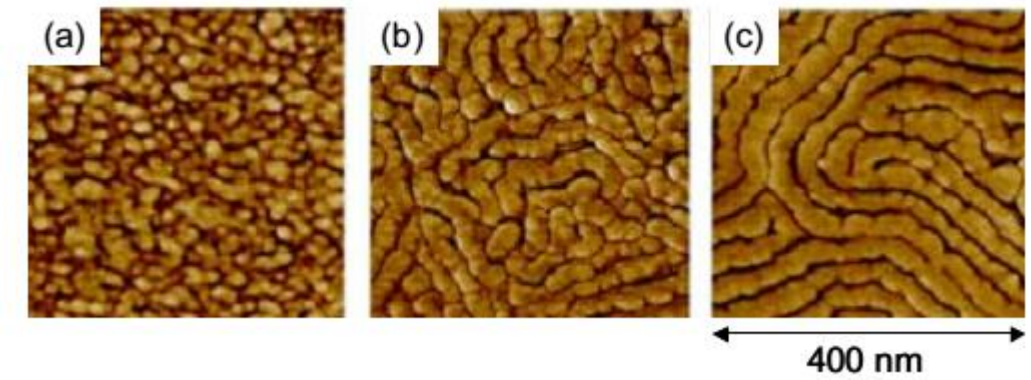

Figure 1.20: Tapping mode AFM phase images of BPSH-PI multiblock copolymer membranes with different block lengths: (a) 5K: 5K; (b) 10K: 10K; (c) 15K: 15K. [99,100]

The tapping mode AFM images of the BPSH-PI multiblock copolymer are shown in Figure 1.20.[100, 101] The phase separation is much more defined than in the BPSH random copolymers. All images show nanophase separation, wherein the hydrophilic channels increase in size as block lengths increase from 5kg/mol to 15kg/mol, resulting in formation of co-continuous hydrophilic channels. These act as pathways for proton transport, leading to improved proton diffusion or proton conductivity as shown in Figure 1.21.

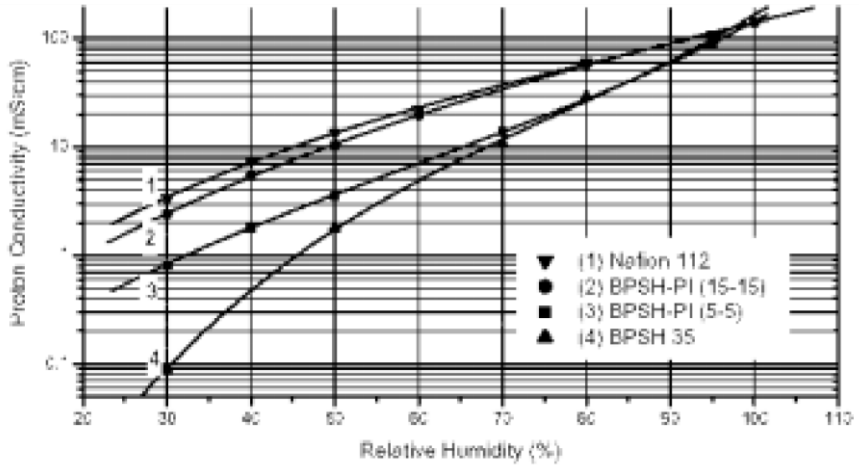

Figure 1.21: Proton conductivity vs. RH plots for BPSH-PI multiblock copolymers, Nafion 112 and BPSH-35 random copolymers. [102]

In recent years, the wholly aromatic poly(arylene ether sulfone) based membranes have improved considerably as proton exchange membranes. Chen and coworkers synthesized PEEK-BPSH100 hydrophobic-hydrophilic multiblock copolymers which show excellent proton conductivity at low relative humidity levels as seen in Figure 1.22.[23] This excellent low relative humidity performance is attributed to the presence of more distinct nanophase morphology and increased phase separation between semi-crystalline hydrophobic and hydrophilic domains.

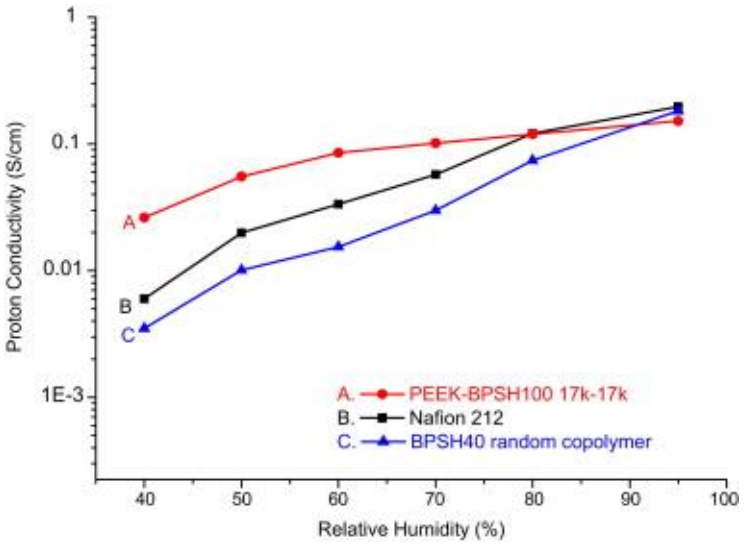

Figure 1.22: Proton conductivity vs. RH of PEEK-BPSH100 17k-17k multiblock copolymers with Nafion® and BPSH40 as references (measured at 80 °C).

In summary, we see that new synthetic techniques and growing knowledge of the structure-property relationships have led to developing alternative hydrocarbon-based proton exchange membranes other than Nafion, which is still the state of the art proton exchange membrane. These alternative PEMs show a balanced combination of proton conductivity, water uptake and durability especially the multiblock copolymer systems. Random copolymers based on the direct synthesis of partially disulfonated monomers have shown similar proton conductivity compared to Nafion at high humidity levels, but their performance deteriorates drastically with decrease in humidity levels. Although high proton conductivity under partially humidified conditions is the primary goal, with the block copolymer systems the challenge remains in discovering ways to maintain mechanical integrity of the system without compromising their performance.

Chapter 2 : Synthesis and Characterization of Novel Trisulfonated Hydrophilic-Hydrophobic Multiblock Copolymers based on Poly(arylene ether sulfone) for Polymer Electrolyte Membranes.

A multiblock copolymer series based on poly(arylene ether sulfone)s containing fully tri-sulfonated hydrophilic blocks was developed and evaluated for use as membranes in proton exchange fuel cell (PEMFCs). The multiblock copolymers were synthesized by coupling decafluorobiphenyl (DFBP) or hexafluorobenzene (HFB) end-capped poly(arylene ether sulfone) hydrophilic block and the phenoxide terminated hydrophobic poly(arylene ether sulfone) hydrophobic blocks, respectively. NMR analysis was used to confirm copolymer composition, and potentiometric titration was used to obtain the ion exchange capacity (IEC). Intrinsic viscosity measurements were used to confirm that high molecular weight copolymers were synthesized. The copolymer series was characterized by means of water uptake, proton conductivity under fully and partially hydrated conditions, and surface morphology using atomic force microscopy (AFM). The nanophase separated morphology developed in the membranes accounted for improved proton conductivity compared to Nafion at reduced relative humidity (RH).

2.1 Introduction

In recent times, with the increasing consumption of fossil fuels and their scarcity, as well as the increase in the resulting pollution and economic costs, it is imperative to develop an alternate energy system which is clean and efficient.[1] Fuel cell technology is a viable alternative to the current fossil fuel based technology as it more energy efficient and produces no greenhouse gases.[54] Fuel cells have a simpler design with no moving parts, higher efficiency, and produces

environmentally benign waste products.[10] One of the primary components of the PEMFCs is the material used for the proton exchange membrane (PEM). An ideal PEM candidate needs to have a number of critical parameters such as high proton conductivity, low electronic conductivity, low permeability to both fuel and oxidant, good oxidative, hydrolytic and thermal stability, good mechanical properties, ease of fabrication into MEAs, and low cost.[9]

Presently, Nafion is the state of the art membranes used in PEMFCs, which exhibits satisfactory properties. Nafion is a poly(perfluorosulfonic acid) ionomer consisting of a tetrafluoroethylene (Teflon) backbone with pendant side chains of perfluorinated vinyl ethers terminated by perfluorosulfonic acid group. It exhibits good proton conductivity under partially humidified conditions, excellent chemical and electrochemical stability. However, the disadvantages of Nafion are that it is expensive and has a low ceiling operating temperature (80^{o} C) due to the plasticization effect of water, and high fuel permeability in the case of direct methanol fuel cells.[18-20, 103, 104] A significant portion of current PEM research is to find alternative membranes that can overcome these disadvantages

A great deal of research has focused on developing sulfonated poly(arylene ether)s, especially poly(arylene ether sulfone)s, as they display much lower fuel permeability, lower cost, higher glass transition temperatures, and better mechanical properties. [9, 105-108] In the McGrath group, the focus has been on developing random and block copolymers consisting of partially sulfonated poly(arylene ether sulfone)s. The random copolymers show comparable proton conductivity under fully hydrated conditions, but their performance deteriorates under partially humidified conditions.[44, 65, 109, 110] However, the hydrophilic-hydrophobic block copolymers show comparable, and sometimes superior, performance compared to Nafion under partially humidified

conditions. One of the reasons for this improved performance is the nanophase separation of the proton-conducting hydrophilic domains and the hydrophobic domains.[71, 72, 111, 112]

In this paper, multiblock (segmented) copolymers were synthesized via coupling reactions of hydrophobic and hydrophilic telechelic oligomers. These materials contain fully hydrophilic trisulfonated poly(arylene ether sulfone) (SQSH100) blocks and hydrophobic poly(arylene ether sulfone) blocks. In the case of the hydrophilic block SQSH100 stands for SQ: sulfonated hydroquinone, S: sulfone, H: the acid form and 100 stands for 100% degree of sulfonation. The general structure of these copolymers studied is shown in Figure 2-1, where a and b denote the relative fractions of the hydrophilic and hydrophobic oligomers. The multiblock copolymers is termed SQSH100-BPS. The synthesis and characterization of the material will be illustrated in detail and the influence of its structures on resulting properties will be discussed.

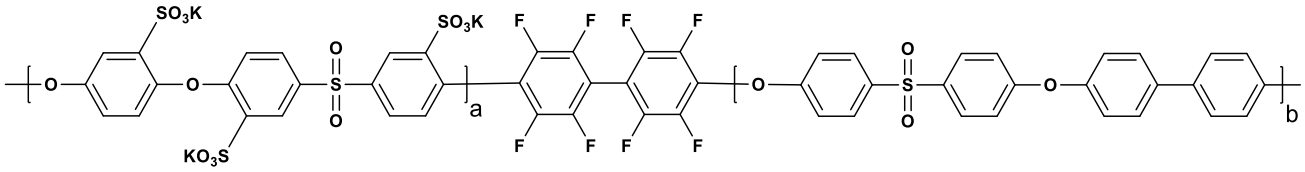

SQS100-BPS

Figure 2.1: Structures of tri-sulfonated hydrophilic-hydrophobic multiblock copolymer

2.2. Experimental

2.2.1. Materials

2,5-Dihydroxybenzenesulfonic acid potassium salt (SHQ) was provided by Sigma Aldrich and recrystallized from deionized water/methanol mixture (10:90 v/v) and then dried under vacuum at 60^{o}C for 24 h. 3,3‘-disulfonated-4,4‘-dichlorodiphenyl sulfone (SDCDPS) and 4,4‘-dichlorodiphenyl sulfone (DCDPS) were provided by Solvay Advanced Polymers, and were dried in vacuum at 180^{o}C and 110^{o}C respectively, for 24 h prior to use. 4,4’-biphenol (BP) was received from Eastman Chemical Company and vacuum dried at 110^{o}C prior to use. Dimethyl sulfoxide (DMSO) and N,N-dimethylacetamide (DMAc) were received from Aldrich and vacuum distilled before use. Potassium carbonate (K_2CO_3), Decafluorobiphenyl (DFBP), hexafluorobenzene (HFB), 2-propanol (IPA), acetone, methanol and toluene were obtained from Aldrich and used as received.

2.3. Polymer synthesis

2.3.1 Synthesis of phenoxide terminated hydrophobic oligomers (BPS)

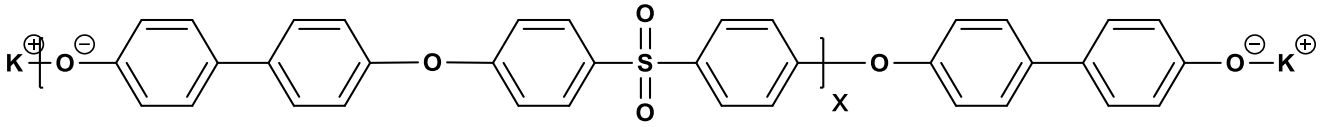

Figure 2.2: Structure of a BPS oligomer.

The synthesis of a phenoxide terminated BPS oligomer with 7 Kg/mol molecular weight, for example, was carried out as follows: DCDPS (14.700 g, 50.428 mmol), biphenol (10.164 g,

54.624 mmol) was added to a three-necked round bottom flask equipped with a mechanical stirrer, condenser, nitrogen inlet, and a Dean-Stark trap. DMAc (135 mL) was added, and the mixture was stirred until dissolved. K_2CO_3 (8.682 g, 62.818 mmol) and toluene (67 mL) were added, and the system was dehydrated at 150^{o}C for 4 h. The reaction bath was then gradually heated to 180^{o}C to remove the toluene. The polymerization was allowed to proceed at 180^{o}C for 48 h. The reaction mixture was isolated by precipitation in methanol. The white polymer was washed with H_2O and methanol, and then dried under vacuum at 120^{o}C for 12 hours before use.

2.3.2. Synthesis of phenoxide terminated fully trisulfonated hydrophilic oligomer (SQS100)

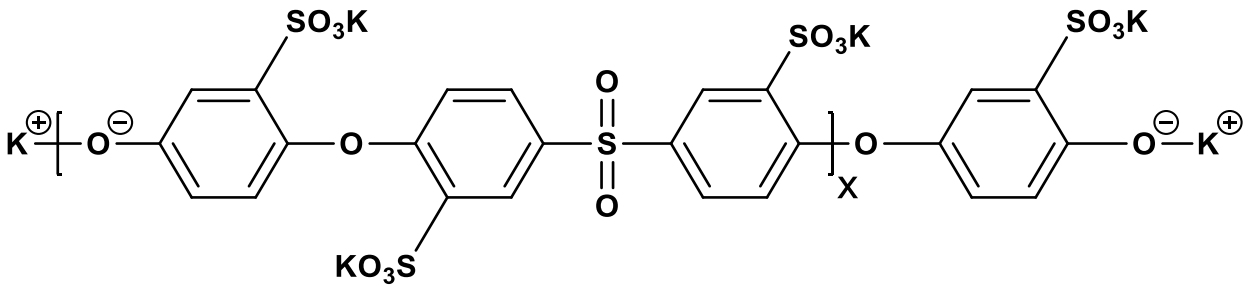

Figure 2.3: Structure of a SQS100 oligomer.

The procedures for the synthesis of 7 Kg/mol phenoxide terminated SQS-100 oligomers are as follows: sulfonated hydroquinone (12.374 g, 54.212 mmol), SDCDPS (24.95 g, 50.027 mmol), and DMSO (69 mL) were charged to a three-necked round bottom flask. The mixture was stirred until dissolved, then K_2CO_3 (8.616 g, 62.344 mmol) and toluene (35 mL) were added. The system was dehydrated at 150^{o}C for 4 h and then the temperature was raised to 155^{o}C with controlled removal of toluene. The polymerization was allowed to proceed at 155^{o}C for at least 96 h. The SQS100 oligomer was filtered to remove salt and precipitated in isopropanol, and then dried under

vacuum at 140°C for 12 hours before use. ^{1}H NMR was performed to determine the molecular weight of the oligomers.

2.3.3. End-capping of phenoxide terminated hydrophilic oligomers with DFBP and HFB (ESQS100)

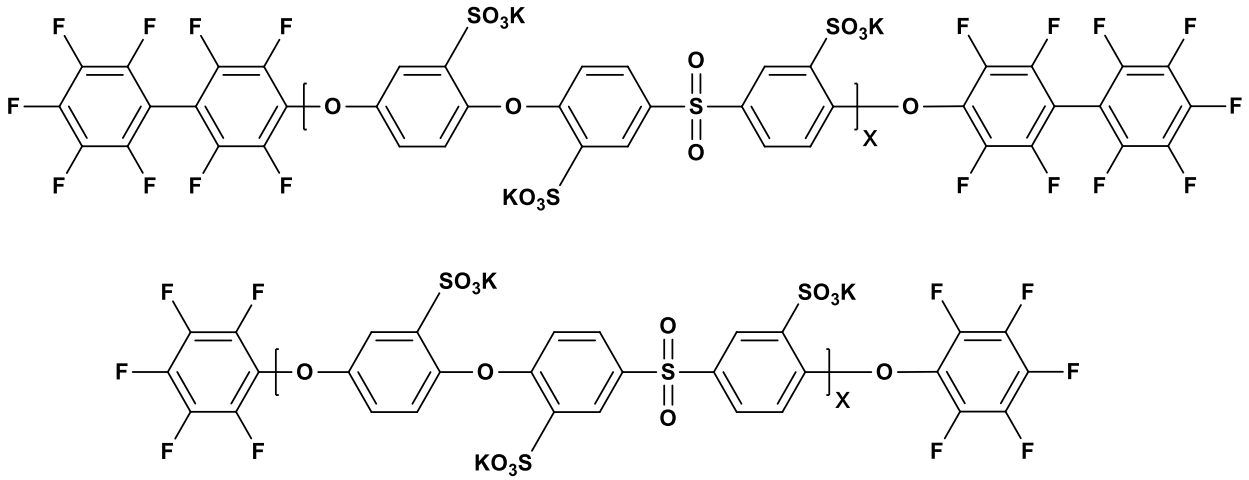

Figure 2.4: Phenoxide terminated hydrophilic SQS100 oligomers with DFBP and HFB, respectively.

Since both the SQS100 and BPS oligomers have the same telechelic functionality (e.g., phenoxide end group), a modification of one of the oligomers is necessary to facilitate a coupling reaction for producing multiblock copolymers. SQS100 hydrophilic blocks were end-capped with DFBP to produce a fluorine-terminated end group functionality (Figure 2-4). The end-capping reagents were used in a 200% molar excess. A typical copolymerization for end-capping the SQS100 oligomers was conducted as follows: Hydrophilic oligomer SQS100, having molecular weight of 7000 kg/mol (7.591 g, 0.973 mmol), and DMSO (40 mL) were charged to a three-necked round bottom flask. The mixture was stirred until dissolved, then K_2CO_3 (0.538 g, 3.89

mmol) and cyclohexane (20 mL) were added. The system was dehydrated at 110°C for 6 h, then the reaction bath was cooled to 105°C and DFBP (1.951 g, 5.839 mmol) was added. The reaction was allowed to proceed at 105°C for 48 h. The product was filtered to remove the salt and precipitated in isopropanol, and then dried under vacuum at 60°C for 12 hours before use. ^{1}H NMR was performed to confirm successful end-capping.

2.3.4. Synthesis of ESQS100-BPS Hydrophobic-Hydrophilic Multiblock Copolymers

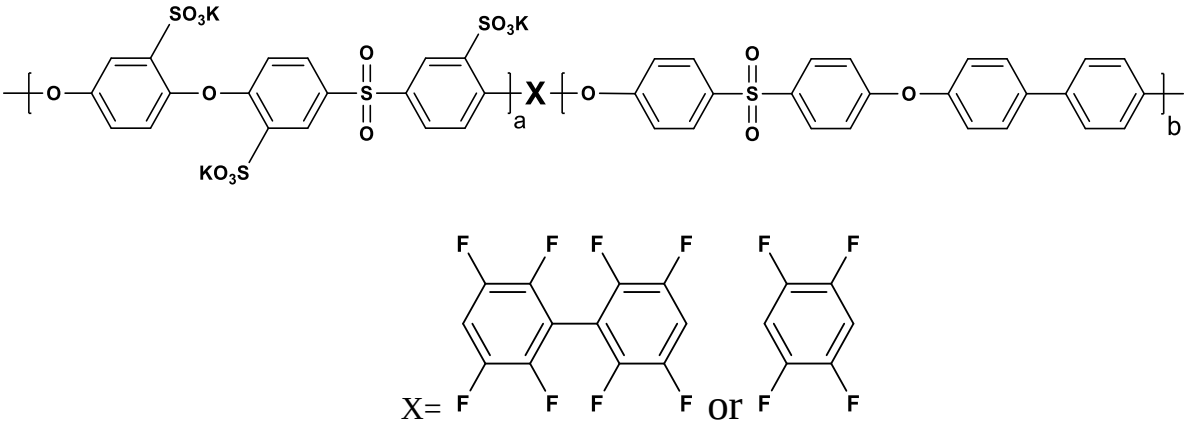

Figure 2.5: ESQS100-BPS Hydrophilic-Hydrophobic Multiblock Copolymers.

Similar, to the procedure of the end-capping reaction, the polymerization of the ESQS100-BPS copolymer took place as follows: the end-capped SQS100 (6.812 g, 0.806 mmol) and DMSO (50 mL) were charged to a three-necked round bottom flask and mixture was stirred till it dissolved completely, then K_2CO_3 (0.446 g, 3.23 mmol) and cyclohexane (25 mL) were added. The system was dehydrated at 110°C for 6 h, and then was cooled to 105°C, and BPS hydrophobic oligomer (5.6443 g, 0.806 mmol) was added. The polymerization was allowed to proceed at 105°C for 24 h then increased to 115°C and reacted for further 24 h. The reaction mixture was then precipitated into isopropanol to obtain a fibrous polymer. The product was washed twice in

deionized water at 60°C to remove salt, then washed twice in acetone and dried to give the polymer fibers.

2.4. Characterization

2.4.1. Nuclear Magnetic resonance (NMR) Spectroscopy

^{1}H and ^{19}F Nuclear Magnetic Resonance (NMR) analysis were conducted on a Varian Unity 400 to obtain the chemical composition of the monomers and polymers. The spectra of SQS100 & BPS oligomers and SQS100-BPS multiblock copolymers were obtained from a DMSO-*d*6 solution (10% w/v) at room temperature. ^{1}H and ^{19}F spectra were referred to tetramethylsilane (TMS) at 0 ppm.

2.4.2. Intrinsic Viscosity Determinations ([η])

The molecular weight analysis and the intrinsic viscosities of the non-sulfonated hydrophobic oligomers were obtained from Agilent 1260 Infinity Multi-Detector SEC with NMP containing 0.05 M LiBr as the mobile phase (60 °C), with 3 PLgel 10 μm mixed-B 300 × 7.5 mm columns in series and a Viscostar II Viscometer. The measurements of intrinsic viscosity of sulfonated hydrophilic poly(arylene ether sulfone)s oligomers and block copolymers were performed using a Cannon- Ubbelohde viscometer, thermostatically controlled in a water bath at 25°C in 0.05M LiBr in NMP solution. Intrinsic viscosities were utilized to obtain information about the size of a molecule in solution and also to obtain a qualitative description of the molecular weights. Intrinsic viscosities were very important because the GPC could not be used for

sulfonated copolymers as the ionic groups present in the block copolymer associate with the chromatographic column, which leads to error in results.[9]

2.4.3. Thermogravimetric Analysis (TGA)

TGA was performed on a TA instrument TGA Q500 in a nitrogen environment to assess the thermal stability of the trisulfonated multiblock poly(arylene ether sulfone) copolymer. The samples were heated at a rate of 10°C/min from 40°C to 700°C. Weight loss was measured in percentage and reported as a function of temperature. The thermal stability of the polymers was reported at the temperature where a weight loss of 5% was observed.

2.4.4. Differential Scanning Calorimetry (DSC)

DSC was used to observe the thermal transition temperatures of the synthesized multiblock copolymers. A TA Instruments DSC Q-1000 was utilized for the DSC. The powder form of the polymer was usually used to provide a suitable sample size (~5 - 10mg). The samples underwent heating and cooling cycles at a rate of 10°C/min from 40°C to 400°C under a nitrogen atmosphere. The onset of the thermal transition during the second heat was used to report the glass transition temperature (T_g).

2.4.5. Potentiometric Titration

Aqueous potentiometric titrations were used to determine the Ion Exchange Capacity (IEC) of the tri-sulfonated multiblock copolymer. From the potentiometric titrations, the milliequivalence (meq) of sulfonic acid groups in sulfonated poly(arylene ether sulfone)s was determined. The IEC

for a polymer is defined as the milliequivalents of reactive $-SO_3H$ sites per gram of polymer and have units of meq/g. The IEC value calculated from the titration was compared to the theoretical IEC value which was based on the amount of the tri-sulfonated oligomers charged in the reaction flask. Potentiometric titrations were performed using a Schott TitroLine alpha^{plus} (TA20) Automatic Titrator.

A typical sulfonated poly(arylene ether sulfone) titration is conducted as follows:

The copolymers were acidified and dried at ~120 ^oC before being weighed (~1gm) and 20 ml of 0.1N aqueous sodium sulphate (Na_2SO_4) solution was added to the copolymer. The solution was equilibrated for 2 days and then was titrated against sodium hydroxide (NaOH) solution (~ 0.02 N). The NaOH solution was standardized against a 0.01N HCl solution immediately before titrating. The end-point was detected as the maximum of the first derivative for the potential versus the used volume of titrant. The average of end points of three titrated samples was then used to calculate the IEC (meq/g) of the sulfonated membrane.

2.4.6. Film Preparation

The film preparation procedure is as follows:

The dried polymer in the salt form was dissolved in DMSO to form a solution with 5 – 15% (w/v) concentration. The variation in concentration allowed some control over the thickness of the films formed. The polymer solution was filtered using a disposable syringe and 0.45µm Teflon disc filters to remove dirt and particulates, followed by sonication to remove air bubbles inside the solution. This polymer solution was uniformly cast on a clean and dry glass substrate and dried under an infrared lamp at 60^oC for 12 hours. After drying, the films were annealed at 220^oC for six hours in a vacuum oven. These films were immersed in deionized water to separate them from the

glass substrate and then dried to remove the moisture. The salt form membrane ($SO_3^-M^+$) was converted to its acid form (SO_3H) by boiling in 0.1M aqueous sulfuric acid solution for 2 h, and was then boiled in deionized water for 2 h. The membrane was then stored in deionized water until it was used for measurements.

2.4.7. Atomic Force Microcopy:

Tapping mode atomic force microscopy (AFM) characterization images were taken using Digital Instruments Dimension 3000 with a microfabricated cantilever. A Veeco silicon probe with an end radius of <10 nm was used to image samples. The force constant was 40 N/m. The acidic form of the copolymer was used as sample and the copolymer film was equilibriated at 40% relative humidity and 30^{o}C for 12 h before imaging.

2.4.8. Characterization of Fuel Cell Related Properties

2.4.8.1 Proton Conductivity

Proton conductivity at 30^{o}C in liquid water was determined using a window cell geometry shown in figure 2.6, with a Solartron (1252 + 1287) Impedance/Gain-Phase Analyzer over the frequency range of 10 Hz to 1 MHz following procedures reported in the literature.[54] In determining proton conductivity in liquid water, membranes were equilibrated at 30^{o}C in DI water for 24 h prior to testing. For determining proton conductivity under partially hydrated conditions, membranes were equilibrated in a humidity-temperature oven (ESPEC, SH-240) at the specified RH and 80^{o}C for 24 h before measurement. An equilibration time of 45 min was allowed in between measurements. The resistance of the film was taken at the frequency which produced the

minimum imaginary response. All impedance measurements were performed at room temperature under full hydration conditions. The proton conductivity is the reciprocal of the resistance and reported in units of Siemens per centimeter (S/cm).

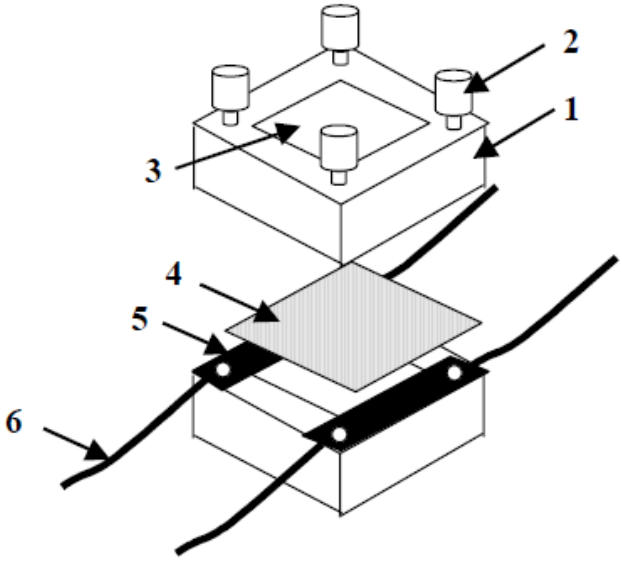

Legend
1. Teflon block
2. Thumbscrew
3. Open area to allow equilibration with environment
4. Membrane sample
5. Blackened Pt foil electrode
6. Pt lead

Figure 2.6: Schematic of a conductivity cell. [54]

2.4.8.2. Water Uptake

The water uptake of all membranes was determined gravimetrically. First, the membranes were equilibrated in DI water at 30°C for 2 days after acidification. Wet membranes were removed from the liquid water, blotted dry to remove surface droplets, and quickly weighed. The membranes were then dried at 120°C under vacuum for at least 24 h and weighed again. The water uptake of the membranes was calculated according to Equation 2.1 where $mass_{dry}$ and $mass_{wet}$ refer to the mass of the dry membrane and the wet membrane, respectively.[54]

$$\text{water uptake} = \frac{\text{mass}_{\text{wet}} - \text{mass}_{\text{dry}}}{\text{mass}_{\text{dry}}} \times 100$$

2.5 Results and Discussion

2.5.1. Synthesis and characterization

2.5.1.1. Synthesis of Hydrophobic Oligomer (BPS)

The hydrophobic oligomers were synthesized using a step-growth polycondensation process. The synthetic scheme for the synthesis of BPS oligomers is shown in Figure 2.7. The desired molecular weights were achieved by off-setting the monomer ratio by using the Carothers equation. Phenoxide terminated oligomers were obtained by using biphenol in order to control the molecular weight. ^{1}H NMR was used to determine the number-average molecular weights (Mn) of the hydrophobic oligomers by using end-group analysis. From the spectra of the BPS, the phenoxide end-groups were determined by the presence of the small peaks at 7.61, 7.34 and 6.81 ppm, while the peaks at 7.92, 7.69, 7.18, and 7.12 ppm were assigned to the protons on the backbone of the main chain as shown in Figure 2.8. By finding the ratio of the integration values between the end-groups and the main chain protons, the number average molecular weight was determined. Molecular weights ranging from 4 to 15 kg/mol were obtained for all of the oligomers. The calculated and experimental molecular weights for the oligomers, as well as intrinsic viscosity values (IV), are listed in Table 2.1. Figure 2.9 shows the plot of ln η as a function of ln M_n.

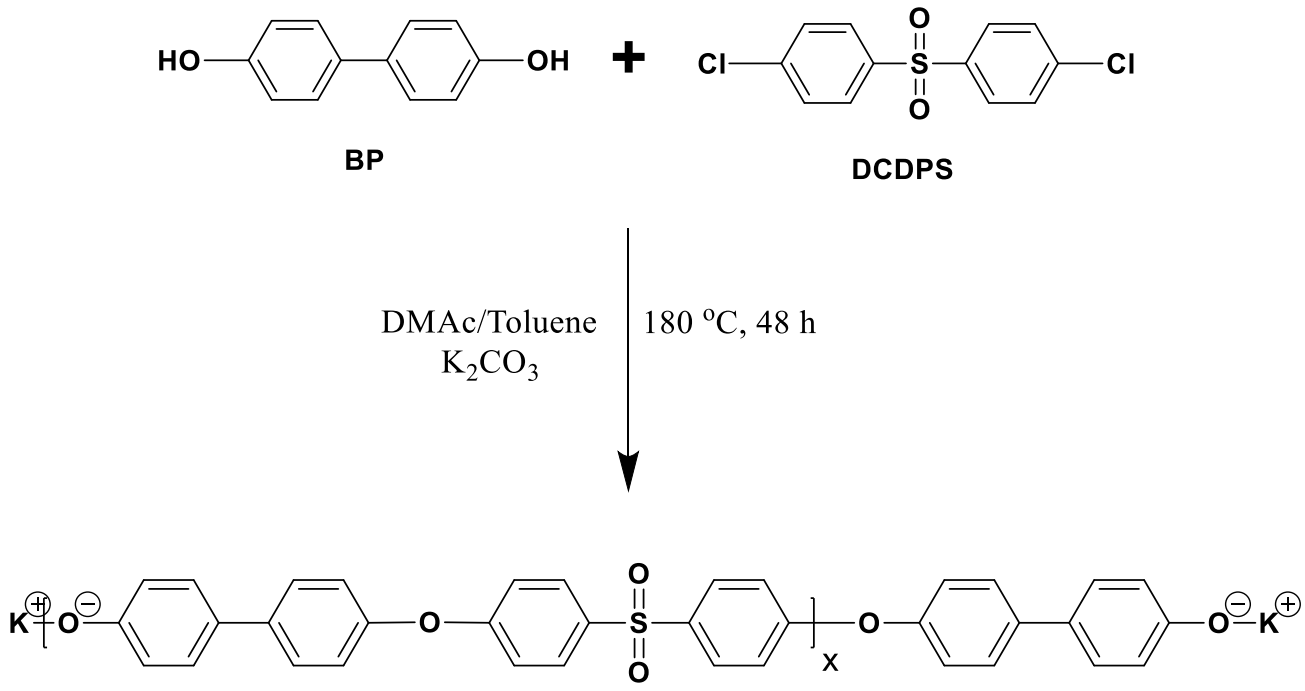

Figure 2.7: Schematic of BPS oligomer synthesis.

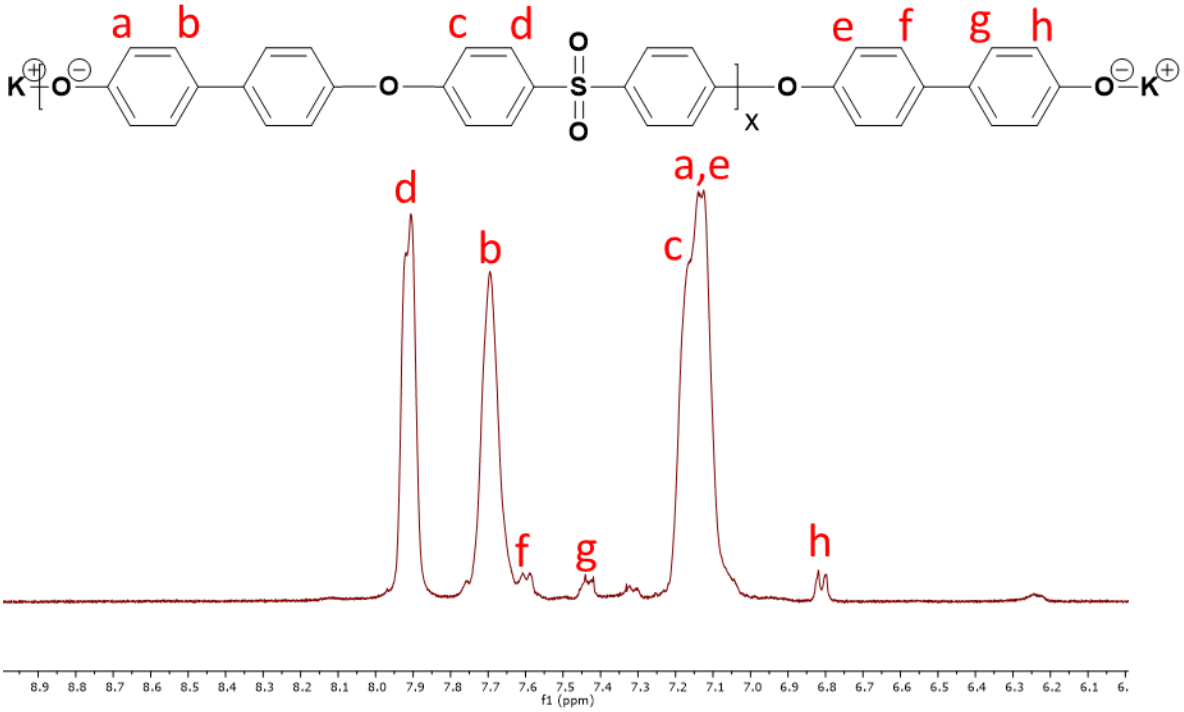

Figure 2.8: ^{1}H NMR spectrum of a BPS oligomer

Table 2.1: Molecular weight characterization of BPS oligomers

Target M_n (g/mol)	**M_n from ^{1}H NMR (g/mol)**	**M_n from GPC[a] (g/mol)**	**Intrinsic Viscosity[a] (dL/g)**
5K	4.9K	4.8K	0.072
7K	7.1K	6.9K	0.092
10K	10.05K	9.8K	0.117
13K	13.02K	13.2K	0.157

a: Measured by SEC with 0.05M LiBr/NMP as mobile phase at 60ºC

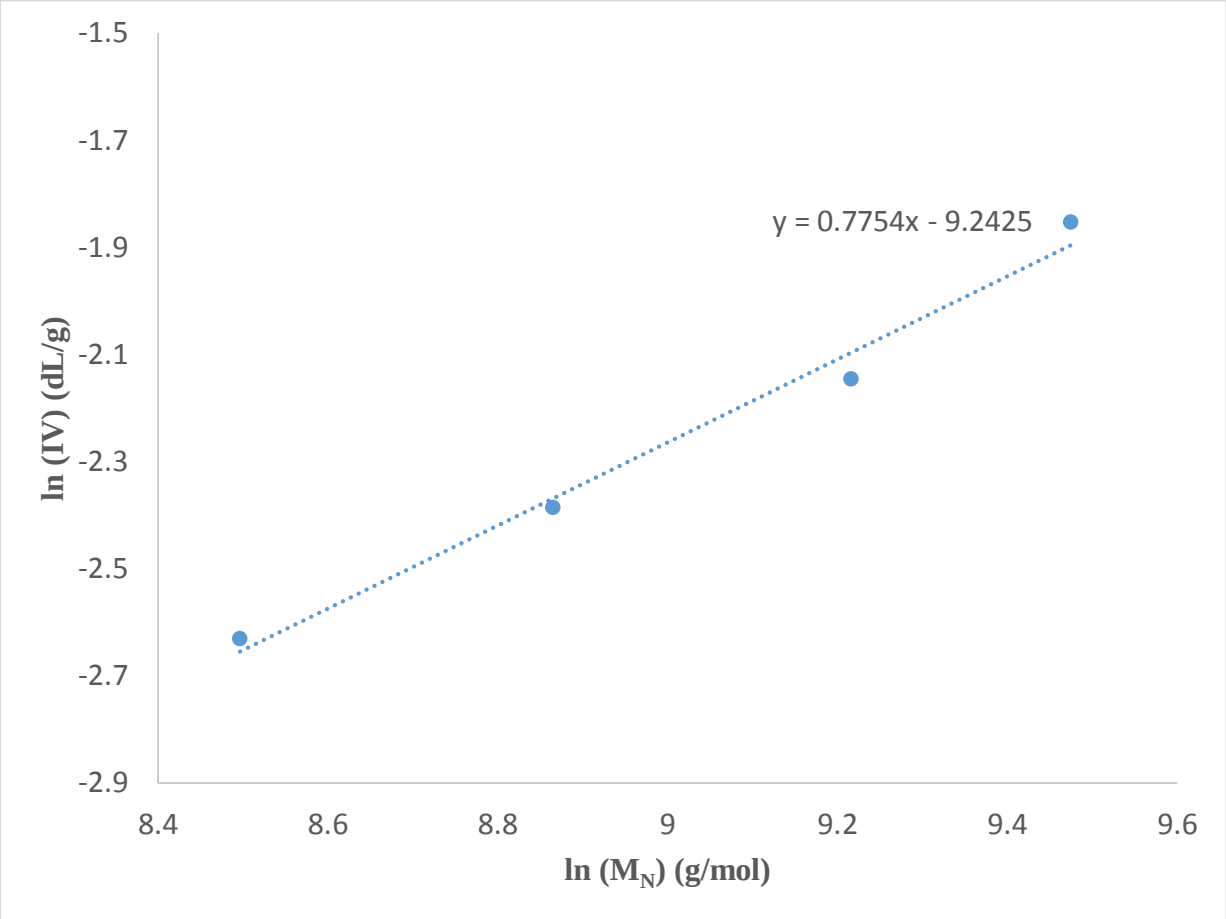

Figure 2.9: ln η vs. ln M_n plot for BPS oligomers

2.5.1.2. Synthesis of fully trisulfonated hydrophilic oligomers (SQS100)

As in the synthesis of disulfonated BPSH-xx random copolymers, the direct polymerization of the sulfonated monomer, SDCDPS, was also used in the synthesis of the fully trisulfonated oligomers. Sulfonated hydroquinone (SHQ) was polymerized with SDCDPS as shown in Figure 2.10. Excess SHQ was used to control the molecular weight in order to produce phenoxide-terminated oligomers.

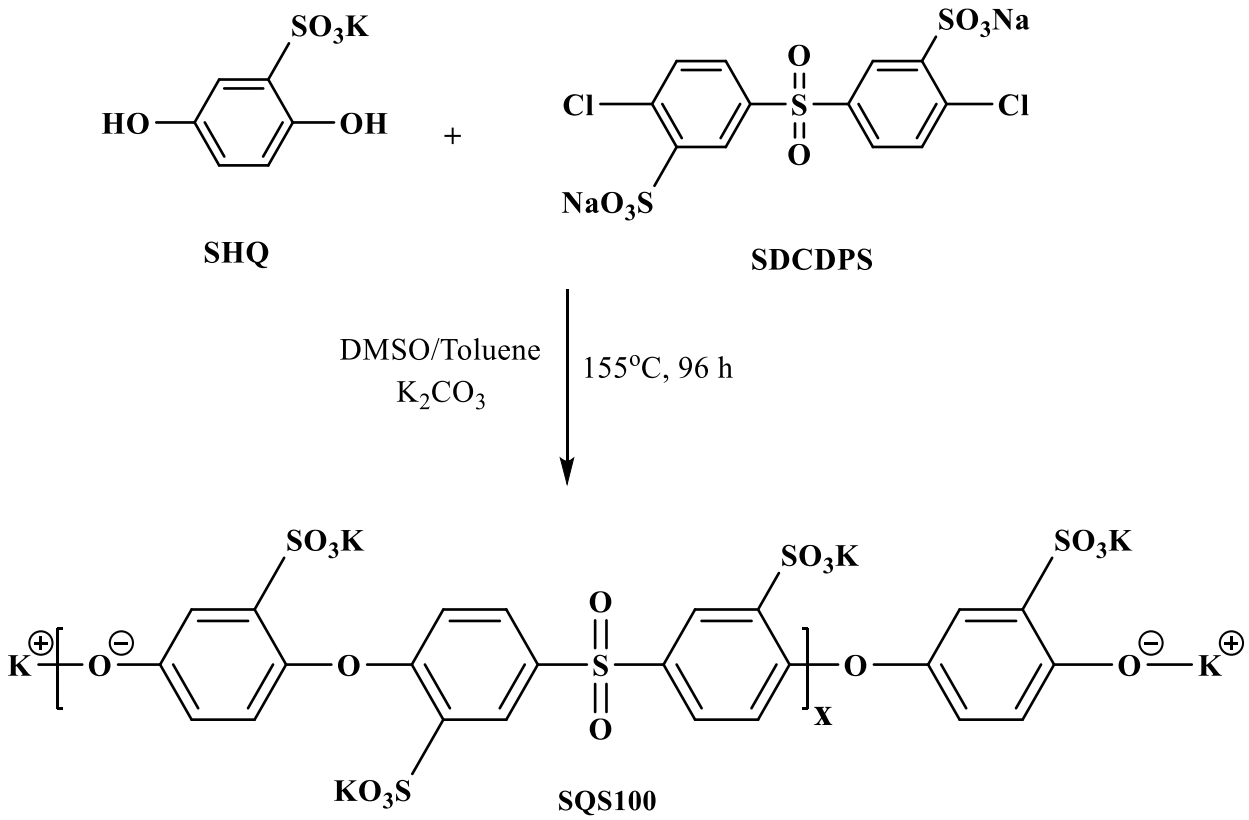

Figure 2.10: Synthesis of fully trisulfonated SQS-100 oligomers

The ^{1}H NMR spectrum of an oligomer is shown in Figure 2.11. To estimate the experimental M_n using the proton spectra, the ratio of the integral of the small peaks at 6.76, 6.70, and 6.46 ppm were attributed to the phenoxide end-groups and the main chain proton peaks at 8.27, 7.86, 7.40, 7.11, and 6.94 ppm. The calculated and experimental molecular weights for the oligomers, as well as intrinsic viscosity values (IV), are listed in Table 2.2. Figure 2.12 shows the plot of ln η as a function of ln M_n.

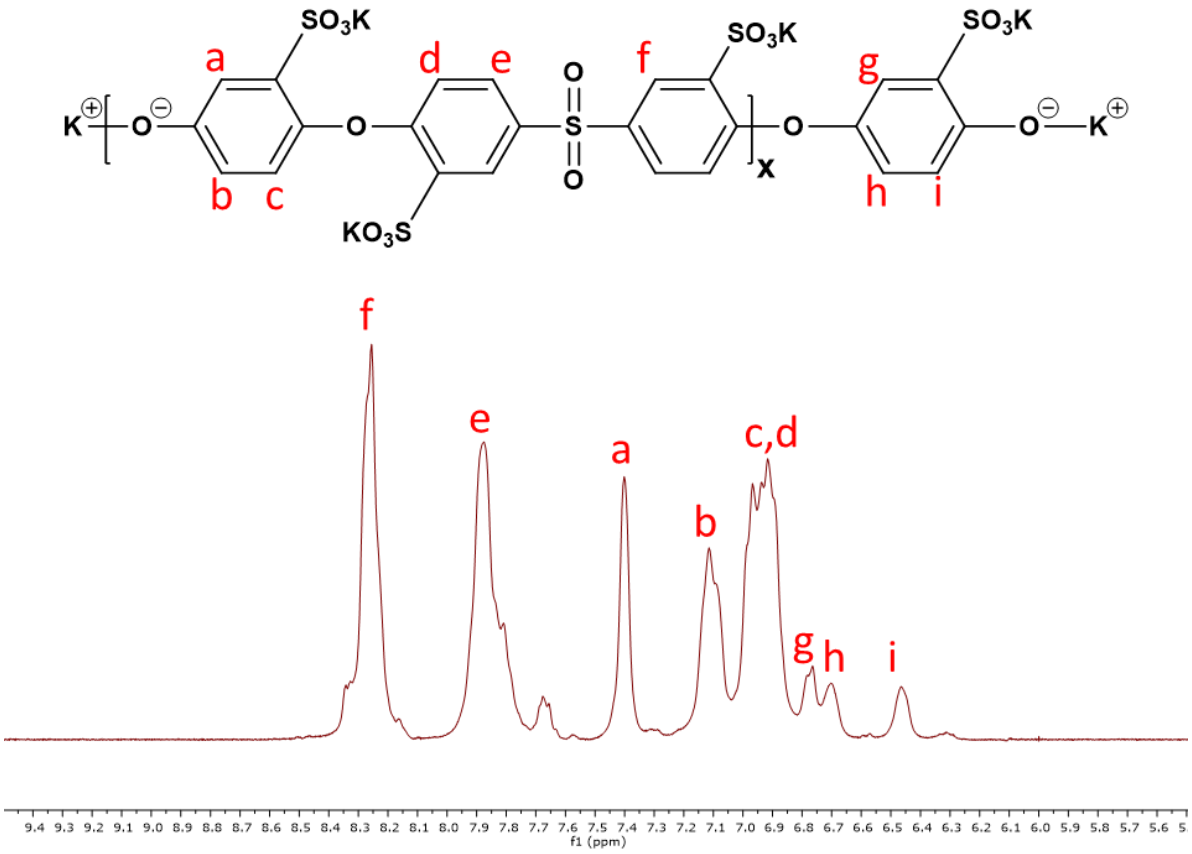

Figure 2.11: ^{1}H NMR spectrum of a SQS-100 oligomer.

Table 2.2: Molecular weight characterizations of SQS100 oligomers

Target M_n (g/mol	**M_n from ^{1}H NMR (g/mol)**	**Intrinsic Viscosity[a] (dL/g)**
7K	6.9K	0.09
8K	8.2K	0.12
9K	9.2K	0.14
10K	9.7K	0.15

a: Measured with 0.05M LiBr/NMP solution at 25^{o}C

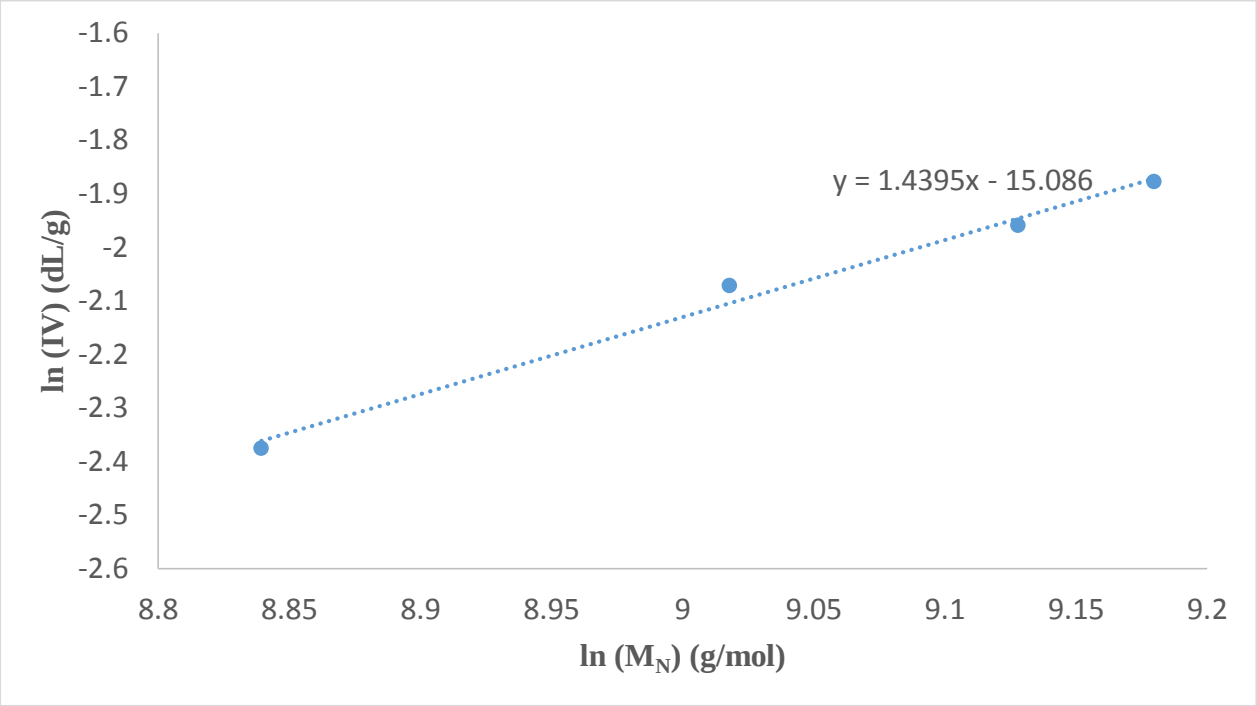

Figure 2.12: ln η vs. ln Mn plot for SQS100 oligomers

2.5.1.3. Synthesis and characterization of DFBP end-capped SQS100 oligomers

The BPS and SQS100 oligomers both possessed the same phenoxide telechelic functionality and therefore it was necessary to modify one of the oligomers to the activated halide functionality in order to produce the final multiblock copolymer. Phenoxide-terminated SQS100 oligomers were end-capped with DFPB to achieve highly reactive fluorine-terminated ESQS100, as shown in Figure 2.13. A large molar excess (6 times the amount of SQS100) of DFBP was added to minimize the inter-oligomer coupling reaction of SQS100 oligomers. Due to the high reactivity of DFBP, a mild reaction temperature (105 °C) and relatively short reaction time (~48 h) were sufficient to get the fluorine-terminated SQS100. The measurement of the M_n of the SQS100 oligomers was very important for the synthesis of multiblock copolymers with proper block lengths (X_n) and IECs. Analysis of a ^1H NMR spectrum shown in Figure 2.14 was utilized to

confirm the completion of the end-capping reaction. On the ^{1}H NMR spectra of the end-capped oligomers, the disappearance of the phenoxide peaks confirmed that all of the phenoxide groups reacted with the end-capping reagents.

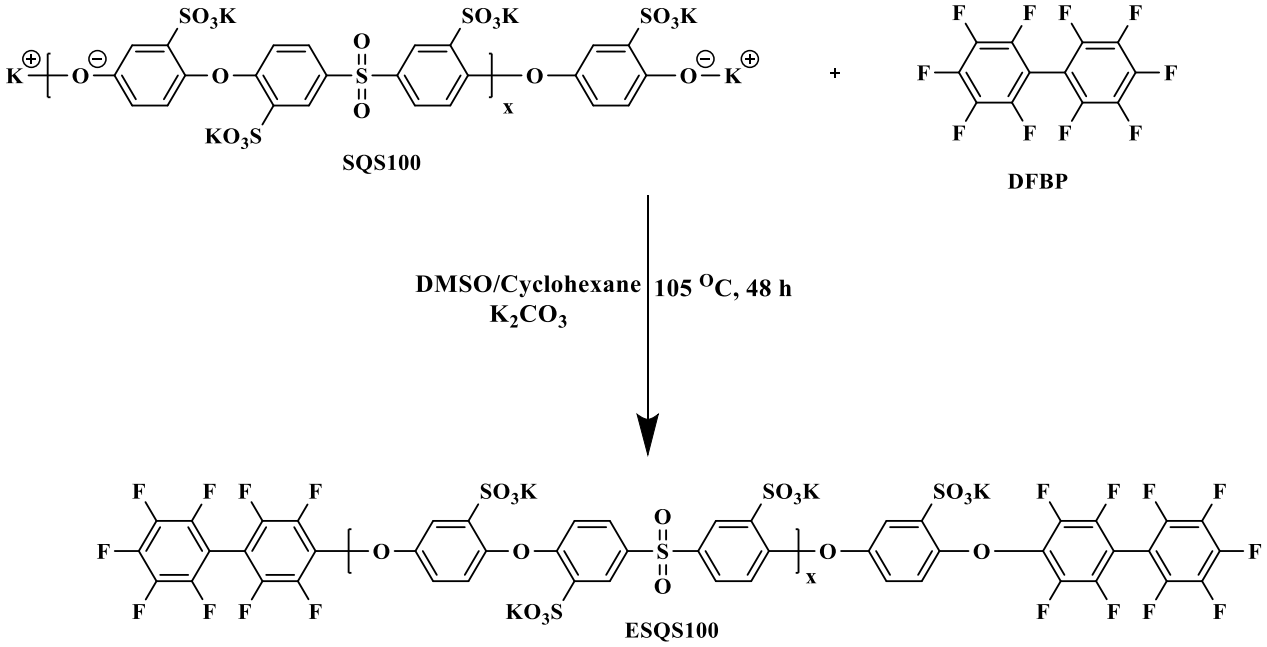

Figure 2.13: Schematic of endcapping of SQS100 oligomers.

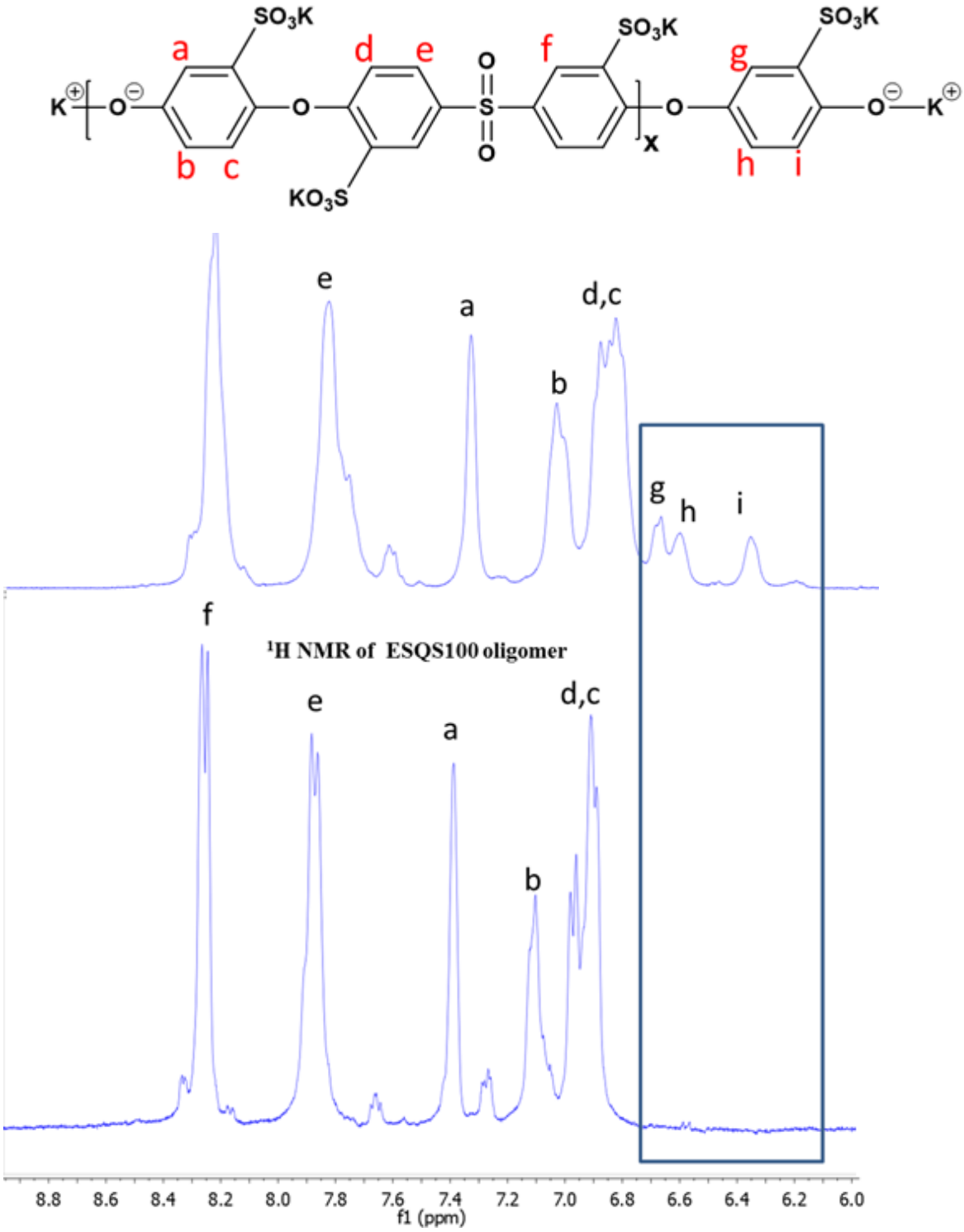

Figure 2.14: ^{1}H NMR of endcapped SQS oligomer.

2.5.1.4. Synthesis of Multiblock Copolymers

A series of amorphous hydrophobic–hydrophilic multiblock copolymers was synthesized via the coupling reaction between phenoxide-terminated BPS and DFBP end-capped SQS100 oligomers. The synthesis of ESQS100-BPS multiblock copolymers is shown in Figure 2.15.

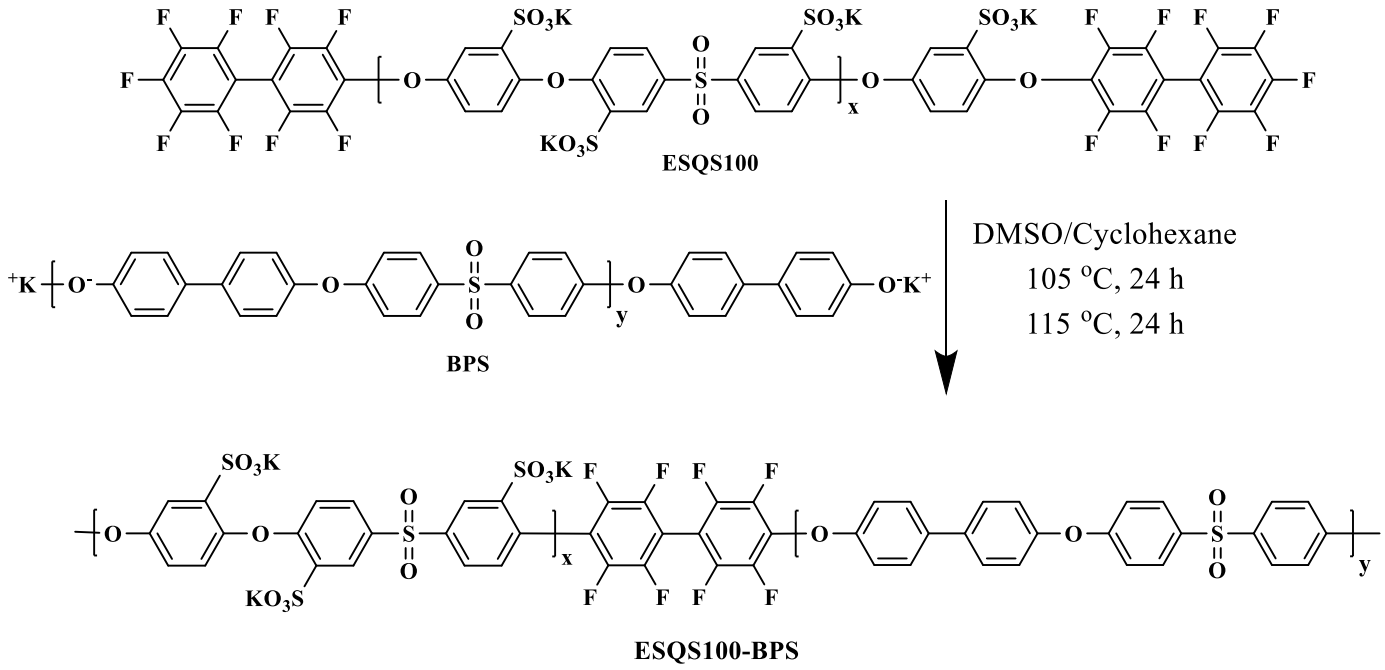

Figure 2.15: Synthesis of ESQS100-BPS multiblock copolymer

The viscosity of the reaction solution increased slowly during the polymerization. In general, the reactions were deemed to be complete and generally stopped 6 hours after the viscosity became constant. It should be noted that reactions tended to proceed more slowly for higher molecular weight oligomers, ranging from 24 h for BPS-SQS100 (3K:3K) to 48 h for BPS-SQS100 (10K:10K). These longer reaction times might have resulted from the differences in solubility of the hydrophobic and hydrophilic oligomers in DMSO. Specifically, we speculate that

the solubility differences might have led to partial phase separation, causing the chain-ends to migrate to the hydrophobic-hydrophilic interfaces in order to meet and react with each other. Nevertheless, the isolated products were completely soluble in DMSO without any gelation observed. Thus, the reactions were thought to have resulted in linear copolymers.

2.5.1.5. Fundamental characterizations of ESQS100- BPS multiblock copolymers

A ^{1}H NMR spectrum for a ESQS100-BPS (7K:7K) copolymer is shown in Figure 2.16. The integration of the peaks attributed to hydrophilic and hydrophobic moieties were utilized to calculate the experimental IEC values of the materials.

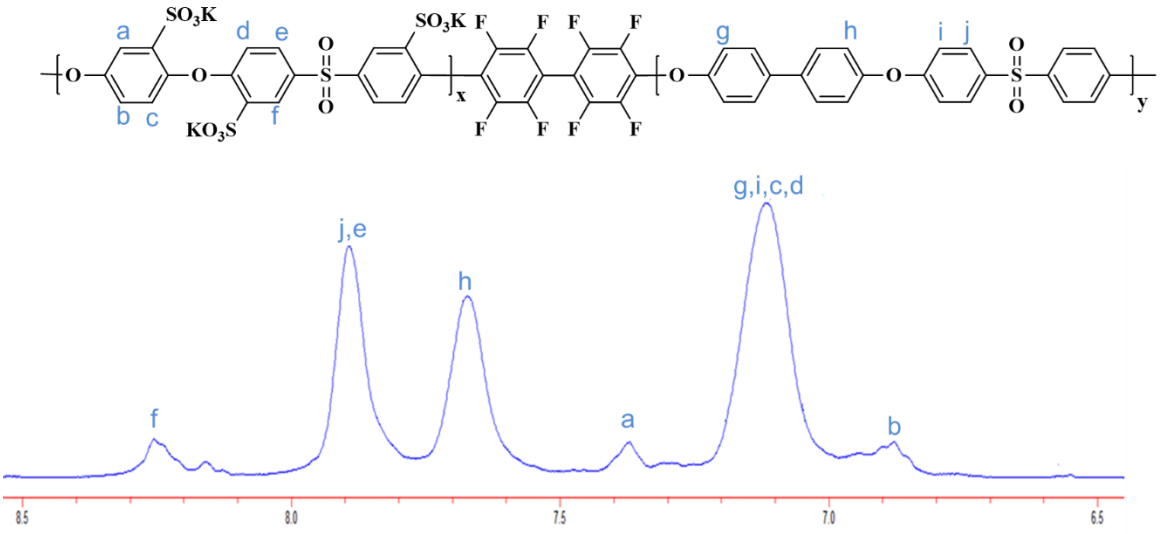

Figure 2.16: ^{1}H NMR spectrum of a ESQS100-BPS multiblock copolymer

Characterization data for a series of the multiblock copolymers are listed in Table 2.3. The copolymers may have different IEC values due to slight differences in the molar charge ratios for the hydrophilic:hydrophobic oligomers. The polymerization yielded multiblock copolymers with

high intrinsic viscosities that were cast into tough, ductile membranes. Unfortunately, due to the association of the multiblock copolymer with the GPC columns, the gel permeation chromatograph (GPC) could not be utilized to determine the molecular weight. Hence, intrinsic viscosity data were required to gain a qualitative measurement of molecular weight.

Table 2.3: Some characterizations of ESQS100-BPSH multiblock copolymers

Copolymer	Block Lengths[a] (g/mol)	Molar Feed Ratio[b]	IEC[c]	Intrinsic Viscosity (dL/g)[d]
ESQS100-BPSH-1	5000:5000	1 : 1.12	1.90	0.69
ESQS100-BPSH-2*	7000:7000	1 : 1.05	1.95	0.86
ESQS100-BPSH-3*	10000:10000	1 : 1	1.84	1.13

a) Block lengths are expressed in the form hydrophilic:hydrophobic

b) Molar ratios are expressed in the form hydrophilic:hydrophobic

c) Measured from titration with 0.02N NaOH solution.

d) Measured at 25^{o}C in DMSO with 0.05M LiBr solution

* : Samples Prepared by Dr.Kwan-Soo Lee

Figure 2.17 shows the DSC trace of a ESQS100-BPS multiblock copolymer. Only one transition was observed around 245^{o}C. The presence of only one T_g is seen in this block ionomer because the molecular motion tends to be hindered by electrostatic interactions among ionic

groups. Dual T_gs are only occasionally seen in block ionomers probably with increased phase separation, i.e. the higher χ parameter caused by the larger differences in their hydrophobicity.[113]

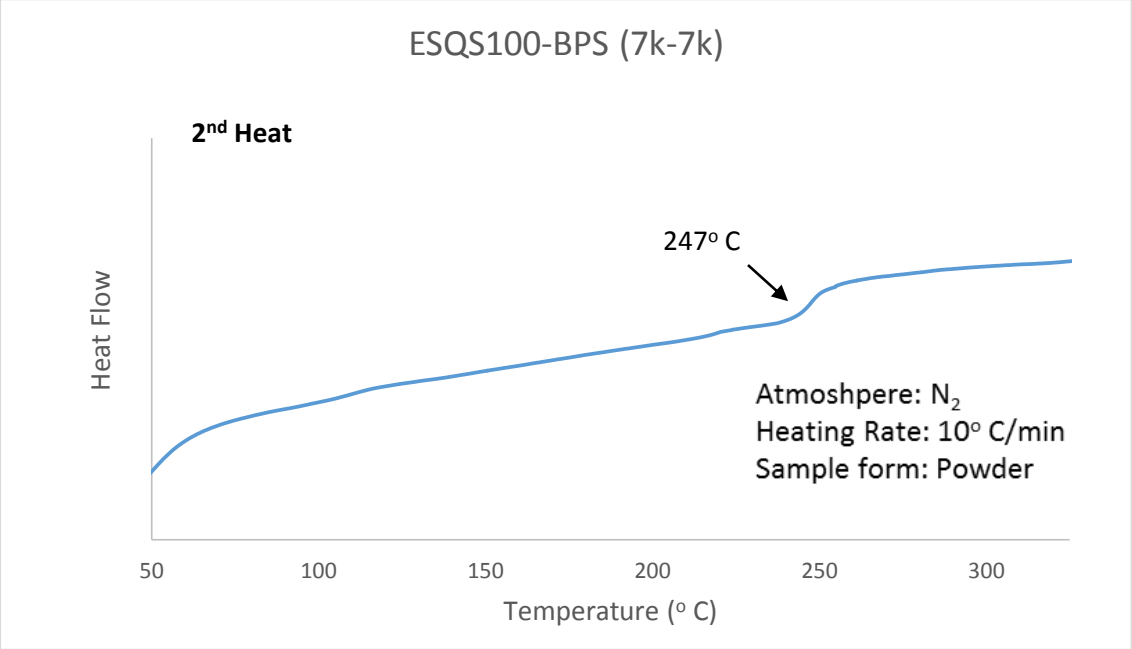

Figure 2.17: DSC trace of a ESQS100-BPSH (10K:10K) multiblock copolymer

Thermogravimetric analysis was used to investigate the thermal stability of the tri-sulfonated poly(arylene sulfone) multiblock copolymers as a function of weight loss. Initially, the sulfonated sample was pre-heated at 150°C for 30 minutes in a TGA furnace to rid the sample from trace solvent and moisture. Then dynamic TGA experiments were conducted from 40 to 700°C, at a heating rate of 10°C/min under nitrogen. The TGA traces of ESQS100-BPS (7K-7K) copolymer is shown in Figure 2.18. The copolymers displayed a distinct two-step degradation. The first weight loss temperature occurred around 280°C, which was attributed to the loss of the sulfonate group. The second weight loss was attributed to the degradation of the polymer backbone, which occurred around 490°C.

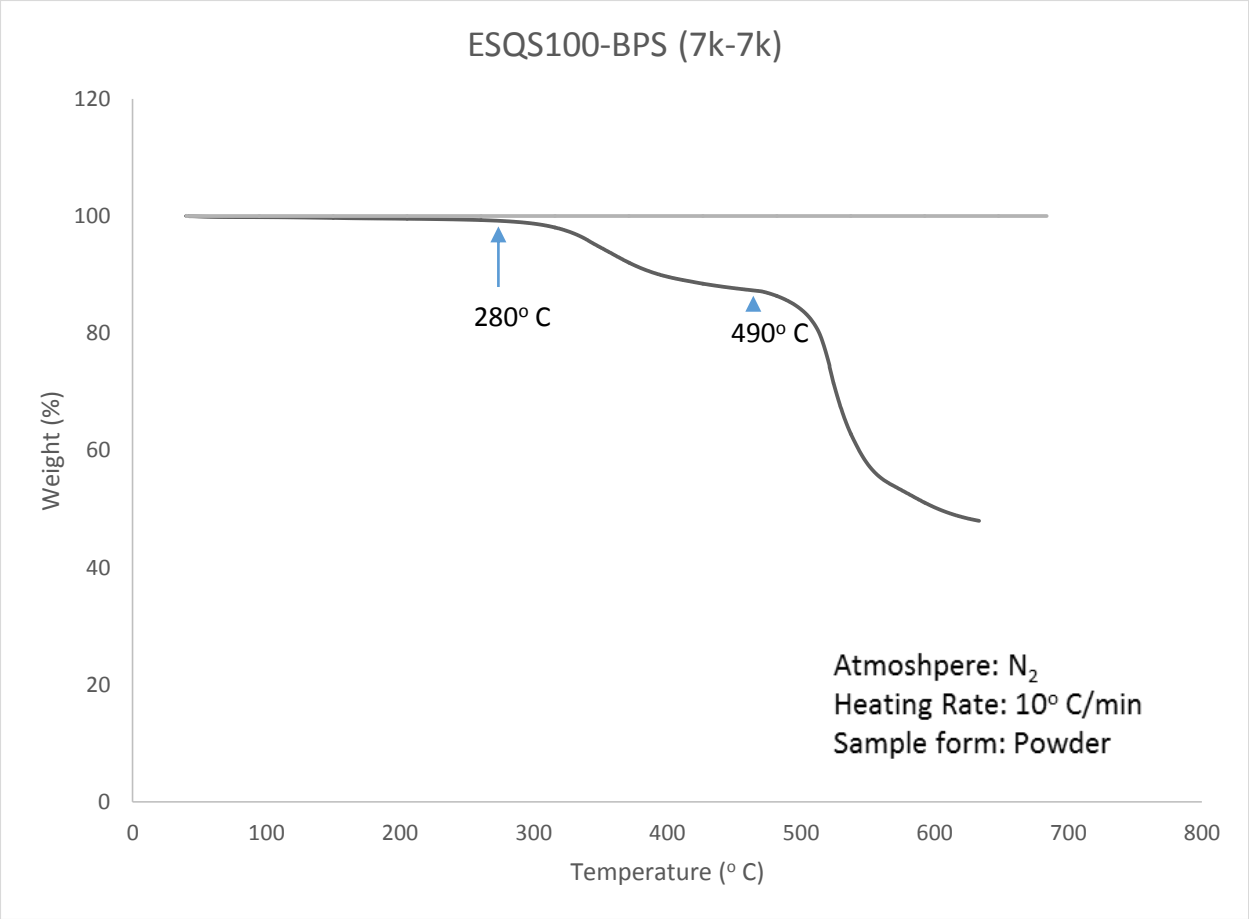

Figure 2.18: TGA traces of ESQS100-BPSH (7K-7K) multiblock copolymers

2.5.1.6. Surface morphological features

Atomic force microscopy images of the tri-sulfonated poly(arylene ether sulfone) block copolymers were reported to examine the ionic clustering under ambient conditions. Before the images were recorded, the sulfonated copolymers were thoroughly dried under vacuum to remove water and trace solvents from the film. In the AFM images, distinct dark and bright phases/regions were observed for the multiblock copolymers. The dark regions are associated to the hydrophilic

phase consisting of the softer pendant sulfonic acid groups (which contain some water), while the bright regions are due to the hydrophobic component. These dark domains are results of the dampening effects in the hydrated ionic groups in the copolymer. The tapping-mode atomic force micrographs of ESQS100-BPS multiblock copolymers, with increasing block lengths, are shown in Figure 2.19. From the phase images it can be seen that, with an increase in block length, the nanophase separation between hydrophobic and hydrophilic domains becomes sharper and, moreover, the hydrophilic domains tend to become increasingly connected.

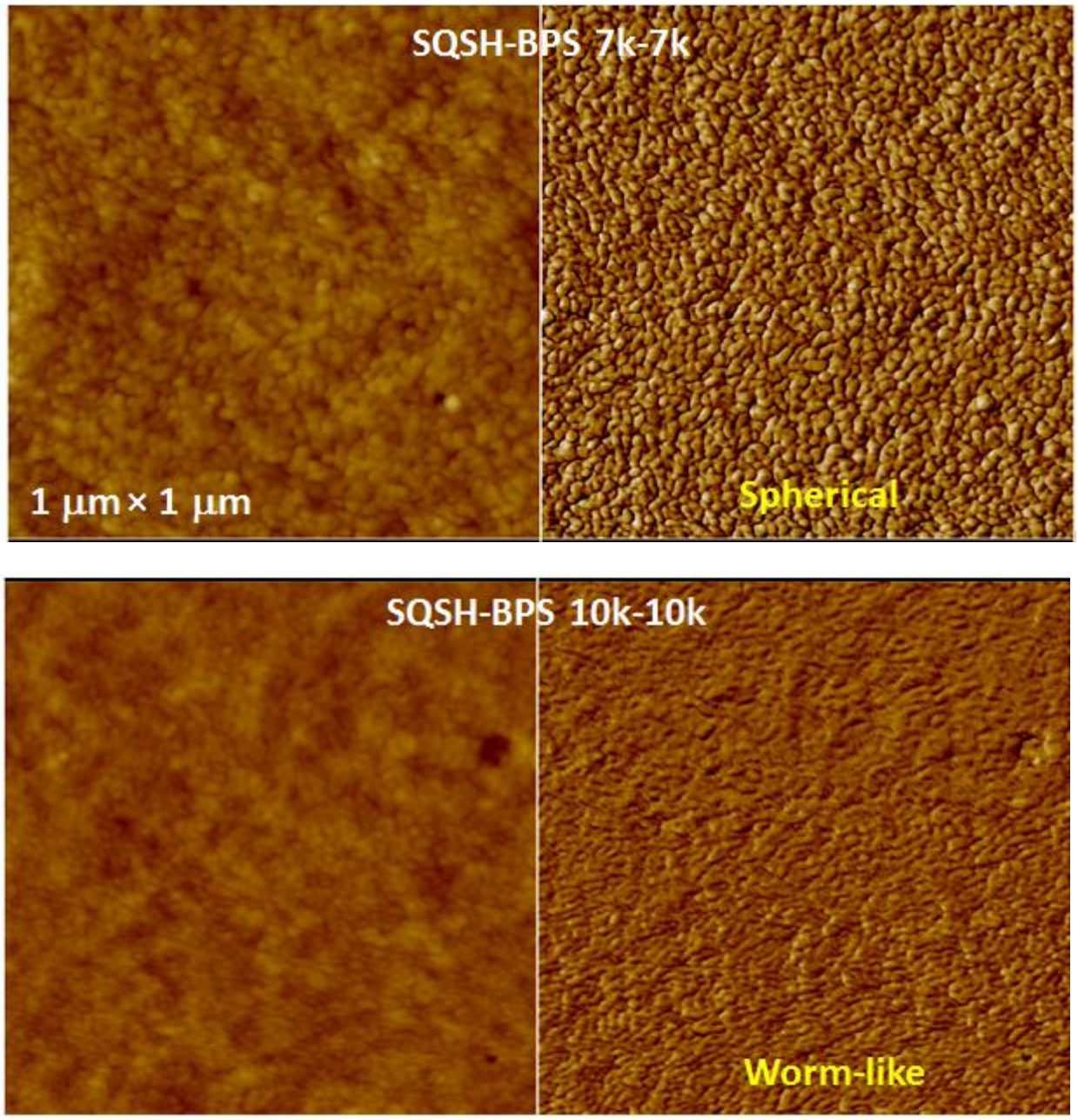

Figure 2.19: Tapping mode AFM height (left) and phase (right) images for ESQS100-BPS (7K-7K), (10K-10K) multiblock copolymer membranes.

Thus, this study demonstrated that the morphological features of these copolymers can be controlled by synthesis.

2.5.2. Fuel Cell Related Characterizations of Multiblock Copolymers

2.5.2.1. Proton conductivity under fully hydrated conditions

The conductivity in a material is dependent upon the charge carrier density and the charge carrier mobility. In case of PEMs, the charge carrier is the proton, which is dependent upon the concentration of the pendent sulfonic acid groups along the polymer chain. Conditions for the measurement are also very important in determining the material conductivity.

Proton conductivities of the ESQSH100-BPS multiblock copolymer were performed at 30^{o}C under fully hydrated conditions using a Solatron 1260 Impedance instrument. The resistance, R, (ohm) of the copolymer membrane was measured and then the proton conductivity was determined by the equation:

$$\partial = \frac{l}{R * A}$$

Where:

∂ = conductivity (S/cm)

R = Resistance (ohms)

l = length between electrodes (cm)

A = cross-sectional area of film (cm^2)

The proton conductivity results are given in Table 2.4. In the table, the water uptake and proton conductivities of the ESQSH100-BPS multiblock copolymers are compared to those of several block copolymer series, as shown in Figure 2.20.

a)

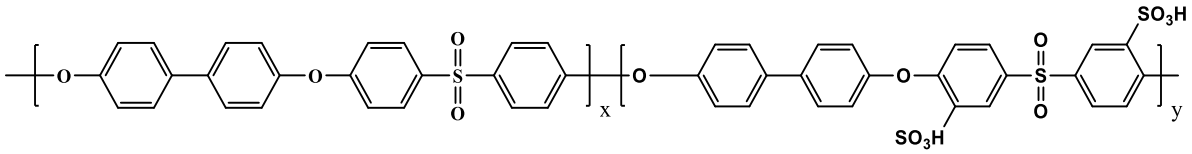

BPS-BPSH100

b)

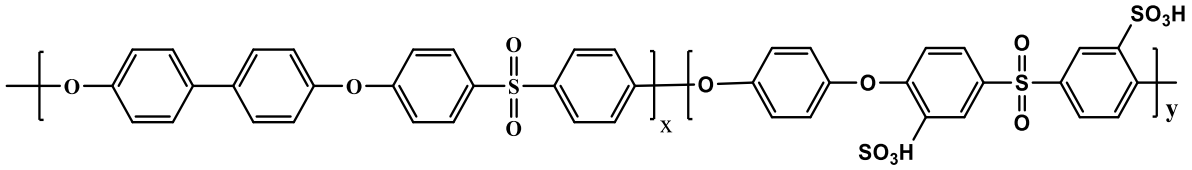

BPS-HQSH100

Figure 2.20: Structures of partially disulfonated block copolymers. (a) BPSH; (b) HQSH.

In the McGrath group, we have previously conducted studies which show that proton conductivity of the disulfonated block copolymer membranes under fully hydrated conditions is a linear function of Ion Exchange Capacity.[23] A similar trend is also observed for tri-sulfonated block copolymer, as shown in Table 2.4.[55, 114] The increase in IEC can be explained due to the increase in concentration of sulfonic acid groups and a corresponding increase in the water uptake. It should also be noted that under fully hydrated conditions, there does not seem to be a significant effect of block length on these properties.

Table 2.4: IEC, water uptake and proton conductivity for fully trisulfonated block copolymers

	IEC (meq/g)[a]	Water uptake (%)[b]	Proton Conductivity (S/cm)[c]
BPS-BPSH100			
5K-5K	1.55	52	0.09
10K-10K	1.57	79	0.10
15k-15k	1.66	79	0.09
BPS-HQSH100			
5K-10K	1.79	112	0.13
10K-10K	1.88	183	0.17
15k-15k	1.67	145	0.16
BPS-ESQSH100*			
5k-5k	1.90	44	0.13
7k-7k	1.95	49	0.14
10k-10k	1.84	38	0.12
Nafion 212	0.90	22	0.12

a: Measured by titration of the sulfonic acid groups with NaOH.

b: Measured in acid form

c: Measured in liquid water at 30^{o}C

*: Samples prepared by Dr. Kwan-Soo Lee

Thus, under fully hydrated conditions, the IEC of the membranes can give a good measure of the expected proton conductivity, regardless of the polymer morphology or the sequence length of sulfonic acid groups.

2.5.2.2. Proton conductivity under partially hydrated conditions

Under fully hydrated conditions, proton conductivity was dependent on IEC of a given membrane. Figure 2.21 shows proton conductivity as a function of relative humidity (RH) for ESQS100-BPS and Nafion 212. It can be seen that below 50% RH, the proton conductivity decreases significantly. However, the decrease in conductivity as RH decreases is less pronounced for the tri-sulfonated block copolymer. We attribute this to the chemical structure of the oligomers, which leads to strong nanophase separation between the hydrophilic and hydrophobic domains, as well as facilitating proton transport under low hydration levels.

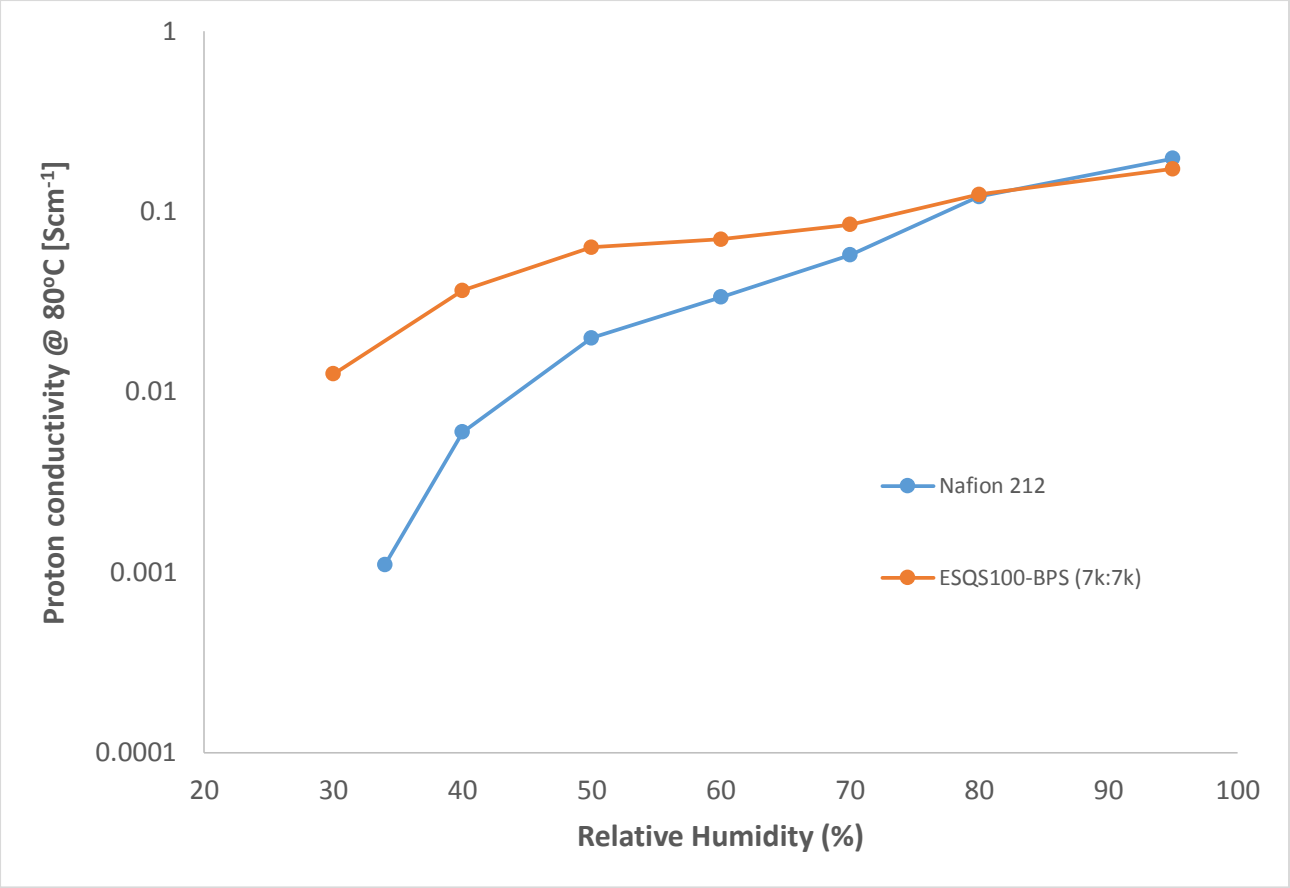

Figure 2.21: Proton conductivity vs. RH plots for Nafion 212, ESQSH100-BPSH block copolymer.

2.6. Conclusions

A series of multiblock copolymers was successfully synthesized from fully trisulfonated hydrophilic poly(arylene ether sulfone)s and biphenol based hydrophobic oligomers for potential application as proton exchange membranes. The copolymers synthesized possessed a variety of oligomer molecular weights with varying ratios of hydrophilic-hydrophobic content. The hydrophilic oligomers were end-capped using the highly reactive decafluorobiphenyl in order to facilitate successful coupling with the hydrophobic oligomer at relatively low temperatures (~105°

C) to avoid ether-ether interchange reactions. Tough ductile films were produced from these multiblock copolymers. Water uptake and proton conductivity under both fully and partially hydrated conditions were measured and compared with Nafion 212 and disulfonated multiblock copolymers. Atomic force microscopy images indicated the development of a nanophase separated morphology, which is one of the reasons for improved performance at low relative humidity.

Chapter 3 : Synthesis and Characterization of Multiblock Copolymers based on Hydrophilic Trisulfonated Poly(arylene ether sulfone) and Hydrophobic partially Fluorinated Poly(arylene ether benzonitrile) for use in Proton Exchange Membranes.

Novel multiblock copolymers were synthesized with a fully tri-sulfonated hydrophilic oligomer incorporating 3,3'-disulfonated-4,4'-dichlorodiphenyl sulfone and 2,5-dihydroxybenzenesulfonic acid potassium salt, and a hydrophobic oligomer consisting of 4,4'-(hexafluoroisopropylidene) diphenol and 2,6-dichlorobenzonitrile. The sulfonated hydroquinone comonomer was incorporated with the intent of forming a multiblock copolymer system with a higher IEC and increased concentration of sulfonic acid moieties. This was hypothesized to lead to improved proton conductivity performance at low RH conditions. Nitrile-activated aryl halide monomer is utilized as it is anticipated that for a fixed block length, there will be more components of 4,4'-(hexafluoroisopropylidene) diphenol, which would lead to increased hydrophobicity and the nitrile functional groups may afford hydrogen bonding sites, which would lead to increased adhesion to the electrode. Tough ductile films were produced from the block copolymers and properties like water uptake, proton conductivity under fully hydrated and partially hydrated conditions were explored. The copolymer showed enhanced conductivities under fully hydrated conditions when compared with Nafion and other fluorinated block copolymer systems (BPSH100-6FPAEB, HQSH100-6FPAEB). Morphological studies with AFM showed nanophase separation occurring with the long-range order developing at higher block lengths.

3.1 Introduction

A fuel cell is a highly efficient device that generates electricity in a single step through an electrochemical process along with production of environmentally benign byproducts (i.e. water).[1] The major developments in the area of polymer electrolyte membrane fuel cells (PEMFC's) as potential energy alternative to hydrocarbon non-renewable energy have been going on since the 1960s, with the first major application in the spacecraft's for the Apollo and Gemini missions. They were used to provide both power and clean drinking water for the astronomers.[4, 7] PEMFCs have the potential to be used as a power generation system in many applications, such as vehicles, stationary power generation and also in portable electronic devices.

Generally, the fuel cells consist of highly active metal catalysts; fuels like hydrogen and methanol, which react to produce radicals at the electrodes; highly acidic and oxidative environments; and temperatures above 100^{o}C. Due to these factors, the conditions in a fuel cell are very harsh.[9] Currently, the state of the art membranes for the fuel cell are made from polymers containing perfluorosulfonic acid groups such as Nafion. Nafion has demonstrated good performance, but is limited by operation temperatures below 90^{o}C, limited performance under partially humidified conditions, and high material cost.[2, 20, 37] Preferably, the disadvantages arising in the fuel cell would be reduced if the operating temperature was increased above 100^{o}C. At elevated temperatures, the reduction in efficiency that takes place due to catalyst poisoning by gases like carbon monoxide would decrease significantly. Moreover, the kinetics of the reactions would improve at high temperatures, leading to better fuel cell performance. Hence this has limited the scope of application for the Nafion membrane and given an impetus to developing alternative membranes that can overcome the disadvantages of Nafion.[20, 21, 37]

Sulfonated poly(arylene ether sulfone)s are of considerable interest as an alternative to Nafion because these materials have excellent thermal, hydrolytic and oxidative stability and also have very good mechanical properties.[29, 35, 115, 116] Sulfonic acid functional groups can be easily introduced in the polysulfone backbone by sulfonating them or sulfonating the monomer initially and directly copolymerizing with another copolymer.[39, 43-45] This has led to synthesis of random and multiblock sulfonated poly(arylene ether sulfone) copolymers and their performance as a fuel cell membrane has been evaluated.[36, 117-120]

The multiblock copolymers that consist of fully disulphonated poly(arylene ether sulfone) hydrophilic blocks (BPSH100, HQSH100) have been considered as much better candidates for the fuel cell membranes as they have shown better proton conduction under partially hydrated conditions.[23, 55, 82, 114, 121-123] These BPSH100 and HQSH100 based multiblock copolymers exhibit nano-phase separated morphologies with well-connected hydrophilic phases. They exhibit high proton conductivity even at low relative humidity conditions comparable or superior to Nafion, while the well-connected hydrophobic phase provides dimensional stability and mechanical strength.[72, 98] An extensive structure-property relationship study showed that the proton conductivity at low RH conditions is a function of the ion exchange capacity (IEC) of a polymer and the hydrophilic and hydrophobic block length.[93, 124, 125] Moreover, there is a need to incorporate fluorinated moieties in the multiblock copolymer system, so as to increase the compatibility of the membrane electrolyte with the electrode material, which contains Nafion as a binder.[36]

With the focus on increasing the conductivity performance by increasing the IEC of the polymer, a possible strategy was developed to increase the volume fraction of hydrophilic segments in the copolymer without decreasing the hydrophobic segment volume fraction.[24] This

strategy was developed so that the resulting copolymer would have better conductivity performance without sacrificing the mechanical properties of the copolymer. This strategy can be implemented by use of a more hydrophilic block in the system, leading to the formation of a multiblock copolymer system with a higher IEC with increased incorporation of sulfonic acid moieties. In addition, higher IEC hydrophilic blocks can lead to a better phase separated morphology in the copolymer membrane due to the increased disparity between hydrophilic–hydrophobic phases.

This paper, therefore, describes the synthesis and characterization of a tri-sulfonated multiblock copolymer system with sulfonated hydroquinone-based hydrophilic oligomers. The IEC of the fully tri-sulfonated hydrophilic oligomer (SQSH100) is 5.31 meq g^{-1}, which is approximately 30% higher than that of HQSH100 and 50% higher than that of BPSH100. Moreover, 4,4'-(hexafluoroisopropylidene) diphenol based poly(arylene ether benzonitrile) hydrophobic oligomer would have increased hydrophobicity because of the incorporation of the fluorine moieties and should assist in better phase separation between the hydrophilic and hydrophobic groups. This will give better morphology leading to better performance in low RH conditions and also help in increasing compatibility with the electrode material. Keeping these factors under consideration, a series of SQSH100-6FPAEB multiblock copolymers was synthesized, and their fundamental membrane properties and morphology will be described below.

3.2. Experimental

3.2.1 Materials

Dimethyl sulfoxide (DMSO) and N,N-dimethylacetamide (DMAc) were purchased from Aldrich and vacuum distilled from calcium hydride before use. Monomer grade 3,3'-disulfonated-4,4'-dichlorodiphenyl sulfone (SDCDPS) was provided by Solvay Advanced Polymers and vacuum dried at 180°C prior to use. 2,5-Dihydroxybenzenesulfonic acid potassium salt (SHQ) was provided by Sigma Aldrich and recrystallized and then vacuum dried according to the procedure reported in the previous section. 4,4'-(hexafluoroisopropylidene) diphenol was purchased from Ciba and sublimated, recrystallized from toluene and dried in a vacuum oven for at least 12 hours at 120°C prior to use. 2,6-dichlorobenzonitrile was purified by recrystallization from methanol and vacuum dried at room temperature before use. Potassium carbonate, decafluorobiphenyl, hexafluorobenzene, isopropanol, acetone, methanol and toluene were obtained from Aldrich and used as received.

3.2.2. Polymer Synthesis

3.2.2.1. Synthesis of 6FPAEB hydrophobic oligomers

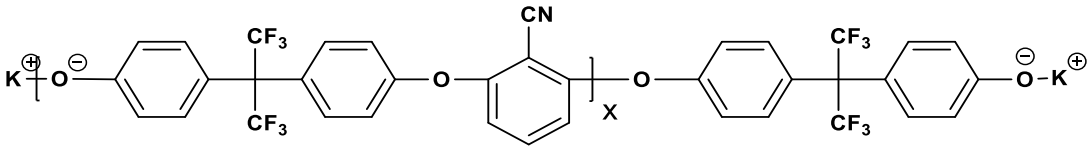

Figure 3.1: Structure of 6FPAEB hydrophobic oligomer.

The synthesis of a 6FPAEB oligomer with 6 Kg/mol molecular weight, for example, was carried out as follows: 6F-BPA (10.189 g, 30.002 mmol) was added to a three-neck round bottom flask equipped with a mechanical stirrer, a condenser, a nitrogen inlet and a Dean-Stark trap.

DMAc (60 mL) was added to the flask and the mixture was dissolved. Then K_2CO_3 (4.768 g, 34.502 mmol) was added, followed by 30 mL of toluene. The reaction bath was heated to 150°C and kept at this temperature for 4 h to dehydrate the system. The reaction was cooled to 140°C, 2,6-dichlorobenzonitrile (4.885 g, 27.833 mmol) was added and the reaction was allowed to proceed at this temperature for 16 h. The mixture was precipitated into methanol and rinsed with water and methanol. The precipitated polymer was dried under vacuum at 120°C.

3.2.2.2. Synthesis of SQS100 hydrophilic oligomers

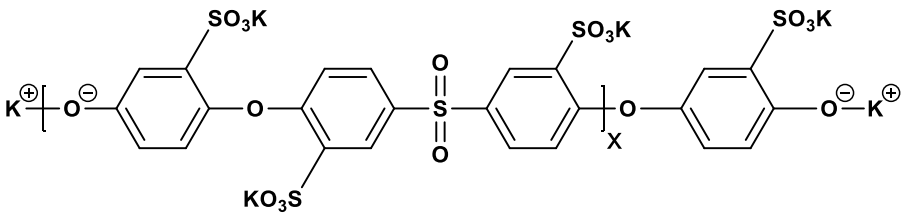

Figure 3.2: Structure of SQS100 hydrophilic oligomer.

SQS100 oligomers with various molecular weights were synthesized and end-capped with highly reactive decafluorobiphenyl or hexafluorobenzene by the same procedures described earlier. The reaction was allowed to proceed for 48 hrs for DFBP and 72 hrs for HFB. The end-capping reaction temperatures were 105 and 75°C for DFBP and HFB, respectively. To prevent a loss of low-temperature boiling HFB (e.g., 80°C) during the reaction, the temperature was chosen in order not to exceed its boiling temperature without a nitrogen purge.

3.2.2.3. Synthesis of SQS100-6FPAEB multiblock copolymers

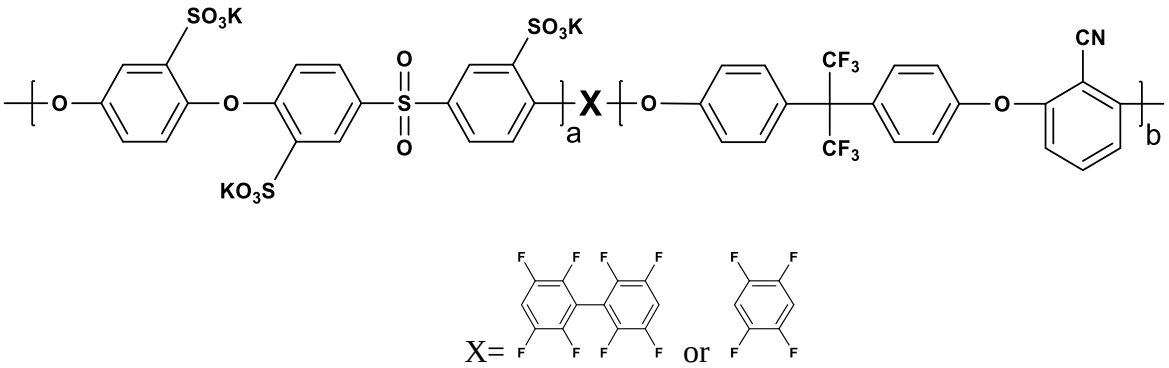

Figure 3.3: Structure of SQS100-6FPAEB hydrophilic-hydrophobic multiblock copolymer.

The ESQS100-6FPAEB multiblock copolymers were synthesized by end-capping the SQS100 moieties using hexafluorobenzene (HFB) or decafluorobiphenyl (DFBP) and then coupling it to hydrophobic 6FPAEB oligomers, using similar procedures described earlier for ESQS100-BPS series. The end-capping reaction using a SQ100 oligomer with hexafluorobenzene and coupling with 6FPAEB oligomer took place in one batch, thus saving time from the precipitation step. The polymerization reaction consisting of the end-capping step with HFB was conducted as follows: Hydrophilic oligomer SQS100 (8.069 g, 0.857 mmol) and DMSO (40 mL) were charged to a three-necked round bottom flask and the mixture was stirred until dissolved. K_2CO_3 (0.571 g, 4.138 mmol) and cyclohexane (20 mL) were added later and the system was dehydrated at 110^{o}C for 6 h. The reaction bath was then cooled to 75^{o}C and HFB (1.155 g, 6.207 mmol) was added. The reaction was allowed to proceed at 75^{o}C for 72 h without a nitrogen purge to prevent loss of low boiling HFB. After the end-capping reaction was finished, the temperature of the reaction was increased to 80^{o}C with nitrogen purge to remove the excessive unreacted HFB. ^{1}H and ^{19}F NMR

were performed to confirm that the end-capping reaction was done successfully and then the unreacted HFB was removed from the system. After the removal of excessive HFB, hydrophobic oligomer 6FPAEB (6.011 g, 0.867 mmol) was added to the system, and the polymerization was conducted at 105ºC for 72 h. After the reaction was completed, the mixture was precipitated into isopropanol to obtain fibers. The product was boiled in deionized water for 6 h to remove salt, then washed twice in acetone and then dried to give the polymer fibers.

3.2.2.4. Membrane preparation

Membranes of the salt form of the EQS100-6FPAEB were prepared by dissolving the copolymer in DMSO to form a transparent solution with 5-10% (wt/v) concentration. The solution was filtered using 0.45µm Teflon filter to remove dust particles. The filtered solution was then cast onto a glass substrate and dried under infrared heat at 60ºC. The film was then annealed at 200ºC under vacuum for 12 h.

3.2.2.5. Acidification of Sulfonated Copolymers Membranes

The tri-sulfonated ESQS100-6FPAEB multiblock copolymer films were converted to their acid-form by boiling the membranes cast in 0.5M sulfuric acid for 2 h. This step was followed by boiling the membrane in deionized water for 2 h to remove the excess acid from the film. The acidified membranes were then stored in deionized water for further characterization.

3.3. Characterization Methods

3.3.1. Nuclear Magnetic Resonance (NMR) Spectroscopy

^{1}H and ^{19}F NMR analysis were conducted on a Varian Unity 400 spectrometer. The spectra of SQS100 & 6FPAEB oligomers and SQS100-6FPAEB multiblock copolymers were obtained from a 10% (w/v) DMSO.d6 solution at room temperature.

3.3.2. Size Exclusion Chromatography (SEC) and Intrinsic Viscosity

The hydrophobic oligomers molecular weight analysis and intrinsic viscosities were obtained from Agilent 1260 Infinity Multi-Detector SEC with NMP with 0.05 M LiBr being the mobile phase (60 °C) with 3 PLgel 10 μm mixed-B 300 × 7.5 mm columns in series and a Viscostar II Viscometer. The intrinsic viscosity measurements for the hydrophilic oligomers and multiblock copolymers were carried out in NMP containing 0.05M LiBr using a Cannon- Ubbelohde viscometer at a constant temperature thermostatically controlled in a water bath at 25^{o}C.

3.3.3. Potentiometric Titration

The titration of the acidified form of the copolymers was conducted to determine the ion exchange capacity (IEC) of the polymer. The acidified films were completely dried at ~120 ^{o}C and ~1gm of the sample was weighed. This film was equilibrated with 20 ml of 0.1N aqueous sodium sulphate (Na_2SO_4) solution for two days. Afterward, this solution was titrated against sodium hydroxide (NaOH) solution (~ 0.02 N) which was standardized against 0.01N HCl solution immediately before titrating. The end-point was detected as the maximum of the first derivative for the potential versus the used volume of titrant. The average end point of three titrated samples was then used to calculate the IEC (meq/g) of the sulfonated membrane.

3.3.4. Thermogravimetric Analysis (TGA)

The thermal stability of the salt form of ESQS100-6FPAEB multiblock copolymer was determined by the thermogravimetric analysis performed on a TA Instruments TGA Q 500. Samples totaled a weight of ~10 mg and were made from the pieces of thin films of the copolymer. These samples were dried under vacuum at 120^{o}C for 12 h to remove trace solvent and water before the analysis and then were evaluated over a range of temperatures from 40^{o}C to 700^{o}C at a heating rate of 10^{o}C/min in nitrogen atmosphere.

3.3.5. Differential Scanning Calorimetry (DSC)

DSC was used to observe the thermal transitions of the ESQS100-6FPAEB multiblock copolymers performed on a TA Instrument DSC Q1000. Powder form of the copolymer was used for the sample weighing (~5 - 10mg). The samples underwent heating cycles at a heating rate of 10^{o}C/min under a nitrogen atmosphere. The onset of the thermal transition during the second heat was used to report the glass transition temperature (T_g).

3.3.6. Atomic Force Microcopy

Atomic force microscopy characterization (AFM) images were taken using Digital Instruments Dimension 3000 with a microfabricated cantilever. The force constant was 40 N/m.

3.3.7. Characterization of Fuel Cell Related Properties

3.3.7.1 Proton Conductivity

Proton conductivity at 30 ^{o}C in liquid water was determined in a window cell geometry using a Solartron (1252 + 1287) Impedance/Gain-Phase Analyzer over the frequency range of 10 Hz to 1 MHz. Membranes were equilibrated at 30^{o}C in DI water for 24 h before determining the proton conductivity in liquid water. For determining proton conductivity under partially hydrated conditions, membranes were equilibrated in a humidity-temperature oven (ESPEC, SH-240) at the specified RH and 80^{o}C for 45 min before each measurement.

3.3.7.2. Water Uptake

The water uptake of all membranes was determined gravimetrically. First, the membranes were soaked in water at 30 °C for 2 days after acidification. Wet membranes were removed from the liquid water, blotted dry to remove surface droplets, and quickly weighed. The membranes were then dried at 120 ^{o}C under vacuum for at least 24 h and weighed again. The water uptake of the membranes was calculated according to Equation 2.1 where mass_{dry} and mass_{wet} refer to the mass of the dry membrane and the wet membrane, respectively.

$$\text{water uptake} = \frac{\text{mass}_{\text{wet}} - \text{mass}_{\text{dry}}}{\text{mass}_{\text{dry}}} \times 100$$

3.4. Results and discussion

3.4.1. Polymer synthesis and characterization

3.4.1.1. Synthesis of fluorinated oligomers

The synthetic scheme for phenoxide terminated 6FPAEB hydrophobic oligomers is shown in Figure 3.4. The procedures for the synthesis of the 6FPAEB oligomers are the similar to those used for the BPS oligomers.

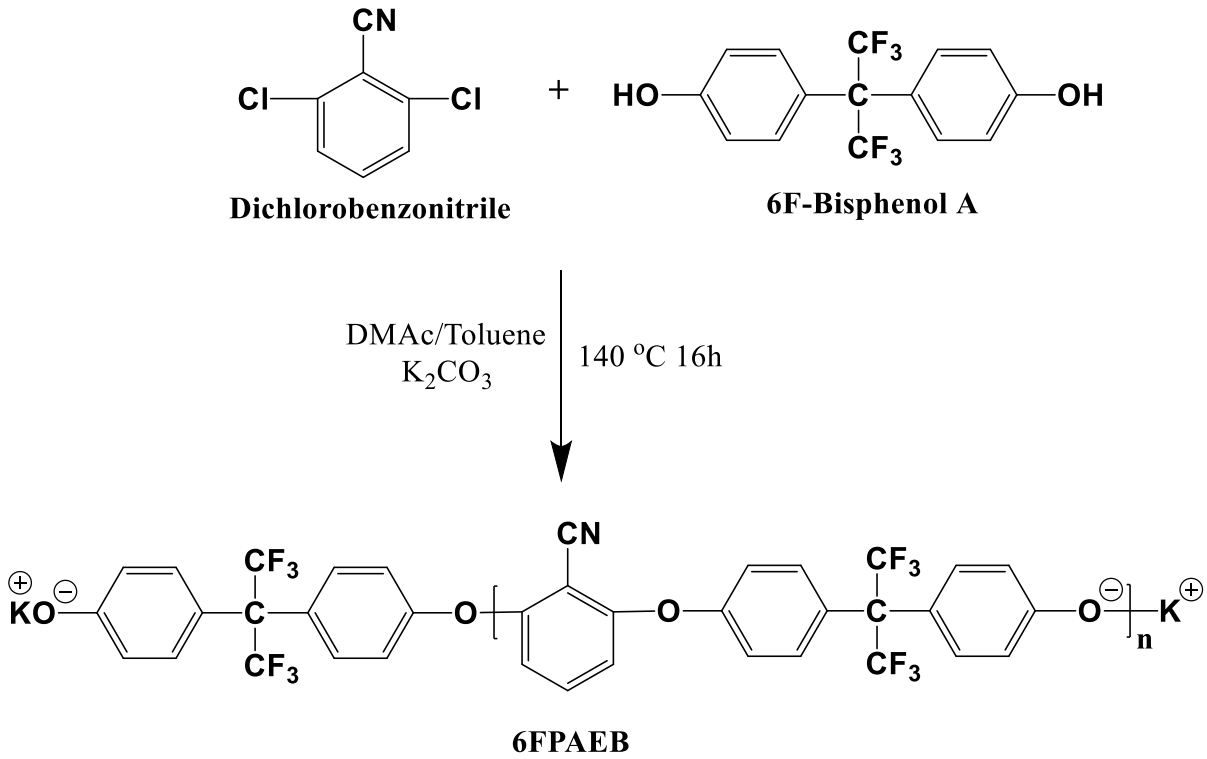

Figure 3.4: Synthesis of phenoxide terminated hydrophobic oligomers.

3.4.1.2. Synthesis of Fully trisulfonated hydrophilic oligomers

Fully trisulfonated SQS100 oligomers were synthesized by the nucleophilic aromatic substitution polymerization of SDCDPS with SHQ. The desired molecular weight was obtained by offsetting the stoichiometric ratio of SDCDPS and SHQ, determined using the Carothers equation. The temperature of the reaction was kept under 155 ^{o}C as DMSO degrades at higher temperatures.

3.4.1.3. Synthesis of SQS100-6FPAEB multiblock copolymers

In the case of synthesis between decafluorobiphenyl end-capped SQS100 and phenoxide-terminated 6FPAEB, a procedure similar to the synthesis of multiblock copolymer described in the previous chapter was used in which the hydrophilic and hydrophobic oligomer were added and dehydrated prior to the reaction taking place. In the case of hexafluorobenzene end-capped SQS100, the multiblock copolymers were synthesized via a sequential addition method. In other words, after the end-capping of SQS100 oligomer was complete, the selected 6FPAEB oligomer was added to the same flask. Hexafluorobenzene, being a volatile liquid, was removed from the solution by heating it at 90 ^{o}C after the end-capping reaction was completed. Under the nitrogen purging, the unreacted HFB was completely removed from the solution. This is illustrated by the ^{19}F NMR taken which is shown in Figure 3.7. The NMR shows that peak at -165 ppm is completely gone, indicating that all of the unreacted HFB was removed from the reaction solution. The SQS100 oligomers were not isolated before the coupling reaction as additional steps would have been needed to remove any residual salt.

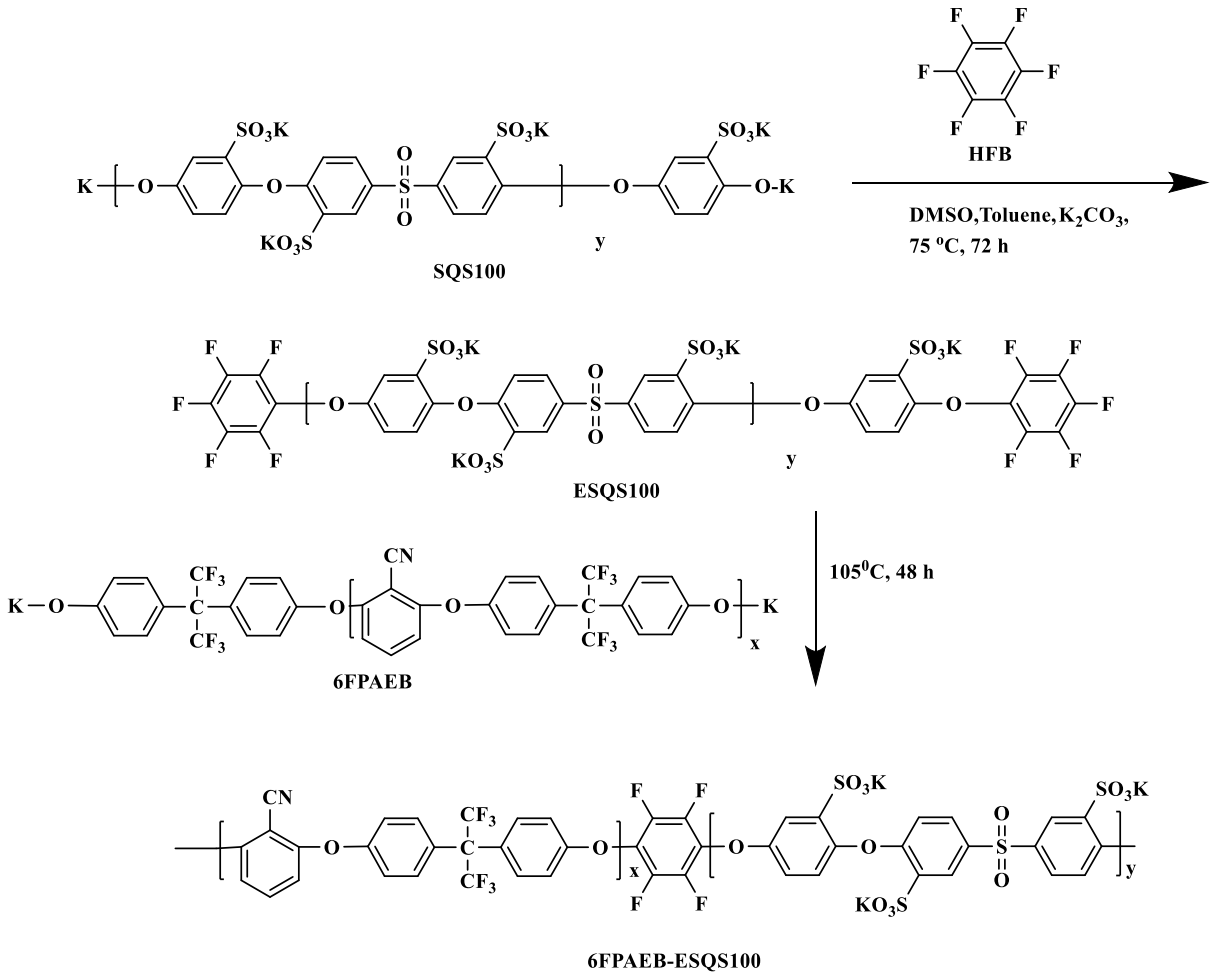

Figure 3.5: Endcapping and coupling of ESQSH100-6FPAEB multiblock copolymers.

The stoichiometry of 6FPAEB and SQS100 oligomers could also be controlled and was not always 1:1. Thus we could independently control the three parameters of a multiblock copolymer: hydrophilic block length, hydrophobic block length, and ion exchange capacity (IEC). The IEC of the multiblock copolymer can be controlled by controlling the block length of the hydrophobic and the hydrophilic oligomer or by controlling the molar ratio of the oligomers. For example, a 5K-10K (hydrophilic-hydrophobic) copolymer, which has shorter hydrophilic blocks than a 10K-10K

specimen, obviously has a lower ion exchange capacity than the latter copolymer. Thus, as IEC values change, the length of either block will also no longer be constant.

Moreover, we can change the ratio of the oligomers. It has been demonstrated before that a 1:1 stoichiometry was not necessary to synthesize block copolymers via oligomeric coupling.[120] This is based on the fact that because the repeat units (blocks) have molecular weights of at least a few thousand g/mol, the degree of polymerization (coupling) does not have to be very high to achieve a substantial total molecular weight. Furthermore, the IEC can be controlled by simply changing the stoichiometry (molar feed ratio) of the oligomers while maintaining the length of the blocks.

3.4.2. Fundamental characterizations

^{1}H NMR is a powerful characterizing tool utilized to identify and characterize the oligomers as well as the multiblock copolymers. The analysis of the NMR spectrum confirmed the structure and composition for each of the oligomers and the subsequent copolymer. The molecular weight and the composition were determined by integrating and analyzing assigned protons of the oligomer and the copolymer.

The ^{1}H NMR spectrum of a 6FPAEB hydrophobic oligomer is shown in Figure 3.6. From the spectrum of the 6FPAEB, the phenoxide end-groups were determined by the presence of the small peaks at 7.25, 7.18, 7.09 and 6.86 ppm, while the peaks at 7.48, 7.42, 7.14, and 6.71 ppm were assigned to the protons on the backbone of the main chain. By finding the ratio of the integration values between the end-groups and the main chain protons, the number average molecular weight was determined. Molecular weights ranging from 4 to 15 kg/mol were obtained

for all of the oligomers. The calculated and experimental molecular weights for the oligomers, as well as intrinsic viscosity values (IV), are listed in Table 3.1. Figure 3.7 shows the plot of lnη as a function of $\ln M_n$.

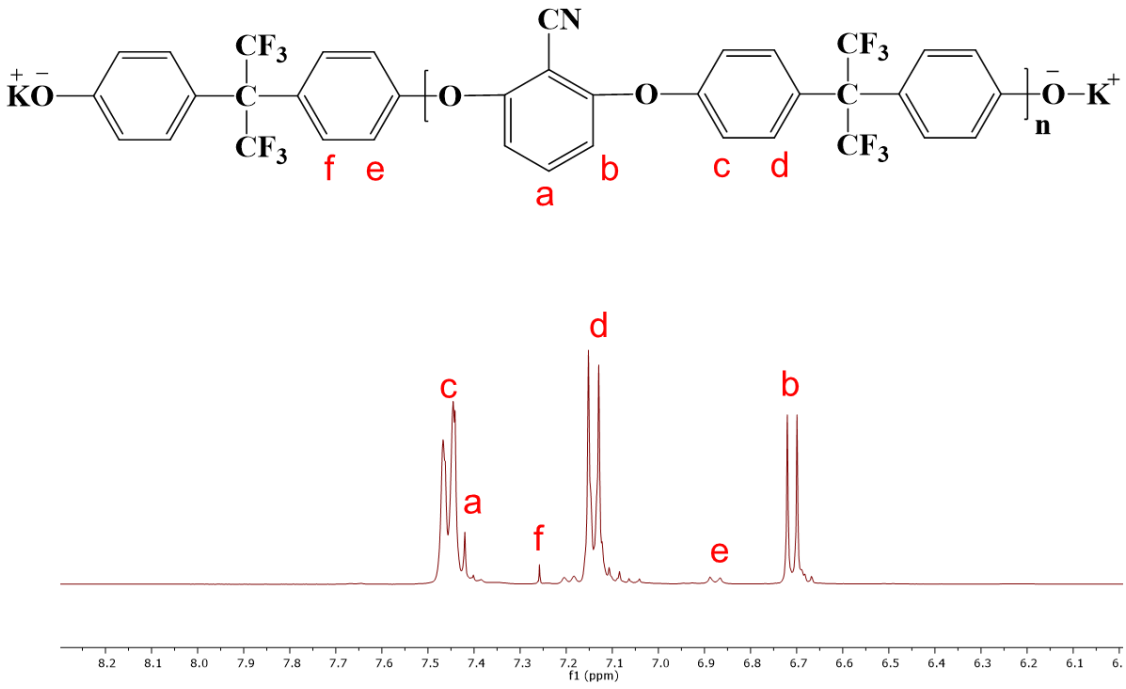

Figure 3.6: ^{1}H NMR spectrum of a 6FPAEB oligomer

Table 3.1: Molecular weight characterizations of 6FPAEB oligomers

Target M_n (g/mol)	M_n from ^1H NMR (g/mol)	M_n from GPC[a] (g/mol)	Intrinsic Viscosity[a] (dL/g)
5K	4.9K	4.8K	0.07
7K	7.2K	6.9K	0.09
10K	10.8K	10.3K	0.13
15K	15.4K	15.2K	0.15

a: Measured by SEC with 0.05M LiBr/NMP as mobile phase at 60°C

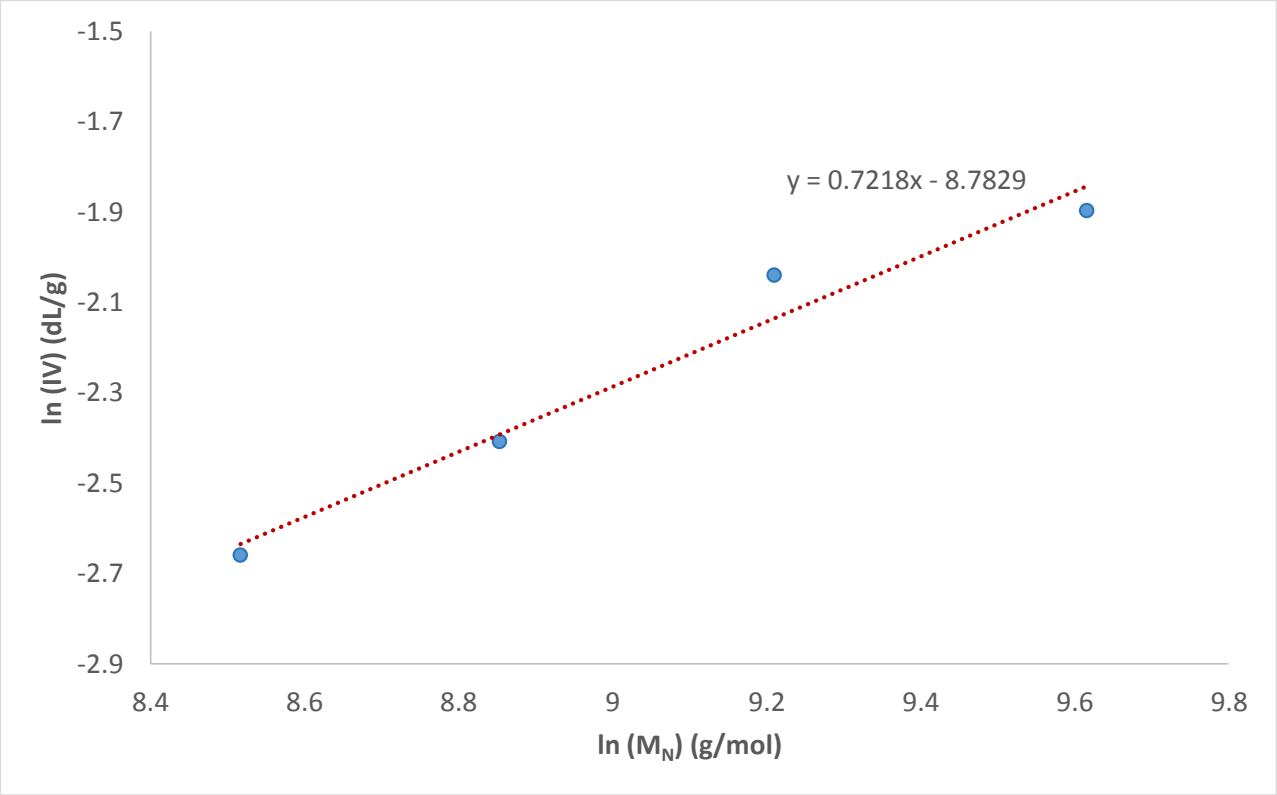

Figure 3.7: ln η vs. ln M_n plot for 6FPAEB oligomers

^{1}H NMR of the SQS100 oligomer is shown in the previous chapter. The ^{19}F and ^{1}H NMR spectra of a multiblock copolymer are shown in Figures 3.8 and 3.9, respectively. Here, the peaks due to the endgroups in the case of the 6FPAEB and SQS100 oligomers were not observed; they either disappeared or shifted. Thus, a high conversion coupling reaction was thought to have been achieved. In the ^{19}F NMR spectrum, only the peaks due to the coupling agent and 6FBPA can be observed. The presence of only 4 peaks related to the coupling agent DFBP indicates that only the terminal fluorine atoms were involved in the reaction thus giving us a linear polymer.

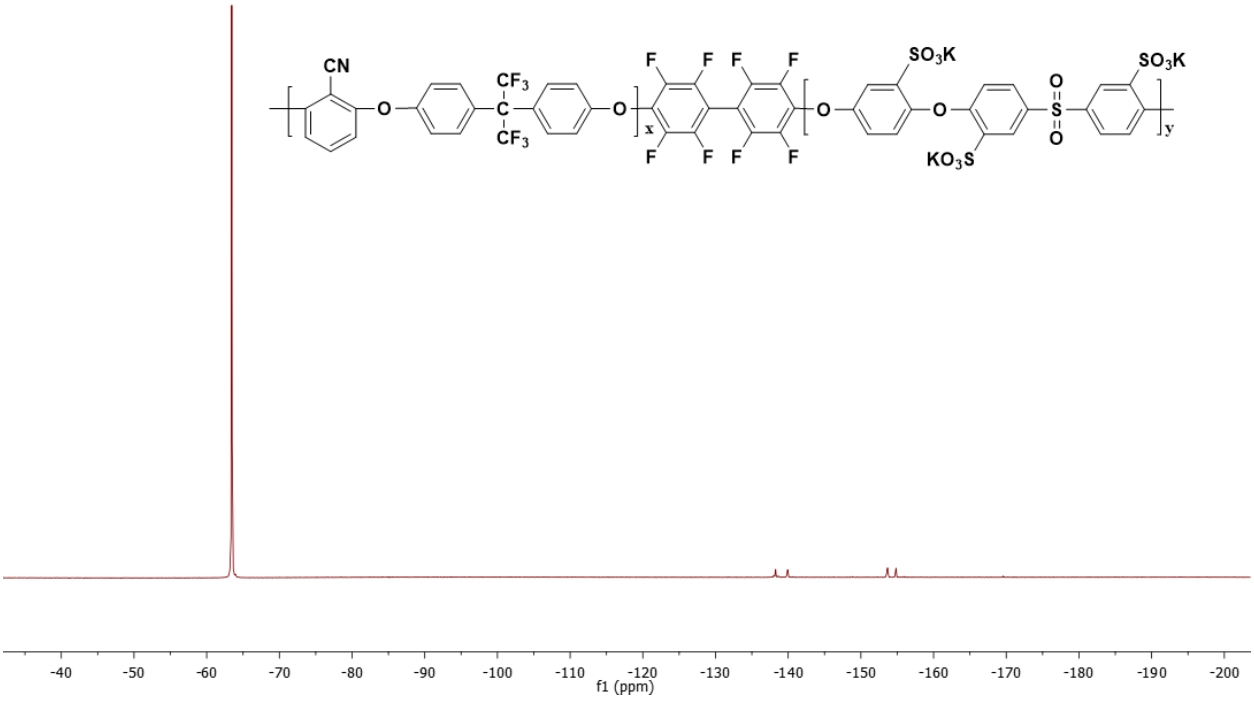

Figure 3.8: ^{19}F NMR spectra of a 6FPAEB-SQS100 multiblock copolymer.

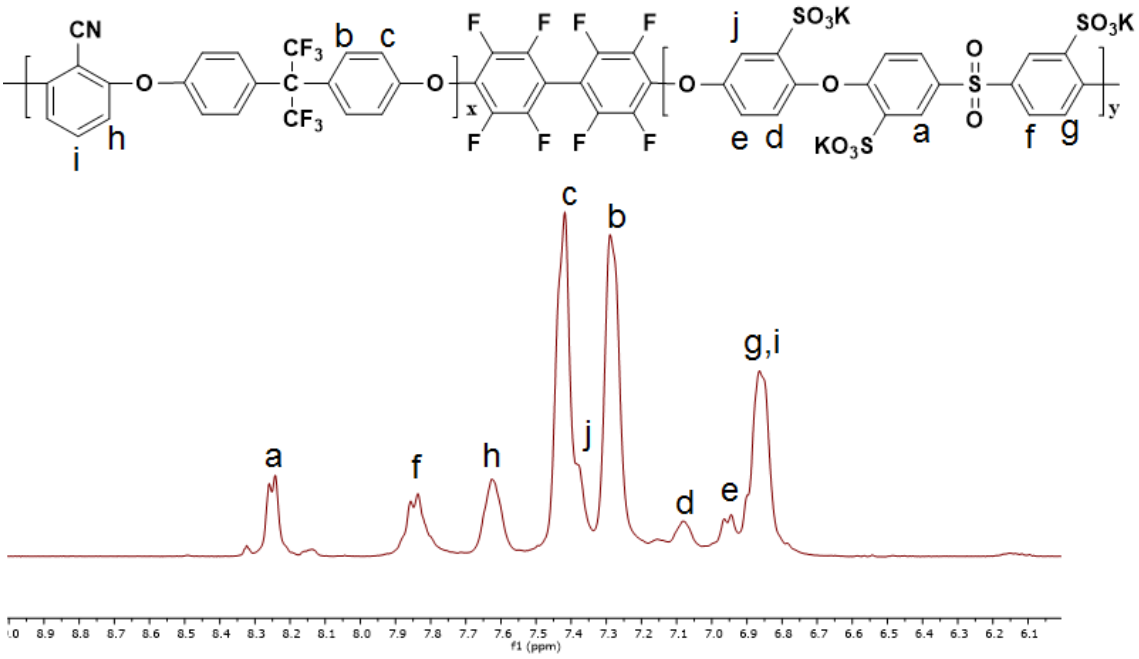

Figure 3.9: ^{1}H NMR spectra of a 6FPAEB-SQS100 multiblock copolymer

In Figure 3.8, it can be observed that the two fluorine peaks anticipated for the 6FPAEB blocks merged into one broad peak in these spectra. Therefore, it is possible that the copolymers might not have formed true solutions in the NMR solvent, DMSO-*d*6, but rather tended to form micelle-like aggregates.[9, 126, 127] Furthermore, as shown in Table 3.2, the copolymer's experimental IEC, obtained from ^{1}H NMR, did not agree with the theoretical value. The titration values, on the other hand, showed better agreement with the target IEC.

Table 3.2: Comparison of target IEC with experimental values for 6FPAEB-SQSH100 multiblock copolymers

Copolymer	Target IEC	IEC from ^{1}H NMR	IEC from Titration
ESQS100-6FPAEB (7K-7K)	2.2	1.7	1.9
ESQS100-6FPAEB (8K-8K)	2.2	1.6	1.8
ESQS100-6FPAEB (10K-10K)	2.1	1.5	1.6

Such large discrepancies cannot be justified by experimental uncertainties. The reason is not clear, but some qualitative hypotheses could be suggested on the basis of the solution properties of the copolymers. In fact, the various hydrophobic oligomer BPS and 6FPAEB, have different solubility in DMSO. The 6FPAEB-ESQSH100 block copolymer chains could, therefore, have very different conformations in DMSO compared to those of BPS-ESQSH100. This may be the reason why experimental IEC values from NMR were not consistent with the target ones. Although the copolymerizations were conducted in DMSO in which both 6FPAEB and ESQS100 oligomers are soluble, there could be differences in solubility. We also propose that there could be more pronounced separation between the hydrophobic and hydrophilic phases, thereby inhibiting the oligomers from migrating toward and reacting with each other.

Characterization data for a series of the multiblock copolymers are listed in Table 3.3. The copolymers may have different IEC values due to slight differences in the molar charge ratios for

the hydrophilic:hydrophobic oligomers. The polymerization yielded multiblock copolymers with high intrinsic viscosities that were cast into tough, ductile membranes.

Table 3.3: Characterization data of ESQS100-BPSH multiblock copolymers.

Copolymer	Block Lengths[a] (g/mol)	Molar Feed Ratio[b]	IEC[c]	Intrinsic Viscosity (dL/g)[d]
ESQS100-6FPAEB-1	6000:6300	1 : 1	2.0	0.84
ESQS100-6FPAEB-2	7200:7000	1 : 1	1.8	0.72
ESQS100-6FPAEB-3	9600:10000	1 : 1	1.6	1.21

e) Block lengths are expressed in the form hydrophilic:hydrophobic

f) Molar ratios are expressed in the form hydrophilic:hydrophobic

g) Measured from titration with 0.02N NaOH.

h) Measured at 25 ^{o}C in 0.05M LiBr DMSO solution

3.4.2.1. Thermal analysis

The DSC thermogram of a ESQS100-6FPAEB multiblock copolymer is shown in Figure 3.10. Even in the case of the ESQS100-6FPAEB multiblock copolymer, only one transition was observed at around 195^{o}C. The presence of only one T_g may be explained due to the hindered

molecular motions caused by the electrostatic interaction among ionic groups present in the block copolymer. This hampers the formation of optimum nanophase separation in the block copolymer.

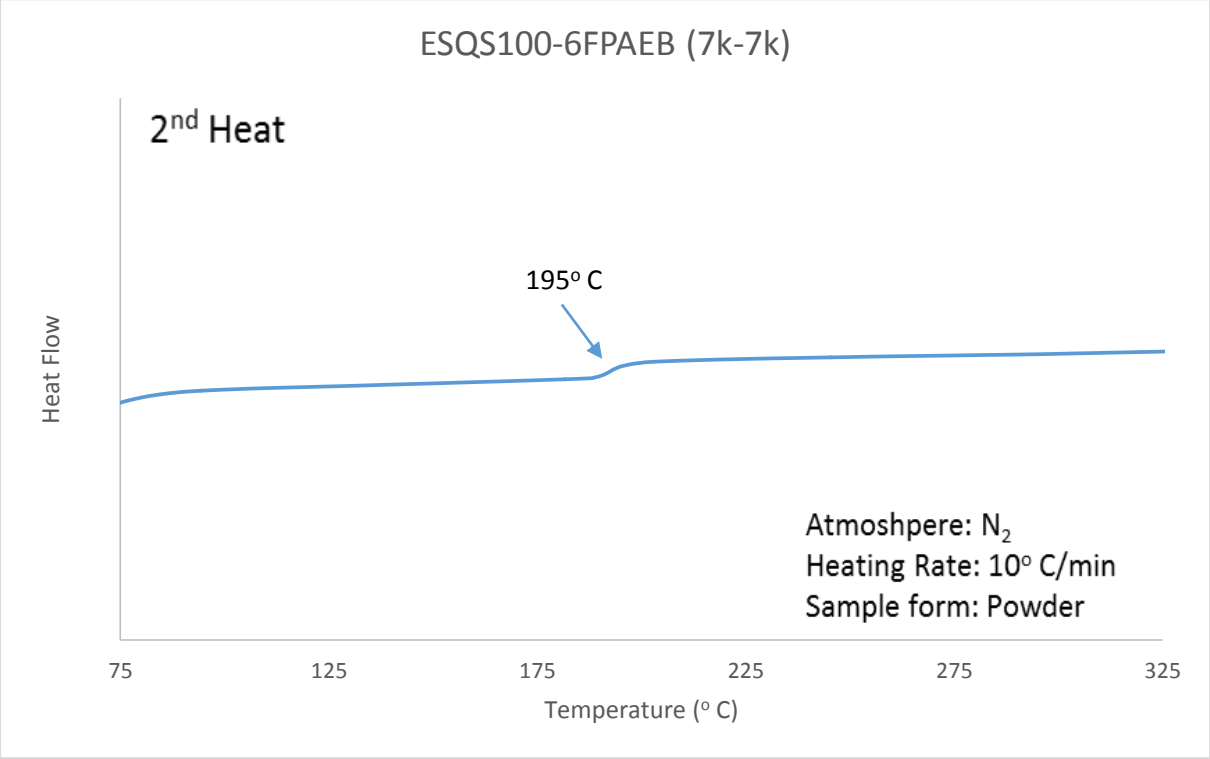

Figure 3.10: DSC of ESQS100-6FPAEB 7K-7K copolymer.

Thermal stability was investigated by thermogravimetric analysis for the salt form of the multiblock copolymer. The TGA was programmed from 30 to 700°C at a heating rate of 10°C/min in nitrogen. Before the analysis, the sulfonated sample was pre-heated at 150°C for 30 minutes in TGA furnace to get rid of any traces of solvent and the moisture from the sample. The degradation process for the multiblock copolymer is shown in Figure 3.11 with the weight loss occurring at 490°C, which was attributed to the degradation of the polymer backbone. The nitrile based multiblock copolymer system does not show the degradation around 320°C observed in SQS100-

BPS copolymer system, which was attributed to the loss of sulfonate group. It is proposed that the nitrile group present in the copolymer interacts with the sulfonate groups and increases their stability. Hence we do not observe the degradation step around 320^{o}C related to the loss of sulfonate groups.

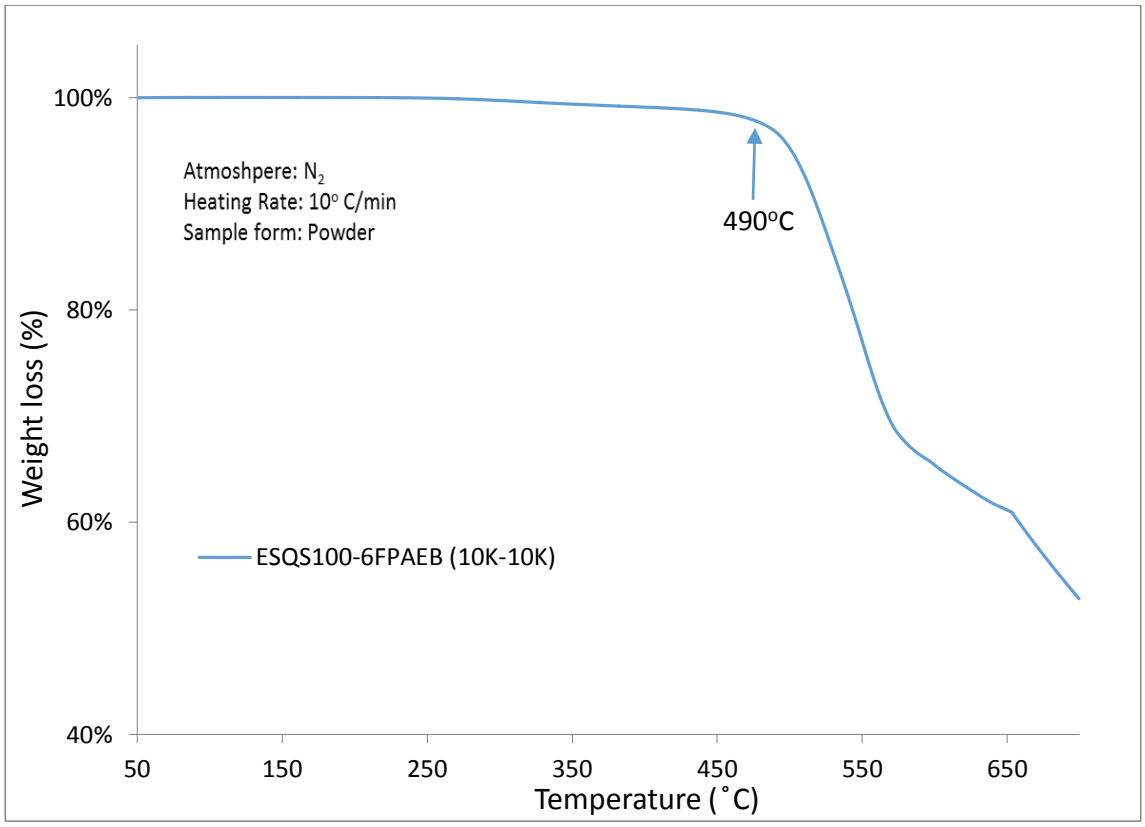

Figure 3.11: TGA traces of ESQS100-BPSH (7K-7K) multiblock copolymer.

3.4.2.2. Surface morphological features

Figure 3.12 display the tapping mode AFM images for the ESQS100-6FPAEB (7K:7K) and ESQS100-6FPAEB (10K:10K) samples. From the Figure, we can observe that the fluorine containing fully tri-sulfonated copolymers display sharp nanophase separation between hydrophobic and hydrophilic domains. From the phase images it can also be observed that, with increasing block length, the nanophase separation becomes more distinct between hydrophobic and hydrophilic domains along with increased connectivity between the hydrophilic domains.

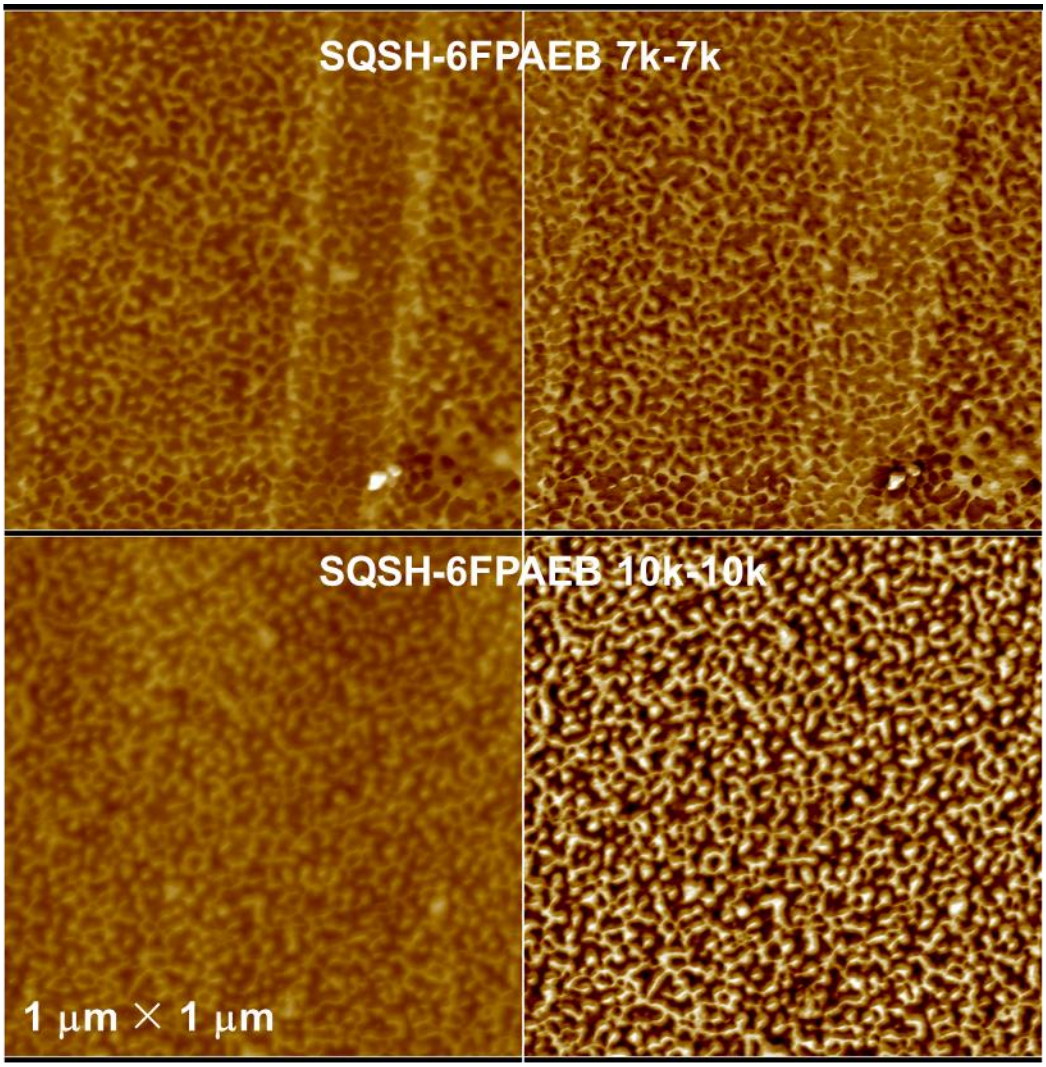

Figure 3.12: Tapping mode AFM height (left) and phase (right) images for ESQS100-6FPAEB (7K-7K), (10K-10K) multiblock copolymer membranes.

3.4.3. Fuel Cell Related Characterizations of Multiblock Copolymers

3.4.3.1. Proton conductivity under fully hydrated conditions

Proton conductivity and water uptake of ESQS100-6FPAEB copolymers are compared with other fluorinated multiblock copolymer series shown in Figure 3.13.

a)

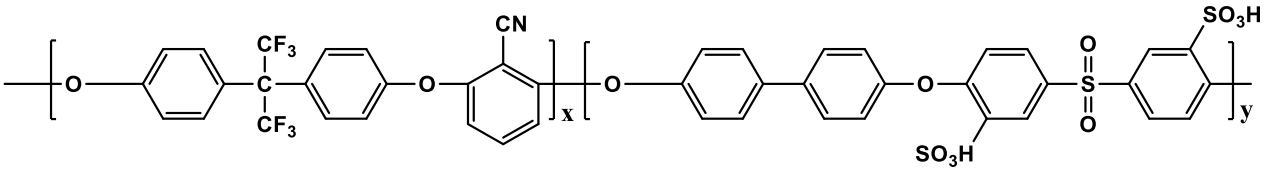

6FPAEB-BPSH100

b)

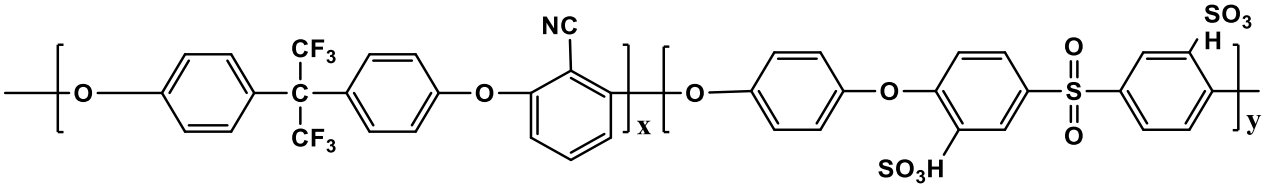

6FPAEB-HQSH100

Figure 3.13: Structures of partially disulfonated block copolymers. (a) BPSH; (b) HQSH

The water uptake and the proton conductivity under fully hydrated conditions of the trisulfonated and the disulfonated block copolymer series are tabulated in Table 3-4. In case of the disulfonated block copolymers, the water uptake and the proton conductivity are a function of the ion exchange capacity.[23] A similar trend is also observed for trisulfonated block copolymer, as shown in Table 3.4.[24, 112] Increase of the water uptake and proton conductivity can be explained due to the increase in ion exchange capacity of the trisulfonated copolymers, which is due to

increased concentration of sulfonic acid groups. The effect of the block length on proton conductivity is not significant under fully hydrated conditions is observed from the results.

It is also noted that the proton conductivity for the fluorinated ESQSH100-6FPAEB is considerably higher than the corresponding non-fluorinated ESQSH100-BPS copolymer. Thus, it can be inferred that the presence of the fluorine helps in increasing the hydrophobicity of the hydrophobic block. An increase in the hydrophobicity leads to an increase in χ parameter leading to increased phase separation, which in turn helps in formation of hydrophilic channels for better proton transport and conductivity.

Table 3.4: IEC, water uptake and proton conductivity for fully tri-sulfonated block copolymers

	IEC (meq/g)[a]	Water uptake (%)[b]	Proton Conductivity (S/cm)[c]
6FK-BPSH100			
5K-5K	1.60	47	0.11
9K-9K	1.65	50	0.12
13K-13K	1.70	53	0.12
6FPAEB-BPSH100			
9K-9K	1.53	44	0.13
13K-13K	1.63	51	0.14
6FPAEB-HQSH100			
7K-7K	1.80	64	0.17
9K-9K	1.65	84	0.15
BPS-ESQSH100			
5k-5k	1.90	44	0.13
7k-7k	1.95	49	0.14
10k-10k	1.84	38	0.12
6FPAEB-ESQSH100			
6k-6k	2.2	76	0.20
7k-7k	2.3	87	0.20

10k-10k	2.2	71	0.18
Nafion 212	0.90	22	0.12

a: Measured by Titration of the sulfonic acid groups with 0.02N NaOH.

b: Measured in acid form

c: Measured in liquid water at 30°C

3.4.3.2. Proton conductivity under partially hydrated conditions

The proton conductivity for the ESQS100-6FPAEB (7k-7k) polymer at 80°C under partially-hydrated conditions is shown in Figure 3.14 and 3.15. The proton conductivity of the ESQS100-6FPAEB copolymer under partially hydrated conditions was investigated using a new process, where, the conductivity vs RH measurements were taken at 80°C first from 95% to 30% humidity, displayed in Figure 3.14, and from 30% to 95% humidity, displayed in Figure 3.15. Prior to each measurements the membranes were equilibrated in a temperature and humidity controlled oven for at least 30 minutes. The resistance, R, (ohm) of the copolymer membrane was measured and then the proton conductivity was determined by the equation:

$$\partial = \frac{l}{R * A}$$

Where:

∂ = conductivity (S/cm)

R = Resistance (ohms)

l = length between electrodes (cm)

A = cross-sectional area of film (cm^2)

In the previous proton conductivity measurement technique, the length of the film measured were taken at each RH level. The film was exposed to atmosphere while measuring the length of the film, this is believed to have increased the human error in the measurements. In the new measurement technique, length of the dry and completely wet film were measured and length measurements were extrapolated at each RH level.

From the Figure 3.14 and 3.15, we can see that the ESQS100-6FPAEB shows excellent proton conductivity vs Nafion at high RH. But as the RH decreases below 70%, the conductivity of the ESQS100-6FPAEB copolymer decreases drastically and shows inferior performance compared to Nafion. In the case of ESQS100-BPS multiblock copolymer, the previous method of measuring conductivity measurement was utilized which showed much better conductivity performance of the copolymer compared to Nafion, even at low RH levels, even though the proton conductivity of ESQS100-BPS in liquid water is much less than ESQS100-6FPAEB.

Thus we attribute the inferior performance of the ESQS100-6FPAEB copolymer to the change in the conductivity measurement technique. There is a need to evaluate both the conductivity measurement techniques and find out which technique gives the most accurate results.

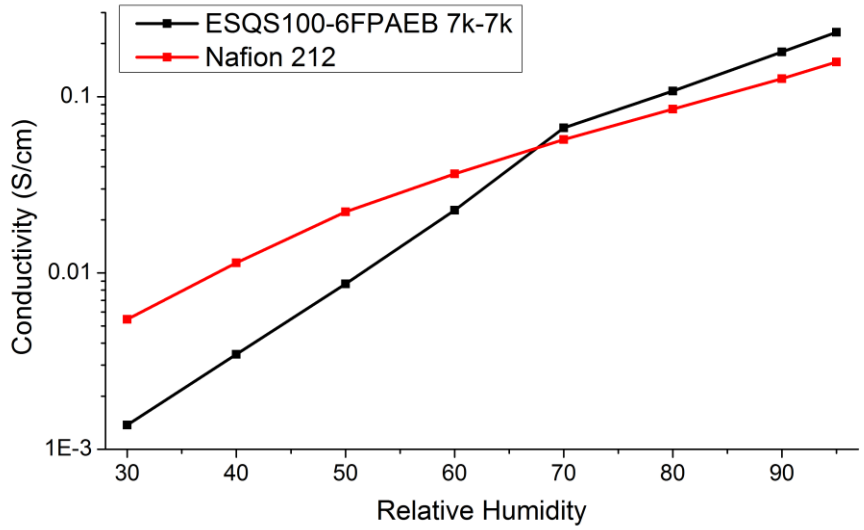

Figure 3.14: Proton conductivity vs. RH plot taken from 95% to 30% humidity for Nafion 212, ESQSH100-6FPAEB block copolymer.

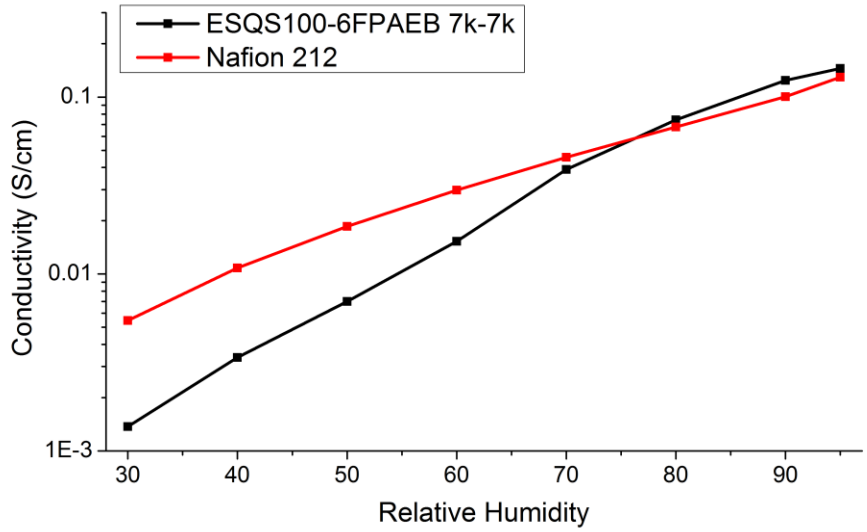

Figure 3.15: Proton conductivity vs. RH plot taken from 30% to 95% humidity for Nafion 212, ESQSH100-6FPAEB block copolymer.

3.5. Conclusion

A series of multiblock copolymers was successfully synthesized from fully trisulfonated hydrophilic poly(arylene ether sulfone)s and biphenol based hydrophobic oligomers for potential application as proton exchange membranes. The copolymers synthesized possessed a variety of oligomer molecular weights with varying ratios of hydrophilic-hydrophobic content. The hydrophilic oligomers were end-capped using the highly reactive decafluorobiphenyl & hexafluorobenzene in order to facilitate successful coupling with the hydrophobic oligomer at relatively low temperatures (~105^{o} C) to avoid ether-ether interchange reactions. Tough ductile films were produced from these multiblock copolymers. Water uptake and proton conductivity under both fully and partially hydrated conditions were measured and compared with Nafion 212 and disulfonated multiblock copolymers. The reduced proton conductivity at low RH was attributed to the change in procedure for the measurement of proton conductivity at different RH levels and more work is needed to determine if the change in the measurement technique leads to a better evaluation of the conductivity for the sulfonated membranes, Atomic force microscopy images indicated the development of a nanophase separated morphology, which is one of the reasons for improved performance in liquid water.

Chapter 4 : Synthesis and characterization of poly(arylene ether sulfone) random copolymer precursors for reverse osmosis membranes.

A precursor for a reverse osmosis membrane was successfully synthesized to produce a poly(arylene ether sulfone) from the reaction of 4,4'-dichlorodiphenyl sulfone, hydroquinone and bis(4-hydroxyphenyl)sulfone . These precursors, after post-sulfonation, shall form mono-sulfonated polysulfone materials with potential applications in reverse osmosis. The chemical structure of these random copolymers were characterized using ^{1}H NMR. Intrinsic viscosity and size exclusion chromatography measurements were used to confirm that high molecular weight copolymers were synthesized and ductile films were produced for these copolymers. The thermal properties were investigated by thermogravimetric analyzer and differential scanning calorimetry while the mechanical properties were determined by the tensile testing machine. The ratio of the amount of hydroquinone and bis(4-hydroxyphenyl)sulfone were varied during the synthesis of the precursor to facilitate control over the post-sulfonation process and the effect of these changes in ratio was investigated for the thermal and mechanical properties. The simple and low cost process of post-sulfonating the random copolymer enables the precursor to be a promising material to be used in the reverse osmosis application.

4.1 Introduction

Water scarcity is a global issue which occurs due to the lack of sufficient water resources where billions of people are impacted by either physical or economic water scarcity.[128] While the earth is mostly covered with water, 97% is sea water, which is not conducive for drinking. Hence

sea water can be an important source for the production of drinking water by desalinating the sea water to produce fresh drinking water. Traditionally, flash distillation has been used for water purification, but recently multi-stage flash distillation (MSF) and multiple-effect distillation (MED) have been used to purify water. One of the drawbacks of the flash distillation, MSF and MED, is the relatively high cost of energy, which is attributed to the rising price of the fuel and the pollution of the environment. Thus alternative technologies need to be explored, which reduces the energy consumption while making the process more efficient. The reverse osmosis (RO) technology can be the answer to the concerns as it less energy consuming and almost as efficient as the conventional methods for desalinating the sea water.[128, 129]

The RO technology incorporates the concept of diffusion of water through a semipermeable membrane, arising due to the difference in concentration gradient of salt in the water, which only allows the pure solvent to pass to the other side, producing fresh water. For the reverse osmosis to take place, osmotic pressure needs to be overcome, which arises from the difference in salt concentration in water on both sides of the membrane, leading to a spontaneous flow of water from the less concentrated solution to the higher concentration solution. Hence a pressure is applied on the feed side containing the higher concentrated solution to overcome the osmotic pressure, which forces the flow of water to the lower concentration solution from the higher concentration.[130, 131] The overall principle of reverse osmosis is shown in the figure 4.1.

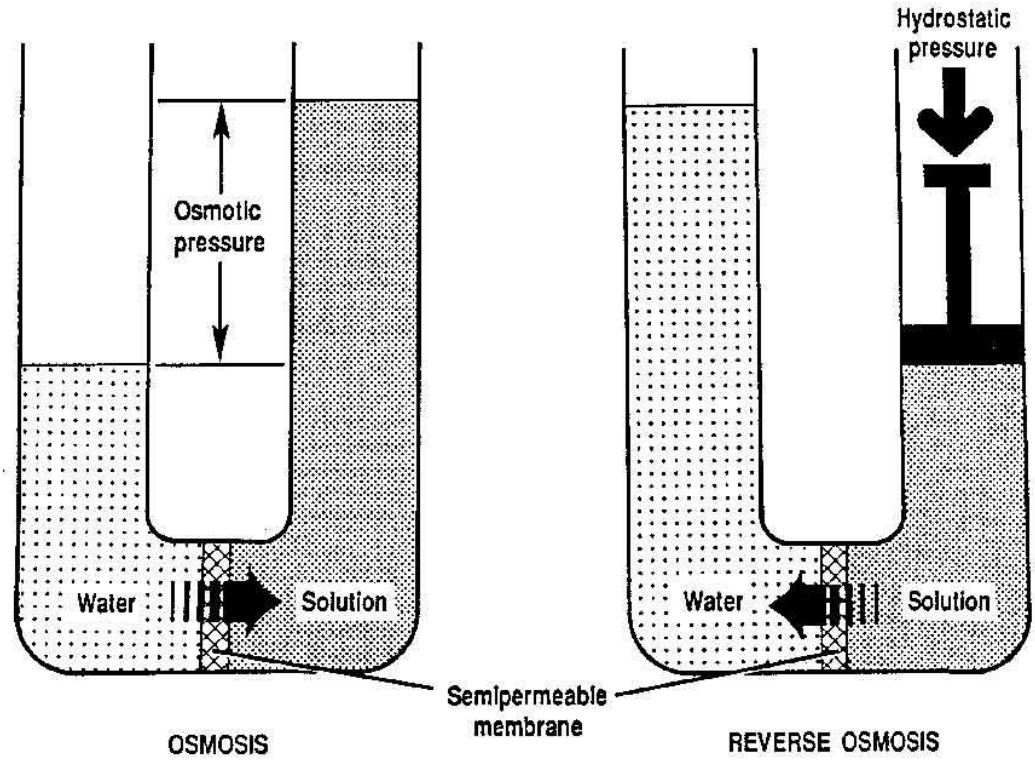

Figure 4.1: Overall Principle of Osmosis Compared to Reverse Osmosis. [132]

The process of water flow through a reverse osmosis membrane takes place via a solution-diffusion mechanism, which is shown in the figure 4.2. In this mechanism, the water particle is absorbed in the membrane and diffuses through the membrane, desorbing at the permeate side of the membrane. An increase in these factors will lead to increased permeability of water through the membrane.[133]

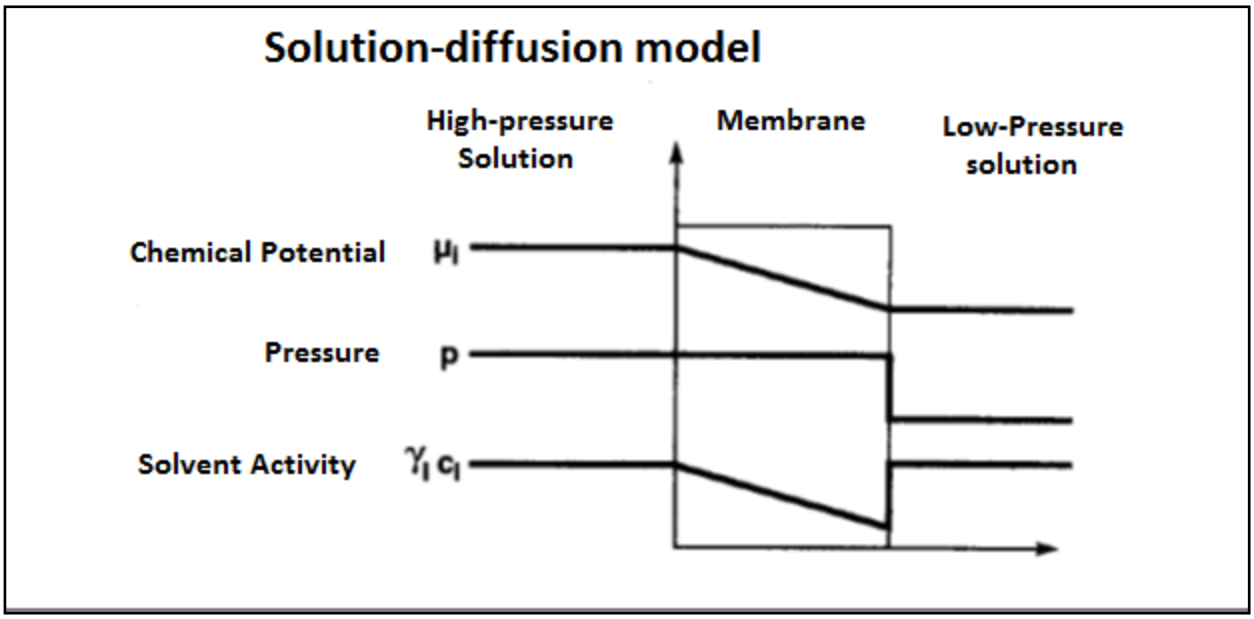

Figure 4.2: Reverse osmosis permeation through membrane by solution-diffusion. [133]

The membranes used for the reverse osmosis constitutes the core of the process. The membrane can either be a dense film, an asymmetric membrane or an interfacially polymerized layer of thin-film composite membrane where the separation occurs only at the skin of the membrane. The function of the membrane is to only allow water to pass through while preventing the solutes like salt ions from passing through it.[132] The reverse osmosis process is shown in figure 4.3.

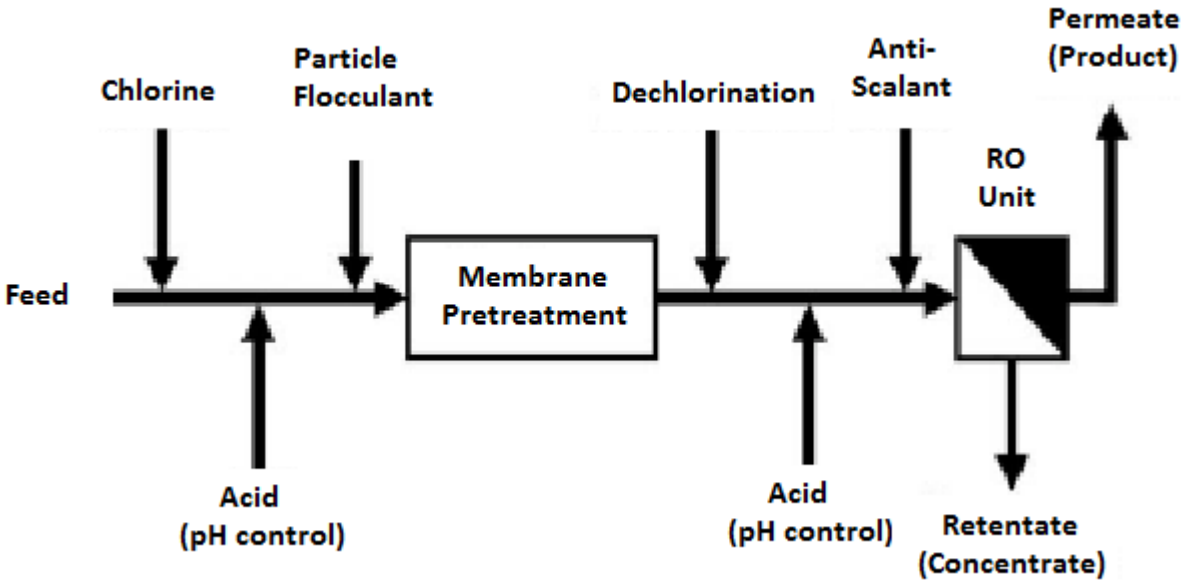

Figure 4.3: Schematic presentation of the reverse osmosis process. [134]

Beasely, J.K. listed some of the properties required by the membrane to be applicable in RO process.[135] They are listed as:

- High salt rejection along with high water flux.
- Need to form thin films with high strength (in case of asymmetric membranes)
- Potential to be fabricated with high surface-to-volume ratio (in case if hollow fibres).
- Versatility to operate in different range and requirements such as: ion content or water source, pressure and temperature.
- Resistant to attack from chemical and biological components.
- Long service life
- Low cost

The state-of-the-art membrane for water purification is a polyamide, FT-30. It is a thin-film composite generally consisting of 3 layers, where the top layer is 100 nm in thickness made up of crosslinked polyamide and does the bulk of the water separation. This top layer is highly selective to water and prevents passage of ionic solutes (salt ions). It also enables a high water flux because of the low thickness of the top layer. The top layer is supported by a microporous support generally made up of polysulfone foam, while the third layer is a woven or non-woven fabric that provides additional mechanical strength to the membrane composite.[135] A schematic diagram of the thin film composite as shown in figure 4.4.

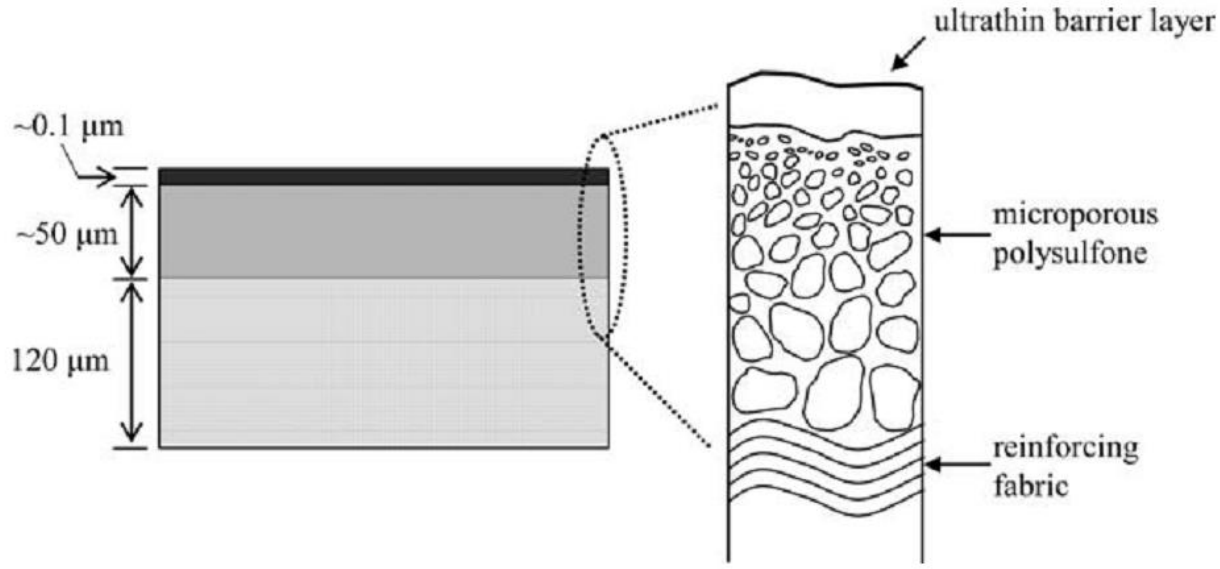

Figure 4.4: Schematic of a thin film composite membrane. [134]

The cross-linked polyamide top layer is formed using interfacial polymerization reaction, in which the microporous support is coated with aqueous solution consisting of the water soluble monomers like m-phenylene diamine. This layer is coated with an organic solution consisting of the other monomer (tri-mesoyl chloride). As both the layer are immiscible with each other, the reaction happens at the interface where the monomers diffuse to the interface and polymerize,

leading to formation of the thin and dense polymer layer. The reaction scheme is shown in figure 4.5.[134-137]

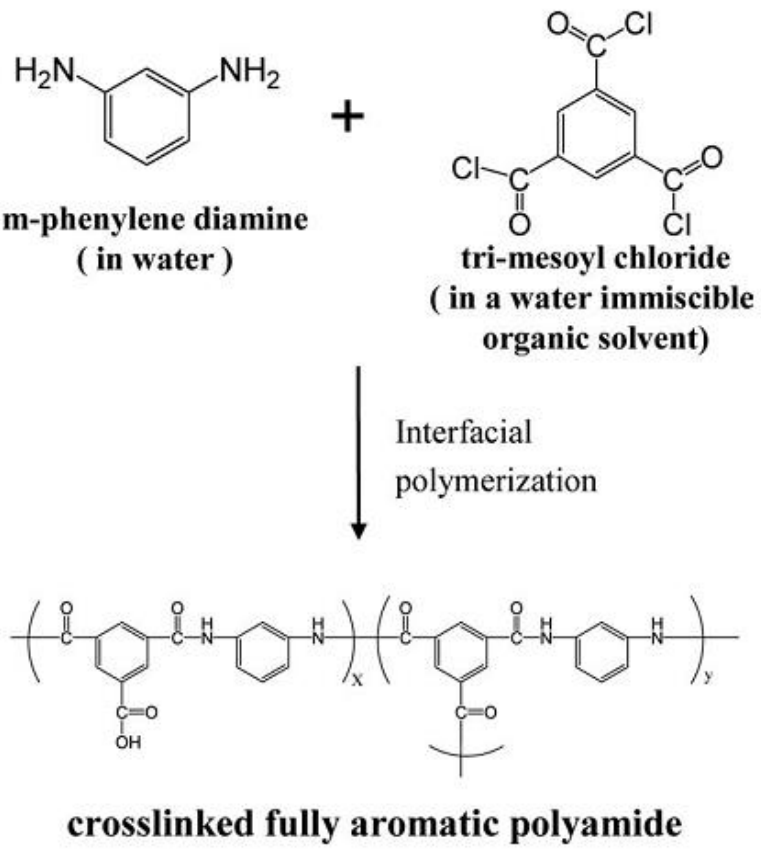

Figure 4.5: Schematic of crosslinked fully aromatic polyamide via interfacial polymerization.[134]

Although the aromatic polyamide based thin-film composites show excellent salt rejection capabilities and resistance to fouling, they are susceptible to degradation by chlorine added as a disinfecting agent and to prevent fouling in the water. These membranes quickly lose their performance even in presence of trace amounts of chlorine which eventually leads to membrane failure.[138-141] The mechanism for the degradation is shown in Figure 4.6. Thus to avoid degradation of the membrane, the feed water needs to be dechlorinated by adding sodium bisulfite before

passing it though the membrane, and the product water is rechlorinated for disinfection. The dechlorination and rechlorination step adds to the cost of production of water, and this has led to the research for chlorine resistant membrane systems.

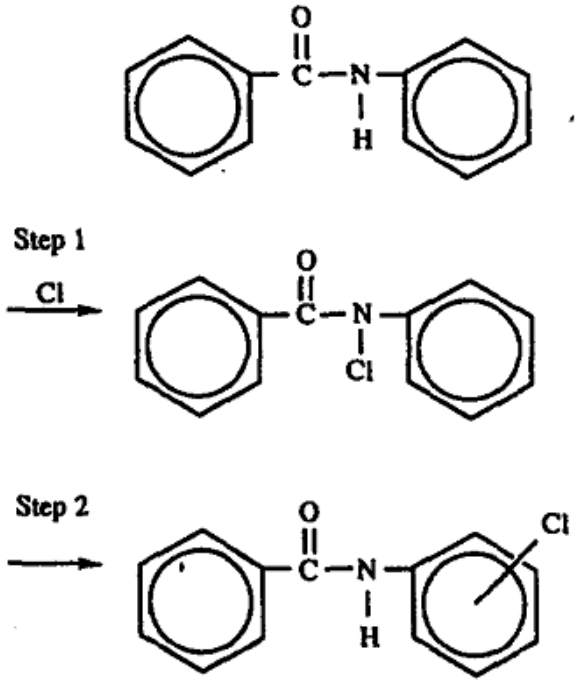

Figure 4.6: Mechanism of chlorination of aromatic polyamide. [141]

Many strategies have been developed to create chlorine resistant membranes[141, 142] and some of them include:

1) Replacing the amidic hydrogen in the polyamide with other groups, such as methyl, phenyl etc.
2) Replacing aromatic amines in polyamide with aliphatic amines.
3) Synthesis of membranes based on more robust systems based as polystyrenes, polysulfones, polyimides, and polybenzimidazoles.[57, 143-148]

New membranes based on more robust systems are the most promising candidates as chlorine tolerant polyamide systems have not been able to produce similar performances compared to conventional aromatic polyamide based membranes. Polymers like polysulfones have an extremely stable backbone structure and exhibit excellent chlorine resistance.[149, 150] However, they are hydrophobic in nature and hence have very low water permeability. To increase the water flux through the polysulfone, it is imperative to attach hydrophilic ionic groups onto the polymer. The introduction of the ionic groups like sulfonates into the backbone of a polysulfone can be either done by post-sulfonating the polysulfone via the electrophilic substitution of proton with sulfonic acid groups on the polymer backbone using concentrated sulfuric acid, fuming sulfuric acid, chlorosulfonic acid, or sulfur trioxide.[37-43] The other strategy is to employ the direct sulfonation method, in which the polymer is prepared using sulfonated monomers. The advantage of this approach was the control on degree of sulfonation and reproducibility of the results.

In the last few years, the McGrath group has been focused on synthesizing wholly aromatic sulfonated polysulfones with varied ion exchange capacity via the direct sulfonation method and Freeman group has evaluated the transport characteristics of these polymers.[9, 44, 45, 99, 114, 118, 119, 151, 152] The BPS random copolymer system developed by McGrath et al.[57] is shown in Figure 4.7, where 'x' denotes the amount of the sulfonated monomer present in the polymer.

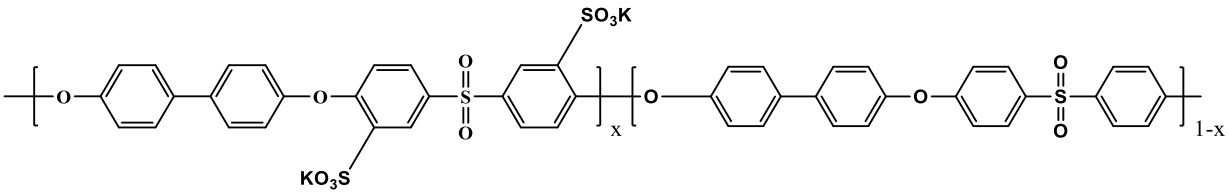

Figure 4.7: Structure of BPS-XX copolymer.

The superior chlorine resistance of the polysulfones (BPS-40) compared to polyamides is shown in Figure. As seen from Figure 4.8, thin-film composite (TFC) made from BPS-40 exhibits a high tolerance to chlorine as well as effective anti-fouling characteristics without compromising on the performance (salt rejection and water flux).[149]

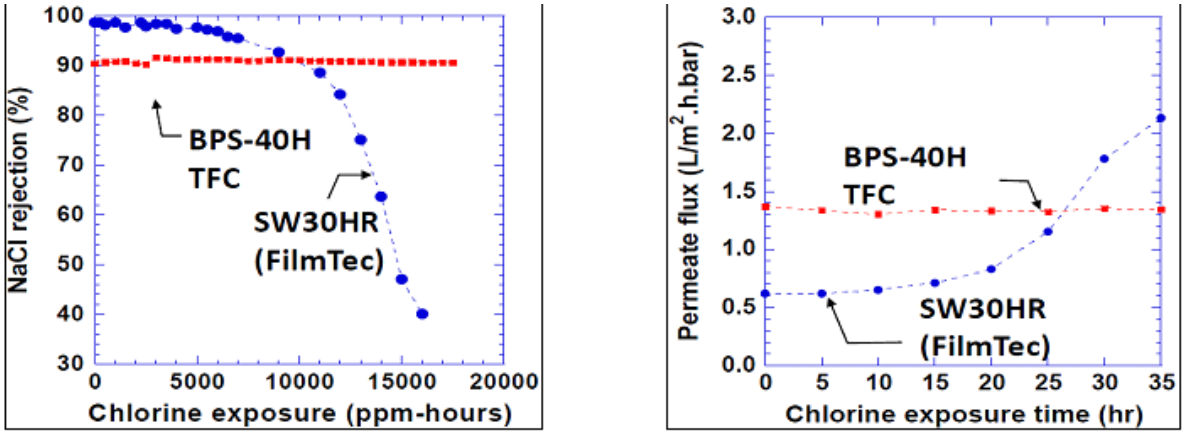

Figure 4.8: Degradation of SW30HR polyamide membrane compared to sulfonated polysulfone. [26]

Recently, asymmetric membranes based on the disulfonated BPS-20 copolymer has been prepared by Stevens et al.[153], showing more than 99% salt rejection, while providing promising water flux. Hence, the disulfonated BPS random copolymer can be said to be promising candidates for the water purification application. One of the drawbacks reported in this work is the increase in the passage of Na^+ ions in the presence of divalent cations as shown in Figure 4.9. In the polysulfone based materials, Stevens et al. proposed that the rejection of the monovalent salt mainly takes place due to the repulsion between the negatively charged SO^{3-} groups on the polymer backbone and anions of the salt present in the feed. But the divalent cations present in the feed binds strongly to negatively charged groups on the polymer backbone, thus decreasing the repulsion between the negative charge on the polymer and the anions in the feed, leading to decrease in the salt rejection.

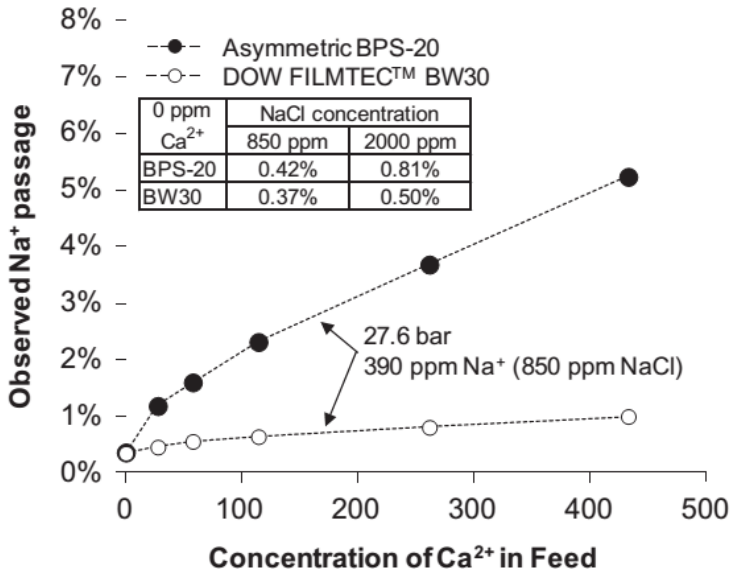

Figure 4.9: Sodium rejection for feeds containing calcium ions.

In this research, we have synthesized random poly(arylene ether sulfone) copolymers called DBH which stands for **D**ichlorodiphenylsulfone**B**isphenolS**H**ydroqionone random copolymer. DBH random copolymer is synthesized using DCDPS, BisS and hydroquinone via nucleophilic aromatic substitution reaction. High molecular weight DBH copolymer is achieved by keeping the moles of DCDPS equal to moles of BisS and hydroquinone. The nomenclature of the DBH copolymer is DBH-xx, where xx denotes the molar equivalent of hydroquinone monomer. For example, DBH-25 denotes a copolymer of DCDPS, BisS and HQ which incorporates 25% of the hydroquinone monomer. The generalized structure of the copolymers studied is shown in Figure 4.10, where X can change depending the ratio of Bisphenol-S to hydroquinone used.

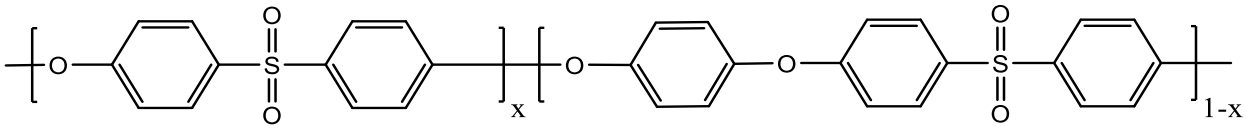

Figure 4.10: Schematic of DBH random copolymer.

These random copolymers on post-sulfonation using concentrated sulfuric acid using the procedure reported by Rose et al.[154] will lead to formation of mono-sulfonated polysulfones. The post-sulfonation process can take place on the only activated ring in the structure, i.e. hydroquinone ring, and will lead to formation of only a mono-sulfonated product, which can be used in reverse osmosis water purification application. The hypothesis for this approach is that the presence of only one sulfonate group in the polymer backbone will hinder the complex formation with the divalent cation present in the feed and not reduce the salt rejection of the membrane. In the following sections, the synthesis and characterization of this material will be illustrated in detail and the influence of their structures on resulting properties will be discussed. The varying amount of the hydroquinone used in the formation of the copolymer will lead to formation of a mono-sulfonated copolymer with varying concentration of sulfonate group, eventually changing the IEC of the polymer.

4.2. Experimental

4.2.1. Materials

4,4'-dichlorodiphenylsulfone (DCDPS) was provided by Solvay Advanced Polymers and recrystallized from toluene and then dried under vacuum at 60°C for 24 h. bis(4-hydroxyphenyl)sulfone was provided by Alfa Aeser, and were dried in vacuum at 110°C for 24 h prior to use. Hydroquinone (HQ) was received from Eastman Chemical Company and vacuum dried at 110°C prior to use. Sulfolane was received from Solvay and N,N-dimethylacetamide (DMAc) were received from Aldrich and vacuum distilled before use. Potassium carbonate (K_2CO_3) and m-xylene were obtained from Aldrich and used as received.

4.2.2: Polymer synthesis

4.2.2.1. Synthesis of DBH random copolymer

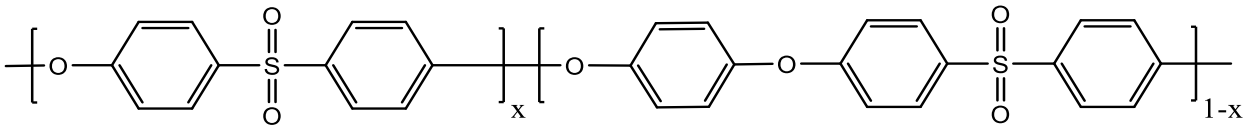

Figure 4.11: Structure of a DBH copolymer.

The synthesis of a DBH-50 random copolymer containing equimolar quantities of BisS and HQ, for example, was carried out as follows: DCDPS (5.75 g, 20.024 mmol), BisS (2.506 g, 10.012 mmol), and hydroquinone (1.102 g, 10.012 mmol) were added to a three-necked round bottom flask equipped with a mechanical stirrer, condenser, nitrogen inlet, and a Dean-Stark trap. Sulfolane (20 mL) was added and the mixture was stirred until dissolved to afford a 33% solids concentration. K_2CO_3 (3.183 g, 23.027 mmol) and m-xylene (10 mL) as an azeotropic agent were

next added and the system was heated under reflux at 180 ^{o}C for 4 h. Then the reaction bath was gradually heated to 230 ^{o}C with the removal of m-xylene. The polymerization reaction proceeded at 230^{o}C for 12 h during which the solution became very viscous. The solution was cooled to room temperature and diluted with DMAc. The solution was filtered to remove most of the salt and the polymer powder was isolated by precipitation in water using a blender. The white polymer then was boiled in deionized H_2O to remove residual solvent and salt and then dried under vacuum at 120 ^{o}C before use. Copolymers with varying content of HQ and BisS were also prepared by the same procedure.

4.1.2.2. Film Preparation

Films of the random copolymers were prepared by dissolving the copolymers in DMAc and casting the solutions on clean glass substrates. About 5-15% (wt/v) concentration solutions were prepared depending upon the desired film thickness. Polymer solutions were filtered to remove any dust particles using a disposable syringe and Teflon disc filters (0.45µm) prior to casting. The filtered solution was then sonicated to remove any trapped air bubbles inside the solution. The solution casted films were dried under IR lamp at 60^{o}C for 12 hrs to remove DMAc followed by drying the films in a vacuum oven at 150^{o}C for 4 hrs. These films were then separated from the glass substrate by immersing them in water. The isolated films were dried in the oven at 120^{o}C.

4.3. Characterization

4.3.1. Nuclear Magnetic Resonance (NMR) Spectroscopy

Proton (^{1}H) Nuclear Magnetic Resonance was used to obtain the chemical composition of polymers, and verify the amount of HQ and BisS incorporated in the polymer. Sample solutions for the NMR were obtained by dissolving the polymer in DMSO-d6 solvent and at a concentration of 5% wt/v (0.1g in 2mL). NMR spectra were obtained on a Varian Unity Spectrometer operating at 400 MHz, and keeping tetramethylsilane as a reference at 0 ppm.

4.3.2. Size Exclusion Chromatography (SEC) and Intrinsic Viscosity

SEC measurements were used to obtain the molecular weight and determine the molecular weight distributions of synthesized copolymers. SEC was conducted on an Agilent 1260 Infinity Multi-Detector SEC, having a multi-angle laser light scattering (MALS) detector (DAWN-HELEOS II), operating at a wavelength of 658 nm, a refractive index detector operating at a wavelength of 658 nm (Optilab T-rEX) and an on-line differential viscometer (Viscostar) coupled in parallel. SEC measurements were performed using an NMP (HPLC grade) as the mobile phase, containing 0.05 M LiBr, at a flow rate of 1.0 ml/min and an injection volume of 200 µl with the polymer concentration of approximately 2~3 mg/ml. The stationary phase was crosslinked polystyrene gel (three Agilent PLgel 10µm Mixed B-LS columns 300×7.5mm) connected in series with a guard column. During the measurements, the column-compartments, lines and detectors were maintained at a constant temperature of 60^{o}C. Astra 6 software (Wyatt Technology) was used to acquire and analyze the results. A series of polystyrene standards having narrow molecular weight distributions

(Agilent Technologies or Varian) were employed to generate a universal calibration curve[155, 156] and were used to determine the number average molecular weight (Mn), weight average molecular weight (Mw) and polydispersity (Mw/Mn) of the synthesized copolymers.

Intrinsic viscosities are utilized to get information on the size of a polymer molecule in solution and provides a qualitative inference of the molecular weight. The measurements of intrinsic viscosity of poly(arylene ether sulfone) random copolymers were performed using the on-line differential viscometer (Viscostar), which was coupled in parallel with the GPC. Intrinsic viscosities were measured at 60^{o}C in NMP with 0.05M LiBr.

4.3.3. Thermogravimetric Analysis (TGA)

Dynamic TGA was performed on a TA instrument TGA Q5000 in nitrogen and the samples were heated at a rate of 10^{o}C/min. % Weight loss was reported as a function of temperature. Thermal stability of the poly(arylene ether sulfone) copolymers and the influence of varying HQ and BisS moieties in the polymer backbone on the thermal stability of these copolymers was reported.

4.3.4. Differential Scanning Calorimetry (DSC)

Differential scanning calorimetry was used to determine the thermal transition temperatures of the synthesized random copolymers. DSC was conducted on a TA instrument DSC Q2000 with a heating rate of 10^{o}C/min under nitrogen atmosphere. The samples were prepared from the powder form of the copolymers and having a suitable sample size of ~10 mg. T_g (glass transition temperature) was reported as the onset of the specific heat increase in the transition region during the second heat.

4.3.5. Tensile testing

The tensile properties of the membrane samples were measured using an Instron 5500R universal testing machine equipped with a 200 lb load cell by mounting the samples in pressure-locking pneumatic grips. The testing was carried out at room temperature and crosshead displacement rate of 5 mm/min. A dogbone die measuring 50 mm in length and 4 mm in width was used to cut out samples from each membrane. A total of 3 samples from each membrane were tested. These membrane samples were dried under vacuum at 60^{o}C for 24 h prior to testing.

4.4 Result and discussions:

4.4.1 Synthesis of Random Copolymers

The synthesis of DBH random copolymers is shown in Figure 4.12.

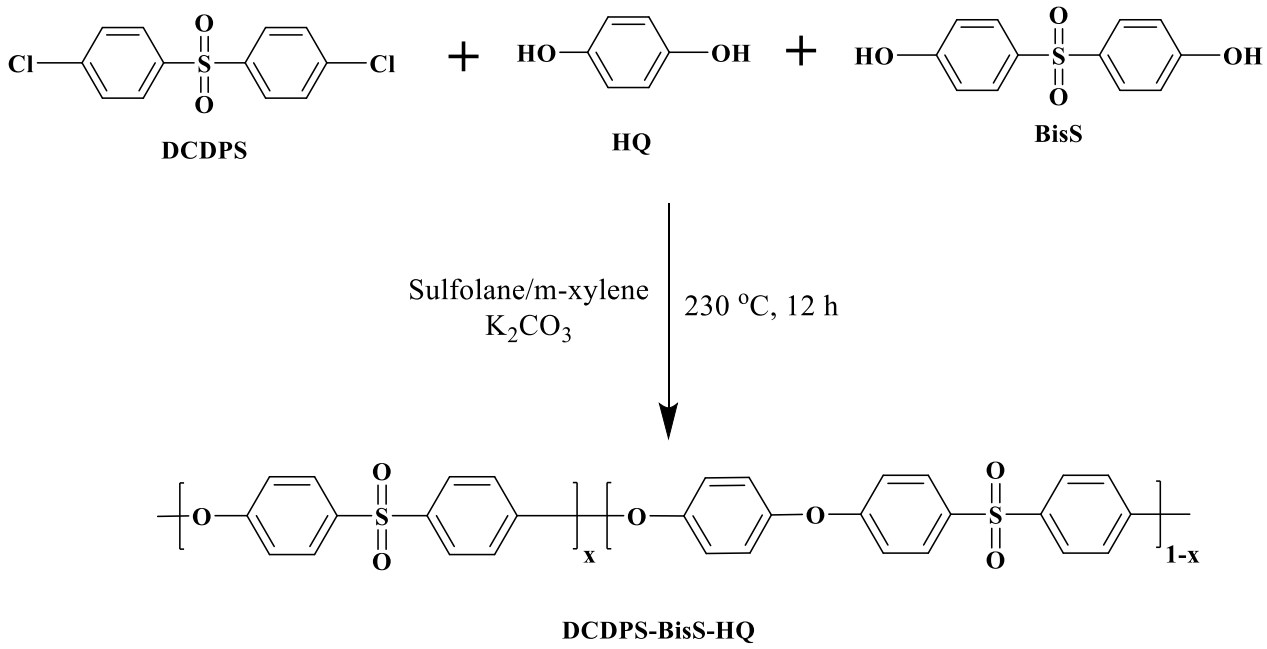

Figure 4.12: Schematic of DBH copolymer synthesis.

Random copolymers were synthesized by using bisphenol S and hydroquinone with 4,4'-dichlorodiphenyl sulfone. Hydroquinone and bisphenol S were polymerized with a stoichiometric amount of dichlorodiphenyl sulfone using the weak base method in which 15 mol% excess of potassium carbonate, based on the amount of HQ and BisS was used.[157] High molecular weight polymers were synthesized in sulfolane as a solvent at a polymerization temperature of 230°C for 12 hours after dehydrating the system with m-xylene at 180°C for 4 hours. The viscosity of the reaction solution increased slowly during the polymerization.

The molecular weights (Mn) and intrinsic viscosity ([η]) of the random copolymer synthesized were ascertained via universal calibrated SEC in NMP and the results are tabulated in Table 4.1.

Table 4.1: Molecular weight (Mn) from Universal calibration GPC and Intrinsic Viscosity [η] of control poly (arylene ether sulfone)s

Polymer	M_n (g/mol)	[η] (dL/g), 25°C
DBH-25	50,500	0.383
DBH-50	45,400	0.47
DBH-75		

4.4.2 Polymer Characterization

Spectroscopic and thermal characterization are two very important techniques to collect more information about the polymers. The structural and compositional information was gathered using the ^{1}H NMR for the random copolymers while the thermal behavior was explored using the thermogravimetric analysis (TGA) and differential scanning calorimetry (DSC). The variation in the thermal behavior with respect to change in the amount of HQ and BisS was also found out.

4.4.2.1. Spectroscopic Analysis

4.4.2.1.1. ^{1}H NMR Spectroscopy

Proton NMR spectroscopy has been employed to provide structural as well as compositional determinations for each copolymer. By integration of known reference protons of the polymer and finding the ratio of the integration of these protons, the relative copolymer composition of the DBH copolymer were determined. The ^{1}H NMR of the DBH-50 random copolymer is a representative ^{1}H NMR spectrum shown in Figure 4.13.

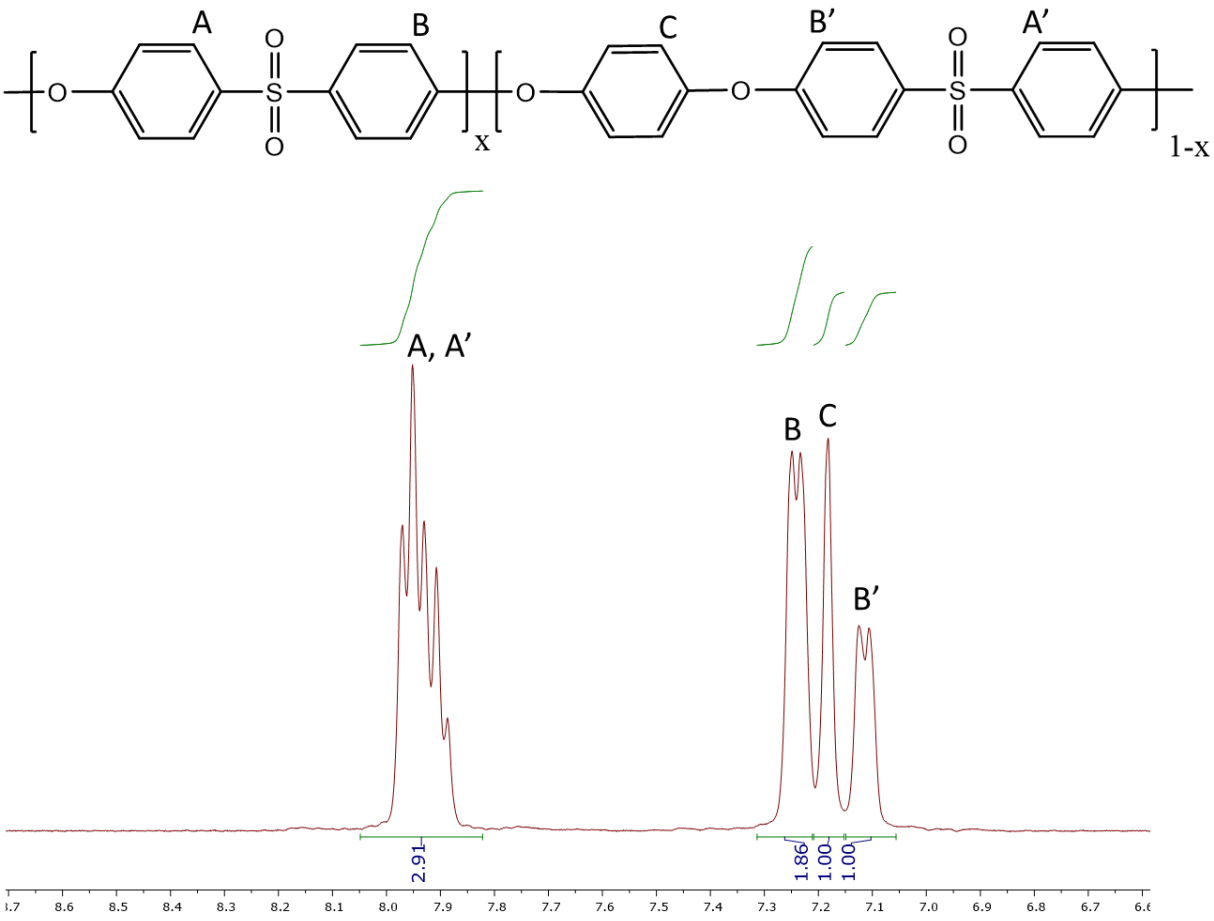

Figure 4.13: ^{1}H NMR and peak assignments of DBH-50 sulfonated copolymer.

The protons meta to the sulfone group (B') (~7.1 ppm) and protons related to the hydroquinone (~7.2 ppm) are used to determine the amount of hydroquinone incorporated in the polymer backbone with respect to BisS. The integration revealed that 54 mol% of HQ and 46 mole% of BisS were incorporated into the polymer, which is close to the charged amounts of 50 mol% of HQ and BisS. Similar integrations and calculations were also performed for other DBH random copolymers and the results were within experimental error (±10% of the expected values). The amount of incorporation of HQ and BisS in the random copolymer is shown in Table 4.2.

Table 4.2: Incorporation of HQ and BisS based on 1H NMR integration calculation for DBH random copolymers

Copolymer	HQ content (%)	BisS content (%)
DBH-25	27	73
DBH-50	54	46
DBH-75	74	26

Sample Calculation: For DBH-50 copolymer:

Integrals for the protons associated with HQ moieties and sulfone moieties,

C = 1.00 and B'=1.00, A+A'=3.91, B =1.86

Amount of protons associated with HQ according to the integral = C, C=1.00

Amount of protons at meta position to the sulfone group related to BisS according to the integral = B-B', B-B'=1.86-1.00 = 0.86

Hence amount of HQ incorporated = 1.00/(1.00+1.86)*100

HQ (mole%) = 54% (rounded to closest 2 digit number)

BisS (mole%) = 100-54 =46%

The synthesis of the DBH random copolymer was monitored using ^{1}H NMR. From the analysis of the NMR spectrum, it was seen that the polymer undergoes a side reaction if the reaction is conducted for more than 12 h. This is shown through the ^{1}H NMR in the fig. 4.14 below. The degradation may be attributed to the rupture of the C-S bond in the polysulfone leading to thermodegradation producing smaller fragments of the polymer molecule.[158] Hence care was taken for the reaction to not proceed for more than the stipulated time.

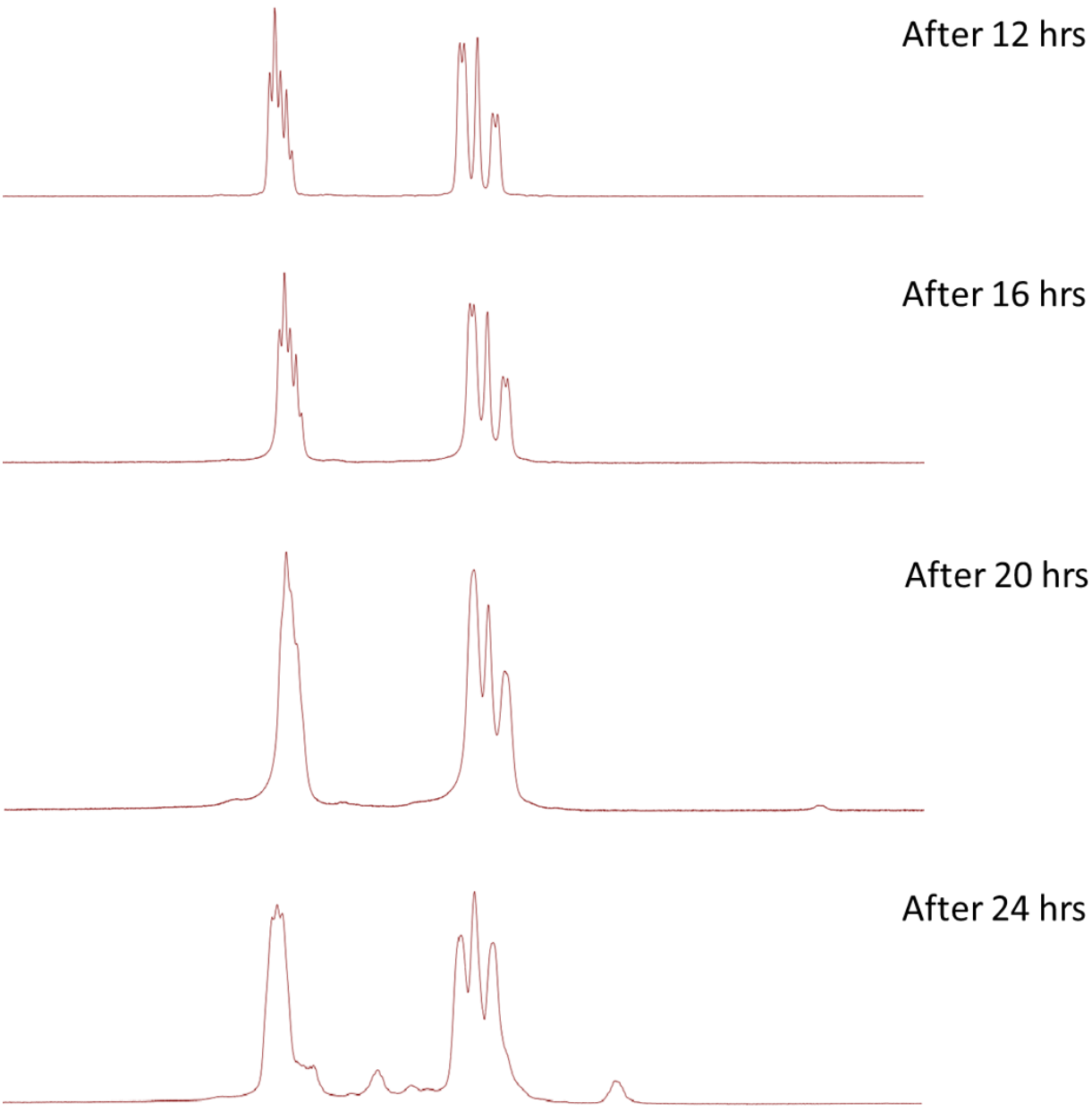

Figure 4.14: Spectra of samples taken at different stages of the reaction.

4.4.2.2. Thermal Characterization

4.4.2.2.1. Differential Scanning Calorimetry (DSC)

The thermal transition properties of the polymer are very important, as they will ascertain the possible applications for the polymer material. DSC was conducted for the DBH copolymers to study the effect of the varying HQ and BisS content on the glass transition temperature (T_g) of the material. The 2nd heat analysis was used to determine T_g's for the DBH random copolymers. The powder form of the polymers was used to prepare the samples, having a weight of ~5-10 mg. A heating rate of 10^{o}C/min was used. The glass transition of the copolymers were well defined and recorded as the onset of the transition. The DSC thermogram for the DBH random copolymers is shown in Figure 4.15. From the figure, we can see a linear, increasing trend in the glass transition temperatures with increasing amount of hydroquinone in the polymer backbone. This can be explained by the increased flexibility imparted by BisS group to the polymer backbone. Hence, the lower the amount of BisS, the higher the glass transition temperature.

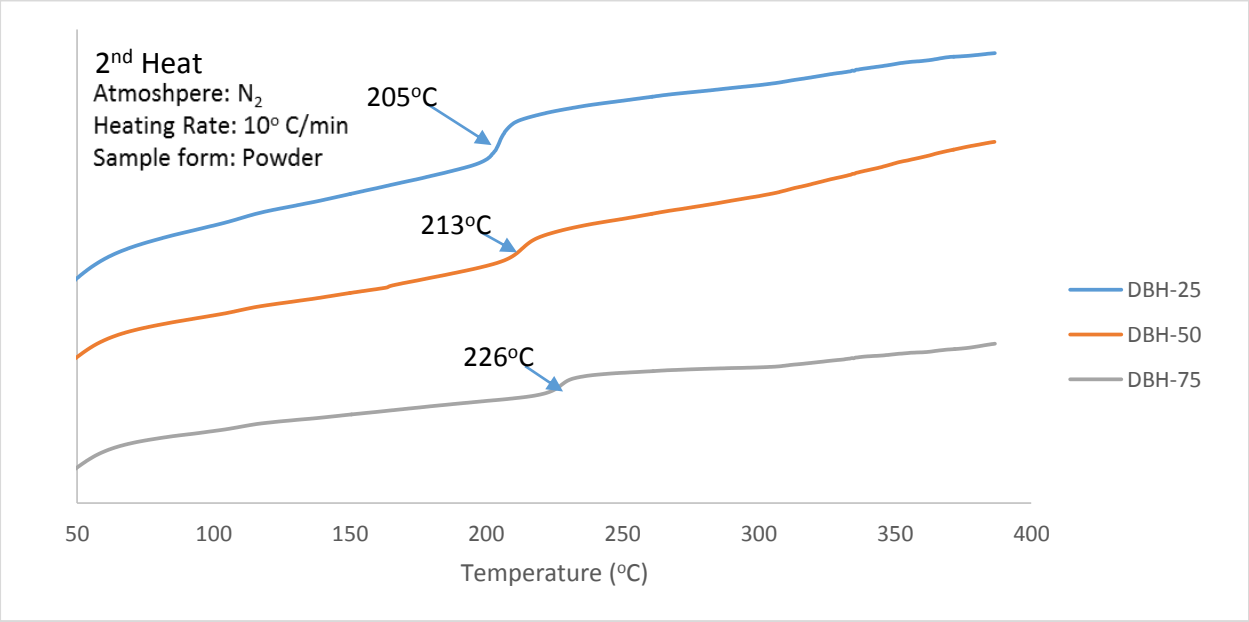

Figure 4.15: DSC of DBH random copolymer series.

4.4.2.2.2. Thermogravimetric Analysis (TGA)

The thermal stability of the random copolymers was investigated as a function of weight loss and shown in Figure 4.16. The influence of the bisphenol content on both weight loss temperature and the residual char yield at 700°C are summarized in Table 4.3. The copolymers synthesized in the DBH series did not show any thermal degradation before 420°C. Thus we can say that the synthesized copolymers afforded highly thermally stable polymers. Figure shows the thermal stability of DBH-25, DBH-50 and DBH-75 as a function of weight loss in nitrogen atmosphere.

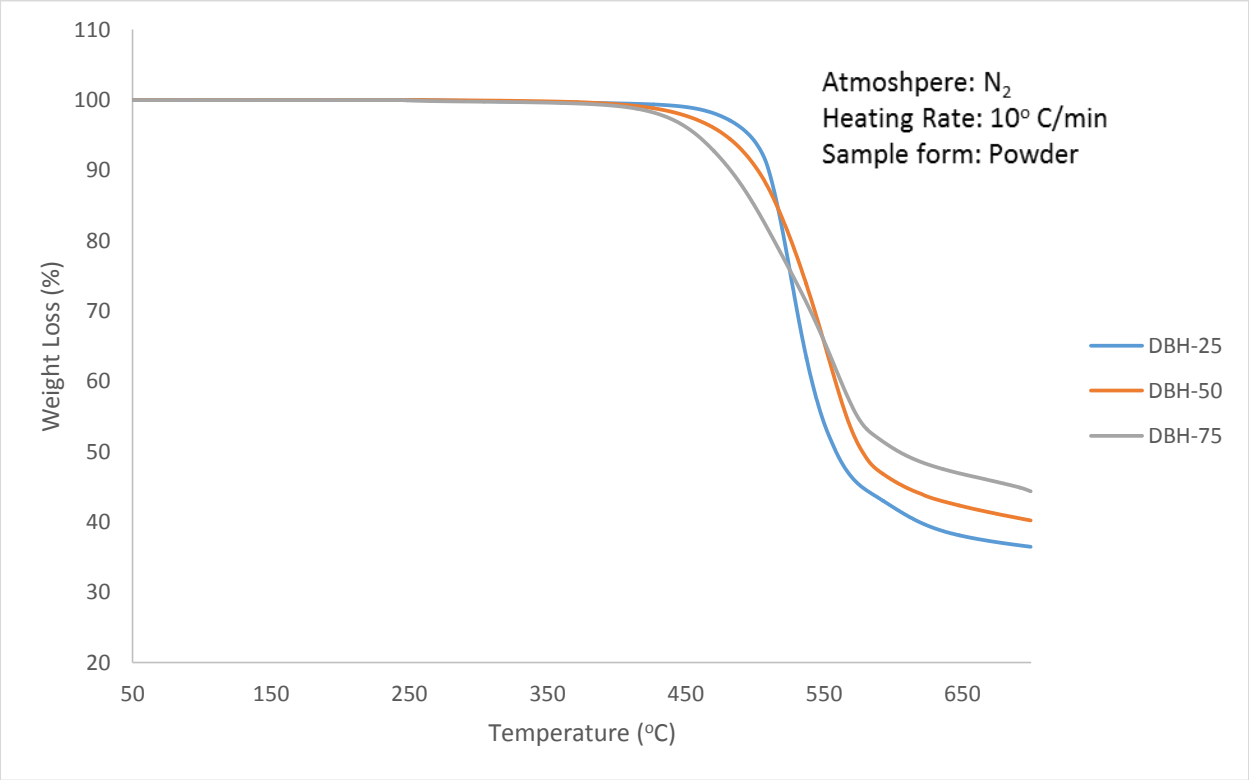

Figure 4.16: TGA thermogram of weight loss of DBH-25, 50 and 75 in N_2.

A trend was observed that the polymers containing higher HQ content produced higher char yields. This can be attributed to the fact that the C-S bond in the poly(arylene ether sulfone) is the most unstable of all the bonds and undergoes thermal degradation above 300°C. The rupture of the C-S bonds leads to formation to SO_2 and fragments of the polymer molecule with terminal phenyl radicals.[158] This also explains the high char yields in the polymer with increased HQ content.

Table 4.3: Influence of amount of HQ and BisS in the copolymer on the TGA behavior in nitrogen

Polymer	Char yields (%) at 700ºC
DBH-25	37.59
DBH-50	41.08
DBH-75	45.86

4.4.2.3. Tensile Testing:

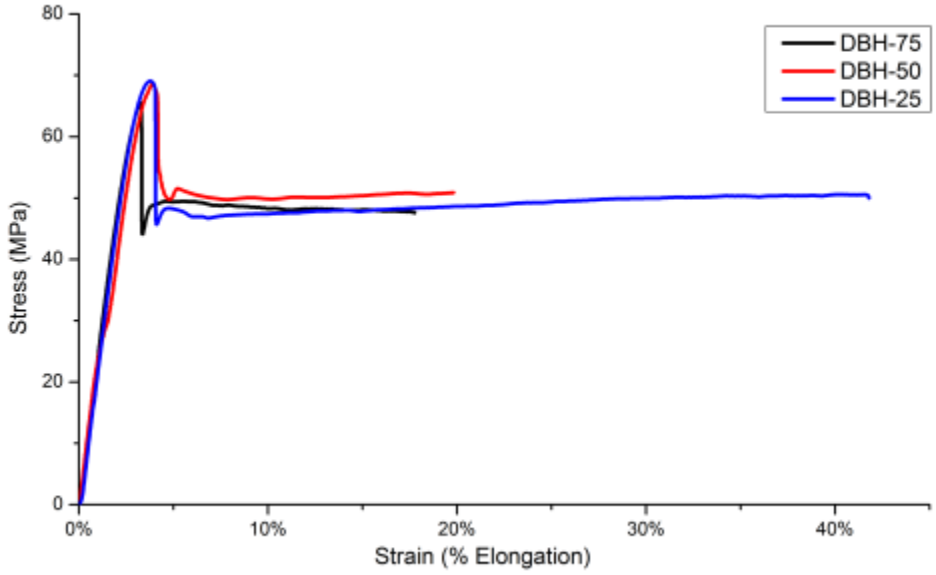

Figure 4.17: Stress–strain behavior of DBH-25, 50 and 75.

Stress-strain test results for the DBH copolymer membranes are illustrated in Figure 4.17. These materials show the typical mechanical response of glassy amorphous polymers. The yield stresses

for these membranes were all between 60 and 70 MPa, with the elongation increasing as the amount of sulfone content of the membranes increase. The DBH-25 based membranes showed the highest yield stress compared to DBH-50 and DBH-75 based membranes. The low hydroquinone containing copolymer, DBH-25, also displayed a higher elongation (45%) than the rest of the samples. The two membranes, DBH-25 and DBH-50, had very similar tensile elongations (17% and 20%). This may be attributed to variation in thickness of the films prepared for measurement. Nevertheless, all the systems showed good mechanical properties and produced tough and ductile membranes. To provide consistency for testing the materials, the membranes were dried in a vacuum oven prior to mechanical testing to remove any water from the systems.

4.5. Conclusion:

A series of poly (arylene ether sulfone)s were synthesized via direct copolymerization of the 4,4'-dichlorodiphenyl sulfone with varying quantities of hydroquinone and bisphenol S. This resulted in the random incorporation of the monomers in the polymer backbone. Varying the stoichiometric ratio of the hydroquinone to bisphenol S comonomer could lead to easy control of the degree of sulfonation (IEC) in the post-sulfonated copolymers.

The varying amount of the HQ and BisS also influenced the thermal as well as mechanical properties of the copolymer. All the synthesized copolymers showed excellent thermal stability up to 420^{o}C in N_2. The glass transition temperature increased with the increasing HQ content in the copolymer. The mechanical strength increased with the increase in Bisphenol S content.

References:

1. Sharaf, O. Z.; Orhan, M. F., An Overview of Fuel Cell Technology: Fundamentals and Applications. *Renewable and Sustainable Energy Reviews* **2014,** *32*, 810.
2. Winter, M.; Brodd, R. J., What Are Batteries, Fuel Cells, and Supercapacitors? *Chemical Reviews* **2004,** *104* (10), 4245-4269.
3. Whittingham, M. S.; Savinell, R. F.; Zawodzinski, T., Introduction: Batteries and Fuel Cells. *Chemical reviews* **2004,** *104* (10), 4243-4244.
4. http://en.wikipedia.org/wiki/Fuel_cell (accessed 03/20/2013).
5. Grove, W. R., Experiments on the Gas Voltaic Battery, with a View of Ascertaining the Rationale of Its Action, and on Its Application to Eudiometry. [Abstract]. *Abstracts of the Papers Printed in the Philosophical Transactions of the Royal Society of London* **1837,** *4*, 463-463.
6. Grove, W. R., Mr. W. R. Grove on a New Voltaic Combination. *The London and Edinburgh Philosophical Magazine and Journal of Science* **1838,** *12*.
7. Handbook of Energy; Volume Ii: Chronologies, Top Ten Lists, and Word Clouds. Book News, Inc: Portland, 2014.
8. http://asabeti8.blogspot.com/ (accessed 03/20/2014).
9. Hickner, M. A.; Ghassemi, H.; Kim, Y. S.; Einsla, B. R.; McGrath, J. E., Alternative Polymer Systems for Proton Exchange Membranes (Pems). *Chem. Rev. (Washington, DC, U. S.)* **2004,** *104* (10), 4587-4611.
10. O'Hayre, R. P., *Fuel Cell Fundamentals*. John Wiley & Sons: Hoboken, N.J, 2009.
11. Letcher, T. M., *Future Energy: Improved, Sustainable and Clean Options for Our Planet*. Elsevier: Amsterdam, 2008.
12. Zawodzinski, T. A.; Neeman, M.; Sillerud, L. O.; Gottesfeld, S., Determination of Water Diffusion-Coefficients in Perfluorosulfonate Ionomeric Membranes. *Journal Of Physical Chemistry* **1991,** *95* (15), 6040-6044.
13. Alberti, G.; Casciola, M.; Palombari, R., Inorgano-Organic Proton Conducting Membranes for Fuel Cells and Sensors at Medium Temperatures. *Journal of Membrane Science* **2000,** *172* (1), 233-239.
14. Roy, A.; Hickner, M.; Glass, T.; Li, Y.; Einsla, B.; Wiles, K. B.; Yu, X.; McGrath, J. E., States of Water- Investigating the Water-Polymer Interactions and Transport Phenomenon in Proton Exchange Membranes. *Prepr. Symp. - Am. Chem. Soc., Div. Fuel Chem.* **2005,** *50* (2), 699-700.
15. Ghassemi, H.; McGrath, J. E., Synthesis and Properties of New Sulfonated Poly(P-Phenylene) Derivatives for Proton Exchange Membranes. I. *Polymer* **2004,** *45* (17), 5847-5854.
16. Wnek, G. In *Sulfonated Styrene-Based Proton Exchange Membranes*, American Chemical Society: 2001; pp POLY-350.
17. Williams, M.; Narayanan, S.; Trulove, P.; Weidner, J. In *Hydrogen Production, Transport, and Storage 3*, The Electrochemical Society: 2009.
18. Yeo, R. S., Ion Clustering and Proton Transport in Nafion Membranes and Its Applications as Solid Polymer Electrolyte. *Journal of The Electrochemical Society* **1983,** *130* (3), 533.
19. Mauritz, K. A.; Moore, R. B., State of Understanding of Nafion. *Chemical Reviews* **2004,** *104* (10), 4535-4585.

20. Kerres, J. A., Development of Ionomer Membranes for Fuel Cells. *Journal of Membrane Science* **2001,** *185* (1), 3-27.
21. Roziere, J.; Jones, D. J., Non-Fluorinated Polymer Materials for Proton Exchange Membrane Fuel Cells. *Annual Review Of Materials Research* **2003,** *33*, 503-555.
22. Chen, Y.; Guo, R.; Lee, M.; Lee, C. H.; McGrath, J. E., Partly Fluorinated Poly(Arylene Ether Ketone Sulfone) Hydrophilic–Hydrophobic Multiblock Copolymers for Fuel Cell Membranes. *International Journal of Hydrogen Energy* **2012,** *37* (7), 6132-6139.
23. Chen, Y.; Lee, C. H.; Rowlett, J. R.; McGrath, J. E., Synthesis and Characterization of Multiblock Semi-Crystalline Hydrophobic Poly(Ether Ether Ketone)-Hydrophilic Disulfonated Poly(Arylene Ether Sulfone) Copolymers for Proton Exchange Membranes. *Polymer* **2012,** *53* (15), 3143-3153.
24. Rowlett, J. R.; Chen, Y.; Shaver, A. T.; Lane, O.; Mittelsteadt, C.; Xu, H.; Zhang, M.; Moore, R. B.; Mecham, S.; McGrath, J. E., Multiblock Poly(Arylene Ether Nitrile) Disulfonated Poly(Arylene Ether Sulfone) Copolymers for Proton Exchange Membranes: Part 1 Synthesis and Characterization. *Polymer* **2013,** *54* (23), 6305-6313.
25. Heitner-Wirguin, C., Recent Advances in Perfluorinated Ionomer Membranes: Structure, Properties and Applications. *Journal of Membrane Science* **1996,** *120* (1), 1-33.
26. Grot, W. G., Perfluorinated Ion Exchange Polymers and Their Use in Research and Industry. *Macromol. Symp.* **1994,** *82*, 161-172.
27. Matyjaszewski, K.; Möller, M.; ebrary, I., *Polymer Science: A Comprehensive Reference*. Elseiver: Amsterdam, 2012.
28. Hay, A. S.; Blanchard, H. S.; Endres, G. F.; Eustance, J. W., Polymerization by Oxidative Coupling. *Journal of the American Chemical Society* **1959,** *81* (23), 6335-6336.
29. Smith, M. B., *March's Advanced Organic Chemistry: Reactions, Mechanisms, and Structure*. Wiley: Chicester, 2013.
30. Pan, H.; Pu, H.; Wan, D.; Jin, M.; Chang, Z., Proton Exchange Membranes Based on Semi-Interpenetrating Polymer Networks of Fluorine-Containing Polyimide and Nafion. *Journal of Power Sources* **2010,** *195* (10), 3077-3083.
31. Chuang, S. W.; Hsu, S. L. C.; Liu, Y. H., Synthesis and Properties of Fluorine-Containing Polybenzimidazole/Silica Nanocomposite Membranes for Proton Exchange Membrane Fuel Cells. *Journal Of Membrane Science* **2007,** *305* (1-2), 353-363.
32. Chuang, S.-W.; Hsu, S. L.-C.; Hsu, C.-L., Preparation of Fluorine-Containing Polybenzimidazole/Montmorillonite Nanocomposite Membranes for Fuel Cell Applications. *PMSE Prepr.* **2007,** *97*, 557-558.
33. Chuang, S.-W.; Hsu, S. L.-C.; Liu, Y.-H., Synthesis and Properties of Fluorine-Containing Polybenzimidazole/Silica Nanocomposite Membranes for Proton Exchange Membrane Fuel Cells. *J. Membr. Sci.* **2007,** *305* (1+2), 353-363.
34. VanHouten, D. J.; Baird, D. G., Generation and Characterization of Carbon Nano-Fiber–Poly(Arylene Ether Sulfone) Nanocomposite Foams. *Polymer* **2009,** *50* (8), 1868-1876.
35. Chakraborty, S.; Pionteck, J.; Krause, B.; Banerjee, S.; Voit, B., Influence of Different Carbon Nanotubes on the Electrical and Mechanical Properties of Melt Mixed Poly(Ether Sulfone)-Multi Walled Carbon Nanotube Composites. *Composites Science And Technology* **2012,** *72* (15), 1933-1940.

36. Kim, Y. S.; Sumner, M. J.; Harrison, W. L.; Riffle, J. S.; McGrath, J. E.; Pivovar, B. S., Direct Methanol Fuel Cell Performance of Disulfonated Poly-Arylene Ether Benzonitrile) Copolymers. *Journal Of The Electrochemical Society* **2004,** *151* (12), A2150-A2156.
37. Kreuer, K. D., On the Development of Proton Conducting Polymer Membranes for Hydrogen and Methanol Fuel Cells. *Journal of Membrane Science* **2001,** *185* (1), 29-39.
38. Johnson, B. C.; Yilgör, İ.; Tran, C.; Iqbal, M.; Wightman, J. P.; Lloyd, D. R.; McGrath, J. E., Synthesis and Characterization of Sulfonated Poly(Acrylene Ether Sulfones). *Journal of Polymer Science: Polymer Chemistry Edition* **1984,** *22* (3), 721-737.
39. Genova-Dimitrova, P.; Baradie, B.; Foscallo, D.; Poinsignon, C.; Sanchez, J. Y., Ionomeric Membranes for Proton Exchange Membrane Fuel Cell (Pemfc): Sulfonated Polysulfone Associated with Phosphatoantimonic Acid. *Journal of Membrane Science* **2001,** *185* (1), 59-71.
40. Bishop, M. T.; Karasz, F. E.; Russo, P. S.; Langley, K. H., Solubility and Properties of a Poly(Aryl Ether Ketone) in Strong Acids. *Macromolecules* **1985,** *18* (1), 86-93.
41. Huang, R. Y. M.; Shao, P.; Burns, C. M.; Feng, X., Sulfonation of Poly(Ether Ether Ketone)(Peek): Kinetic Study and Characterization. *Journal of Applied Polymer Science* **2001,** *82* (11), 2651-2660.
42. Bailly, C.; Williams, D. J.; Karasz, F. E.; MacKnight, W. J., The Sodium Salts of Sulphonated Polyaryletheretherketone (Peek): Preparation and Characterization. *Polymer* **1987,** *28* (6), 1009-1016.
43. Ueda, M.; Toyota, H.; Ouchi, T.; Sugiyama, J. I.; Yonetake, K.; Masuko, T.; Teramoto, T., Synthesis and Characterization of Aromatic Poly(Ether Sulfone)S Containing Pendant Sodium-Sulfonate Groups. *Journal Of Polymer Science Part A-Polymer Chemistry* **1993,** *31* (4), 853-858.
44. Wang, F.; Hickner, M.; Kim, Y. S.; Zawodzinski, T. A.; McGrath, J. E., Direct Polymerization of Sulfonated Poly(Arylene Ether Sulfone) Random (Statistical) Copolymers: Candidates for New Proton Exchange Membranes. *J. Membr. Sci.* **2002,** *197* (1-2), 231-242.
45. Harrison, W. L.; Wang, F.; Kim, Y.; Hickner, M.; McGrath, J. E. In *Synthesis, Characterization and Morphologial Influence of Bisphenol Structure on the Direct Synthesis of Sulfonated Poly(Arylene Ether Sulfone) Copolymers*, American Chemical Society: 2002; pp POLY-228.
46. Harrison, W. L.; Wang, F.; O'Connor, K.; Arnett, N. Y.; Kim, Y. S.; McGrath, J. E. In *Sulfonated Poly(Arylene Ether Sulfones) Containing Hexafluoroisopropylidene Unit: Influence of Sulfonic Acid Position on Stability and Other Properties*, 2003; pp 849-849.
47. Badami, A. S., *Morphological and Structure-Property Analyses of Poly(Arylene Ether Sulfone)-Based Random and Multiblock Copolymers for Fuel Cells*. University Libraries, Virginia Polytechnic Institute and State University: [Blacksburg, Va. :, 2007.
48. Wang, F.; Glass, T. E.; Li, X.; Hickner, M.; Kim, Y.; McGrath, J. E. In *Synthesis and Characterization of Controlled Molecular Weight Poly(Arylene Ether Sulfone) Copolymers Bearing Sulfonate Groups by Endgroup Analysis*, American Chemical Society: 2002; pp POLY-113.
49. Bae, B.; Miyatake, K.; Watanabe, M., Sulfonated Poly(Arylene Ether Sulfone Ketone) Multiblock Copolymers with Highly Sulfonated Block. Synthesis and Properties. *Macromolecules* **2010,** *43* (6), 2684-2691.
50. Mikami, T.; Miyatake, K.; Watanabe, M., Poly(Arylene Ether)S Containing Superacid Groups as Proton Exchange Membranes. *ACS Appl. Mater. Interfaces* **2010,** *2* (6), 1714-1721.

51. Lane, O.; Lee, H.-S.; McGrath, J. E., Morphology and Proton Transport Behavior of Multiblock Copolymers with Hydrophilic-Hydrophobic Sequences for Proton Exchange Membranes. *Prepr. Symp. - Am. Chem. Soc., Div. Fuel Chem.* **2008,** *53* (2), 750-751.
52. Roy, A.; Lee, H.-S.; McGrath, J. E., Hydrophilic-Hydrophobic Multiblock Copolymers Based on Poly(Arylene Ether Sulfone)S as Novel Proton Exchange Membranes - Part B. *Polymer* **2008,** *49* (23), 5037-5044.
53. Roy, A.; Lee, H.-S.; Yu, X.; Paul, M.; Riffle, J. S.; McGrath, J. E. In *Structure-Property Relationships of Proton Exchange Membranes*, American Chemical Society: 2008; pp FUEL-095.
54. Roy, A.; Yu, X.; Dunn, S.; McGrath, J. E., Influence of Microstructure and Chemical Composition on Proton Exchange Membrane Properties of Sulfonated-Fluorinated, Hydrophilic-Hydrophobic Multiblock Copolymers. *J. Membr. Sci.* **2009,** *327* (1+2), 118-124.
55. Lee, H.-S.; Lane, O.; McGrath, J. E., Development of Multiblock Copolymers with Novel Hydroquinone-Based Hydrophilic Blocks for Proton Exchange Membrane (Pem) Applications. *Journal of Power Sources* **2010,** *195* (7), 1772-1778.
56. Harrison, W.; Wang, F.; Mecham, J. B.; O'Connor, K.; McGrath, J. E. In *Influence of Bisphenol Structure on the Direct Synthesis of Sulfonated Poly(Arylene Ether)S*, American Chemical Society: 2000; pp POLY-124.
57. Paul, M.; Park, H. B.; Freeman, B. D.; Roy, A.; McGrath, J. E.; Riffle, J. S., Synthesis and Crosslinking of Partially Disulfonated Poly(Arylene Ether sulfone) Random Copolymers as Candidates for Chlorine Resistant reverse Osmosis Membranes. *Polymer* **2008,** *49* (9), 2243-2252.
58. Paul, M.; Roy, A.; Park, H. B.; Freeman, B. D.; Riffle, J. S.; McGrath, J. E., Synthesis and Crosslinking of Poly(Arylene Ether Sulfone) Blend Membranes. *Abstracts Of Papers Of The American Chemical Society* **2007,** *233*.
59. Li, Y.; Wang, F.; Yang, J.; Liu, D.; Roy, A.; Case, S.; Lesko, J.; McGrath, J. E., Synthesis and Characterization of Controlled Molecular Weight Disulfonated Poly(Arylene Ether Sulfone) Copolymers and Their Applications to Proton Exchange Membranes. *Polymer* **2006,** *47* (11), 4210-4217.
60. Harrison, W. L.; Wang, F.; Mecham, J. B.; Bhanu, V. A.; Hill, M.; Kim, Y. S.; McGrath, J. E., Influence of the Bisphenol Structure on the Direct Synthesis of Sulfonated Poly(Arylene Ether) Copolymers. I. *J. Polym. Sci., Part A: Polym. Chem.* **2003,** *41* (14), 2264-2276.
61. Einsla, B. R.; Hong, Y.-T.; Kim, Y. S.; Wang, F.; Gunduz, N.; McGrath, J. E., Sulfonated Naphthalene Dianhydride Based Polyimide Copolymers for Proton-Exchange-Membrane Fuel Cells. I. Monomer and Copolymer Synthesis. *J. Polym. Sci., Part A: Polym. Chem.* **2004,** *42* (4), 862-874.
62. Einsla, B. R.; Kim, Y. S.; Hickner, M. A.; Hong, Y. T.; Hill, M. L.; Pivovar, B. S.; McGrath, J. E., Sulfonated Naphthalene Dianhydride Based Polyimide Copolymers for Proton-Exchange-Membrane Fuel Cells Ii. Membrane Properties and Fuel Cell Performance. *Journal Of Membrane Science* **2005,** *255* (1-2), 141-148.
63. Wang, F.; Mecham, J.; Harrison, W.; Hickner, M.; Kim, Y.; McGrath, J. E., Synthesis of Sulfonated Poly(Arylene Ether Phosphine Oxide Sulfone)S Via Direct Polymerization. *Abstracts Of Papers Of The American Chemical Society* **2001,** *221*, U435-U435.
64. Gui, L.; Zhang, C.; Kang, S.; Tan, N.; Xiao, G.; Yan, D., Synthesis and Properties of Hexafluoroisopropylidene-Containing Sulfonated Poly(Arylene Thioether Phosphine Oxide)S for Proton Exchange Membranes. *International Journal of Hydrogen Energy* **2010,** *35* (6), 2436-2445.

65. Roy, A.; Hickner, M. A.; Einsla, B. R.; Harrison, W. L.; McGrath, J. E., Synthesis and Characterization of Partially Disulfonated Hydroquinone-Based Poly(Arylene Ether Sulfone)S Random Copolymers for Application as Proton Exchange Membranes. *J. Polym. Sci., Part A: Polym. Chem.* **2009,** *47* (2), 384-391.
66. Noshay, A.; McGrath, J. E., *Block Copolymers*. Academic Press: New York, 1977.
67. Petit, F.; Iliopoulos, I.; Audebert, R.; Szonyi, S., Associating Polyelectrolytes with Perfluoroalkyl Side Chains: Aggregation in Aqueous Solution, Association with Surfactants, and Comparison with Hydrogenated Analogues. *Langmuir* **1997,** *13* (16), 4229-4233.
68. Kennedy, J. P., Novel Designed Polyisobutylene-Based Biopolymers - Synthesis, Characterization, and Biological Testing of Amphiphilic Chameleon Networks. *Journal Of Macromolecular Science-Pure And Applied Chemistry* **1994,** *A31* (11), 1771-1790.
69. Elabd, Y. A.; Napadensky, E.; Sloan, J. M.; Crawford, D. M.; Walker, C. W., Triblock Copolymer Ionomer Membranes Part I. Methanol and Proton Transport. *Journal Of Membrane Science* **2003,** *217* (1-2), 227-242.
70. Roy, A.; Hickner, M. A.; Yu, X.; Li, Y.; Glass, T. E.; McGrath, J. E., Influence of Chemical Composition and Sequence Length on the Transport Properties of Proton Exchange Membranes. *J. Polym. Sci., Part B: Polym. Phys.* **2006,** *44* (16), 2226-2239.
71. Chen, Y.; Lane, O.; McGrath, J. E., Synthesis and Characterization of Multiblock Hydrophobic (Polyarylene Ether Nitrile)-Hydrophilic (Disulfonated Polyarylene Ether Sulfone) Copolymers for Proton Exchange Membranes. *Prepr. Symp. - Am. Chem. Soc., Div. Fuel Chem.* **2008,** *53* (2), 762-764.
72. Rowlett, J.; Chen, Y.; Lee, C. H.; McGrath, J. E., Hydroquinone Based Hydrophilic-Hydrophobic Block Copolymers for Proton Exchange Membranes. *PMSE Prepr.* **2012**, No pp. given.
73. Ghassemi, H.; Ndip, G.; McGrath, J. E., New Multiblock Copolymers of Sulfonated Poly(4'-Phenyl-2,5-Benzophenone) and Poly(Arylene Ether Sulfone) for Proton Exchange Membranes. Ii. *Polymer* **2004,** *45* (17), 5855-5862.
74. Lee, H. S.; Badami, A. S.; Roy, A.; McGrath, J. E., Segmented Sulfonated Poly(Arylene Ether Sulfone)-B-Polyimide Copolymers for Proton Exchange Membrane Fuel Cells. I. Copolymer Synthesis and Fundamental Properties. *Journal Of Polymer Science Part A-Polymer Chemistry* **2007,** *45* (21), 4879-4890.
75. Kim, D. J.; Lee, H. J.; Nam, S. Y., Sulfonated Poly(Arylene Ether Sulfone) Membranes Blended with Hydrophobic Polymers for Direct Methanol Fuel Cell Applications. *Int. J. Hydrogen Energy* **2013**, Ahead of Print.
76. Badami, A. S.; Lee, H.-S.; Li, Y.; Roy, A.; Wang, H.; McGrath, J. E., Molecular Weight Effects on Poly(Arylene Ether Sulfone)-Based Random and Multiblock Copolymers Characteristics for Fuel Cells. *ACS Symp. Ser.* **2010,** *1040* (Fuel Cell Chemistry and Operation), 65-81.
77. Ghassemi, H.; McGrath, J. E.; Zawodzinski Jr, T. A., Multiblock Sulfonated–Fluorinated Poly (Arylene Ether) S for a Proton Exchange Membrane Fuel Cell. *Polymer* **2006,** *47* (11), 4132-4139.
78. Yu, X.; Roy, A.; Dunn, S.; Badami, A. S.; Yang, J.; Good, A. S.; McGrath, J. E., Synthesis and Characterization of Sulfonated-Fluorinated, Hydrophilic-Hydrophobic Multiblock Copolymers for Proton Exchange Membranes. *J. Polym. Sci., Part A: Polym. Chem.* **2009,** *47* (4), 1038-1051.

79. VanHouten, R. A., *Synthesis and Characterization of Hydrophobic-Hydrophilic Segmented and Multiblock Copolymers for Proton Exchange Membrane and Reverse Osmosis Applications*. University Libraries, Virginia Polytechnic Institute and State University: [Blacksburg, Va :2009].
80. Li, Y.; Roy, A.; Badami, A. S.; Hill, M.; Yang, J.; Dunn, S.; McGrath, J. E., Synthesis and Characterization of Partially Fluorinated Hydrophobic-Hydrophilic Multiblock Copolymers Containing Sulfonate Groups for Proton Exchange Membrane. *J. Power Sources* **2007,** *172* (1), 30-38.
81. Lee, H. S.; Roy, A.; Lane, O.; Lee, M.; McGrath, J. E., Synthesis and Characterization of Multiblock Copolymers Based on Hydrophilic Disulfonated Poly (Arylene Ether Sulfone) and Hydrophobic Partially Fluorinated Poly (Arylene Ether Ketone) for Fuel Cell Applications. *Journal of Polymer Science Part A: Polymer Chemistry* **2010,** *48* (1), 214-222.
82. Chen, Y.; Rowlett, J. R.; Lee, C. H.; Lane, O. R.; Van Houten, D. J.; Zhang, M.; Moore, R. B.; McGrath, J. E., Synthesis and Characterization of Multiblock Partially Fluorinated Hydrophobic Poly(Arylene Ether Sulfone)-Hydrophilic Disulfonated Poly(Arylene Ether Sulfone) Copolymers for Proton Exchange Membranes. *J. Polym. Sci., Part A: Polym. Chem.* **2013,** *51* (10), 2301-2310.
83. Ghassemi, H.; Zawodzinski, T. In *Multiblock Sulfonated-Fluorinated Poly(Arylene Ether)S Membranes for a Proton Exchange Membrane Fuel Cell*, American Chemical Society: 2005; pp FUEL-049.
84. Hu, H.; Xiao, M.; Wang, S.; Meng, Y., Poly (Fluorenyl Ether Ketone) Ionomers Containing Separated Hydrophilic Multiblocks Used in Fuel Cells as Proton Exchange Membranes. *International Journal of Hydrogen Energy* **2010,** *35* (2), 682-689.
85. Mikami, T.; Miyatake, K.; Watanabe, M., Synthesis and Properties of Multiblock Copoly (Arylene Ether) S Containing Superacid Groups for Fuel Cell Membranes. *Journal of Polymer Science Part A: Polymer Chemistry* **2011,** *49* (2), 452-464.
86. Chen, K.; Hu, Z.; Endo, N.; Higa, M.; Okamoto, K.-i., Sulfonated Multiblock Copolynaphthalimides for Polymer Electrolyte Fuel Cell Application. *Polymer* **2011,** *52* (10), 2255-2262.
87. Sung, K. A.; Kim, W.-K.; Oh, K.-H.; Choo, M.-J.; Nam, K.-W.; Park, J.-K., Proton Exchange Membranes Based on Hydrophilic-Hydrophobic Multiblock Copolymers Using Different Hydrophobic Oligomers. *Int. J. Hydrogen Energy* **2011,** *36* (6), 3956-3964.
88. Li, N.; Liu, J.; Cui, Z.; Zhang, S.; Xing, W., Novel Hydrophilic–Hydrophobic Multiblock Copolyimides as Proton Exchange Membranes: Enhancing the Proton Conductivity. *Polymer* **2009,** *50* (19), 4505-4511.
89. Li, X.; Yu, Y.; Liu, Q.; Meng, Y., Synthesis and Properties of Anion Conductive Multiblock Copolymers Containing Tetraphenyl Methane Moieties for Fuel Cell Application. *Journal of Membrane Science* **2013,** *436* (0), 202-212.
90. Lee, H.-J.; Lee, D. H.; Henkensmeier, D.; Jang, J. H.; Cho, E. A.; Kim, H.-J.; Kim, H., Synthesis and Characterization of H3po4 Doped Poly(Benzimidazole-Co-Benzoxazole) Membranes for High Temperature Polymer Electrolyte Fuel Cells. *Bull. Korean Chem. Soc.* **2012,** *33* (10), 3279-3284.
91. Lee, H.-S.; Roy, A.; Lane, O.; McGrath, J. E., Synthesis and Characterization of Poly (Arylene Ether Sulfone)-*b*-Polybenzimidazole Copolymers for High Temperature Low Humidity Proton Exchange Membrane Fuel Cells. *Polymer* **2008,** *49* (25), 5387-5396.

92. Lee, J. K.; Kerres, J., Synthesis and Characterization of Sulfonated Poly(Arylene Thioether)S and Their Blends with Polybenzimidazole for Proton Exchange Membranes. *J. Membr. Sci.* **2007,** *294* (1+2), 75-83.
93. Badami, A. S.; Roy, A.; Lee, H.-S.; Li, Y.; McGrath, J. E., Morphological Investigations of Disulfonated Poly(Arylene Ether Sulfone)-B-Naphthalene Dianhydride-Based Polyimide Multiblock Copolymers as Potential High Temperature Proton Exchange Membranes. *J. Membr. Sci.* **2009,** *328* (1+2), 156-164.
94. Roy, A.; Lee, H.-S.; McGrath, J. E., Hydrocarbon Based Bpsh-Bps Multiblock Copolymers as Novel Proton Exchange Membranes. *ECS Trans.* **2008,** *6* (26, Membranes for Electrochemical Applications), 1-7.
95. Roy, A.; Lee, H.-S.; McGrath, J. E., Hydrophilic–Hydrophobic Multiblock Copolymers Based on Poly(Arylene Ether Sulfone)S as Novel Proton Exchange Membranes – Part B. *Polymer* **2008,** *49* (23), 5037-5044.
96. Serpico, J.; Ehrenberg, S.; Fontanella, J.; Jiao, X.; Perahia, D.; McGrady, K.; Sanders, E.; Kellogg, G.; Wnek, G., Transport and Structural Studies of Sulfonated Styrene-Ethylene Copolymer Membranes. *Macromolecules* **2002,** *35* (15), 5916-5921.
97. Yu, X.; Roy, A.; Dunn, S.; Badami, A. S.; Yang, J.; Good, A. S.; McGrath, J. E., Synthesis and Characterization of Sulfonated-Fluorinated, Hydrophilic-Hydrophobic Multiblock Copolymers for Proton Exchange Membranes. *Journal of Polymer Science Part A: Polymer Chemistry* **2009,** *47* (4), 1038-1051.
98. Roy, A.; Lee, H.-S.; Yu, X.; Paul, M.; Riffle, J. S.; McGrath, J. E., Structure-Property Relationships of Proton Exchange Membranes. *Prepr. Symp. - Am. Chem. Soc., Div. Fuel Chem.* **2008,** *53* (2), 752-754.
99. Kim, Y. S.; Hickner, M. A.; Dong, L.; Pivovar, B. S.; McGrath, J. E., Sulfonated Poly(Arylene Ether Sulfone) Copolymer Proton Exchange Membranes: Composition and Morphology Effects on the Methanol Permeability. *J. Membr. Sci.* **2004,** *243* (1-2), 317-326.
100. Lee, H.-S.; Badami, A. S.; Roy, A.; McGrath, J. E., Segmented Sulfonated Poly(Arylene Ether Sulfone)-B-Polyimide Copolymers for Proton Exchange Membrane Fuel Cells. I. Copolymer Synthesis and Fundamental Properties. *J. Polym. Sci., Part A: Polym. Chem.* **2007,** *45* (21), 4879-4890.
101. Lee, H.-S.; Roy, A.; Badami, A. S.; McGrath, J. E., Synthesis and Characterization of Sulfonated Poly (Arylene Ether) Polyimide Multiblock Copolymers for Proton Exchange Membranes. *Macromolecular Research* **2007,** *15* (2), 160-166.
102. Lee, H.-S.; Roy, A.; Badami, A. S.; McGrath, J. E., Synthesis and Characterization of Sulfonated Poly(Arylene Ether) Polyimide Multiblock Copolymers for Proton Exchange Membranes. *Macromol. Res.* **2007,** *15* (2), 160-166.
103. Banerjee, S.; Curtin, D. E., Nafion Perfluorinated Membranes in Fuel Cells. *J. Fluorine Chem.* **2004,** *125* (8), 1211-1216.
104. Thiam, H. S.; Daud, W. R. W.; Kamarudin, S. K.; Mohamad, A. B.; Kadhum, A. A. H.; Loh, K. S.; Majlan, E. H., Nafion/Pd-Sio2 Nanofiber Composite Membranes for Direct Methanol Fuel Cell Applications. *Int. J. Hydrogen Energy* **2013,** *38* (22), 9474-9483.
105. Wu, X.; He, G.; Li, X.; Nie, F.; Yan, X.; Yu, L.; Benziger, J., Improving Proton Conductivity of Sulfonated Poly (Ether Ether Ketone) Proton Exchange Membranes at Low Humidity by Semi-Interpenetrating Polymer Networks Preparation. *J. Power Sources* **2014,** *246*, 482-490.

106. Chen, L.; Pu, Z.; Yang, J.; Yang, X.; Liu, X., Synthesis and Properties of Sulfonated Polyarylene Ether Nitrile Copolymers for Pem with High Thermal Stability. *J. Polym. Res.* **2013,** *20* (1), 1-8.
107. Li, X.; Liu, C.; Zhang, S.; Yu, G.; Jian, X., Acid Doped Polybenzimidazoles Containing 4-Phenyl Phthalazinone Moieties for High-Temperature Proton Exchange Membrane Fuel Cell. *J. Membr. Sci.* **2012,** *423-424*, 128-135.
108. Kern, K. E.; Abdellatif, M.; Fossum, E., Poly(Arylene Ether)S Carrying Pendant (3-Sulfonated) Phenylsulfonyl Groups. *Polym. Int.* **2012,** *61* (8), 1249-1255.
109. Rowlett, J. R.; Shaver, A. T.; Lane, O.; Mittelsteadt, C.; Xu, H.; Zhang, M.; Moore, R. B.; Mecham, S.; McGrath, J. E. In *Properties and Performance of Multiblock Copolymers Based Upon a Varying Hydrophilicity Backbone*, American Chemical Society: 2014; pp ENFL-76.
110. McGrath, J. e. E.; Roy, A.; Lee, H. S.; Paul, M.; Lane, O.; Yu, X.; Riffle, J. S., Structure-Property Relationships of Ion Containing Proton Exchange Membranes. *PMSE Prepr.* **2010**, No pp. given.
111. Chen, B.-K.; Wu, T.-Y.; Kuo, C.-W.; Peng, Y.-C.; Shih, I. C.; Hao, L.; Sun, I. W., 4,4'-Oxydianiline (Oda) Containing Sulfonated Polyimide/Protic Ionic Liquid Composite Membranes for Anhydrous Proton Conduction. *Int. J. Hydrogen Energy* **2013,** *38* (26), 11321-11330.
112. Chen, Y.; Guo, R.; Lee, C. H.; Lee, M.; McGrath, J. E., Partly Fluorinated Poly (Arylene Ether Ketone Sulfone) Hydrophilic–Hydrophobic Multiblock Copolymers for Fuel Cell Membranes. *International Journal of Hydrogen Energy* **2012,** *37* (7), 6132-6139.
113. Yu, X., *Synthesis and Characterization of Hydrophilic-Hydrophobic Disulfonated Poly(Arylene Ether Sulfone)-Decafluoro Biphenyl Based Poly(Arylene Ether) Multiblock Copolymers for Proton Exchange Membranes (Pems)*. University Libraries, Virginia Polytechnic Institute and State University: [Blacksburg, Va: 2008].
114. Lee, H.-S.; Roy, A.; Lane, O.; Dunn, S.; McGrath, J. E., Hydrophilic–Hydrophobic Multiblock Copolymers Based on Poly(Arylene Ether Sulfone) Via Low-Temperature Coupling Reactions for Proton Exchange Membrane Fuel Cells. *Polymer* **2008,** *49* (3), 715-723.
115. McGrath, J. E. In *Proton Exchange Membranes Based on Engineering Thermoplastics*, American Chemical Society: 2003; pp POLY-455.
116. Robeson, L.; Farnham, A.; McGrath, J., Dynamic Mechanical Characteristics of Polysulfone and Other Polyarylethers. *Molecular Basis of Transitions and Relaxations, Gordon and Breach Science Publishers, New York* **1978**, 405-425.
117. Chen, Y.; Lane, O. R.; McGrath, J. E. In *Synthesis and Characterization of Multiblock Hydrophobic (Polyarylene Ether Nitrile)-Hydrophilic (Disulfonated Polyarylene Ether Sulfone) Copolymers for Proton Exchange Membranes*, American Chemical Society: 2008; pp FUEL-099.
118. Ghassemi, H.; McGrath, J. E.; Zawodzinski, T. A., Multiblock Sulfonated–Fluorinated Poly(Arylene Ether)S for a Proton Exchange Membrane Fuel Cell. *Polymer* **2006,** *47* (11), 4132-4139.
119. Harrison, W. L.; Hickner, M. A.; Kim, Y. S.; McGrath, J. E., Poly(Arylene Ether Sulfone) Copolymers and Related Systems from Disulfonated Monomer Building Blocks: Synthesis, Characterization, and Performance - a Topical Review. *Fuel Cells (Weinheim, Ger.)* **2005,** *5* (2), 201-212.
120. Li, Y. The Influence of Aromatic Disulfonated Random and Block Copolymers' Molecular Weight, Composition, and Microstructure on the Properties of Proton Exchange Membranes for Fuel Cells. 2007.

121. Badami, A. S.; Lane, O.; Lee, H.-S.; Roy, A.; McGrath, J. E., Fundamental Investigations of the Effect of the Linkage Group on the Behavior of Hydrophilic-Hydrophobic Poly(Arylene Ether Sulfone) Multiblock Copolymers for Proton Exchange Membrane Fuel Cells. *J. Membr. Sci.* **2009,** *333* (1+2), 1-11.
122. Lee, H.-S.; Lane, O.; McGrath, J. E., Synthesis and Characterization of Multiblock Copolymers with Hydrophilic-Hydrophobic Sequences for Proton Exchange Membranes. *Prepr. Symp. - Am. Chem. Soc., Div. Fuel Chem.* **2008,** *53* (2), 760-761.
123. Lee, H.-S.; Lane, O. R.; McGrath, J. E. In *Synthesis and Characterization of Multiblock Copolymers with Hydrophilic-Hydrophobic Sequences for Proton Exchange Membranes*, American Chemical Society: 2008; pp FUEL-098.
124. Roy, A.; Lee, H.-S.; Badami, A. S.; Yu, X.; Li, Y.; Glass, T. E.; McGrath, J. E. In *Proton Conduction under Partially Hydrated Condition for Pems*, American Chemical Society: 2006; pp FUEL-044.
125. Roy, A.; Lee, H.-S.; Badami, A. S.; Yu, X.; Li, Y.; Glass, T. E.; McGrath, J. E., Transport Properties of Multiblock Hydrophilic-Hydrophobic Proton Exchange Membranes for Fuel Cells. *Prepr. Symp. - Am. Chem. Soc., Div. Fuel Chem.* **2006,** *51* (2), 660-661.
126. Gohy, J.-F., Block Copolymer Micelles. In *Block Copolymers Ii*, Springer: 2005; pp 65-136.
127. Loh, W., Block Copolymer Micelles. *Encyclopedia of surface and colloid science* **2002**, 802-813.
128. Santos Pereira, L.; Cordery, I.; Iacovides, I.; SpringerLink, *Coping with Water Scarcity: Addressing the Challenges*. Springer Netherlands: Dordrecht, 2009.
129. Kucera, J., *Desalination: Water from Water*. Wiley: Hoboken, New Jersey, 2014.
130. Fritzmann, C.; Lowenberg, J.; Wintgens, T.; Melin, T., State-of-the-Art of Reverse Osmosis Desalination. *Desalination* **2007,** *216* (1-3), 1-76.
131. Charcosset, C., A Review of Membrane Processes and Renewable Energies for Desalination. *Desalination* **2009,** *245* (1), 214-231.
132. http://www.aquatechnology.net/reverse_osmosis.html (accessed 04/08/2014).
133. Wijmans, J. G.; Baker, R. W., The Solution-Diffusion Model: A Review. *Journal of Membrane Science* **1995,** *107* (1), 1-21.
134. Geise, G. M.; Lee, H. S.; Miller, D. J.; Freeman, B. D.; McGrath, J. E.; Paul, D. R., Water Purification by Membranes: The Role of Polymer Science. *Journal Of Polymer Science Part B-Polymer Physics* **2010,** *48* (15), 1685-1718.
135. Beasley, J., The Evaluation and Selection of Polymeric Materials for Reverse Osmosis Membranes. *Desalination* **1977,** *22* (1), 181-189.
136. Petersen, R. J., Composite Reverse Osmosis and Nanofiltration Membranes. *Journal of Membrane Science* **1993,** *83* (1), 81-150.
137. Xie, W.; Geise, G. M.; Freeman, B. D.; Lee, H. S.; Byun, G.; McGrath, J. E., Polyamide Interfacial Composite Membranes Prepared from M-Phenylene Diamine, Trimesoyl Chloride and a New Disulfonated Diamine. *Journal Of Membrane Science* **2012,** *403*, 152-161.
138. Kang, G.-D.; Gao, C.-J.; Chen, W.-D.; Jie, X.-M.; Cao, Y.-M.; Yuan, Q., Study on Hypochlorite Degradation of Aromatic Polyamide Reverse Osmosis Membrane. *Journal of Membrane Science* **2007,** *300* (1), 165-171.
139. Kwon, Y.-N.; Leckie, J. O., Hypochlorite Degradation of Crosslinked Polyamide Membranes. *Journal of Membrane Science* **2006,** *283* (1), 21-26.

140. Konagaya, S.; Watanabe, O., Influence of Chemical Structure of Isophthaloyl Dichloride and Aliphatic, Cycloaliphatic, and Aromatic Diamine Compound Polyamides on Their Chlorine Resistance. *Journal Of Applied Polymer Science* **2000,** *76* (2), 201-207.
141. Glater, J.; Hong, S.-k.; Elimelech, M., The Search for a Chlorine-Resistant Reverse Osmosis Membrane. *Desalination* **1994,** *95* (3), 325-345.
142. Shintani, T.; Matsuyama, H.; Kurata, N., Development of a Chlorine-Resistant Polyamide Reverse Osmosis Membrane. *Desalination* **2007,** *207* (1), 340-348.
143. Choi, J.-H.; Willis, C. L.; Winey, K. I., Structure–Property Relationship in Sulfonated Pentablock Copolymers. *Journal of Membrane Science* **2012,** *394-395*, 169-174.
144. Geise, G. M.; Freeman, B. D.; Paul, D. R., Characterization of a Sulfonated Pentablock Copolymer for Desalination Applications. *Polymer* **2010,** *51* (24), 5815-5822.
145. Park, H. B.; Freeman, B. D.; Zhang, Z.-B.; Fan, G.-Y.; Sankir, M.; McGrath, J. E. In *Water and Salt Transport Behavior through Hydrophilic-Hydrophobic Copolymer Membranes and Their Relations to Reverse Osmosis Membrane Performance*, American Chemical Society: 2006; pp PMSE-495.
146. Lee, C. H.; McCloskey, B. D.; Cook, J.; Lane, O.; Xie, W.; Freeman, B. D.; Lee, Y. M.; McGrath, J. E., Disulfonated Poly(Arylene Ether Sulfone) Random Copolymer Thin Film Composite Membrane Fabricated Using a Benign Solvent for Reverse Osmosis Applications. *Journal Of Membrane Science* **2012,** *389*, 363-371.
147. Brinegar, W. C. Reverse Osmosis Process Employing Polybenzimidazole Membranes. 1901.
148. Wang, K. Y.; Chung, T.-S.; Qin, J.-J., Polybenzimidazole (Pbi) Nanofiltration Hollow Fiber Membranes Applied in Forward Osmosis Process. *Journal of Membrane Science* **2007,** *300* (1), 6-12.
149. Park, H. B.; Freeman, B. D.; Zhang, Z.-B.; Sankir, M.; McGrath, J. E., Highly Chlorine-Tolerant Polymers for Desalination. *Angewandte Chemie (International ed. in English)* **2008,** *47* (32), 6019-6024.
150. Xie, W.; Park, H.-B.; Cook, J.; Lee, C. H.; Byun, G.; Freeman, B. D.; McGrath, J. E., Advances in Membrane Materials: Desalination Membranes Based on Directly Copolymerized Disulfonated Poly(Arylene Ether Sulfone) Random Copolymers. *Water science and technology : a journal of the International Association on Water Pollution Research* **2010,** *61* (3), 619-624.
151. Einsla, B. R.; Harris, L. A.; Hill, M. L.; McGrath, J. E., Direct Copolymerization of Wholly Aromatic and Partially Fluorinated Disulfonated Poly(Arylene Ether Sulfone)S. *Prepr. Symp. - Am. Chem. Soc., Div. Fuel Chem.* **2005,** *50* (2), 571-572.
152. Li, Y.; Mukundan, T.; Harrison, W.; Hill, M.; Sankir, M.; Yang, J.; McGrath, J. E., Direct Synthesis of Disulfonated Poly(Arylene Ether Ketone)S and Investigation of Their Behavior as Proton Exchange Membrane (Pem). *Prepr. Symp. - Am. Chem. Soc., Div. Fuel Chem.* **2004,** *49* (2), 536-537.
153. Stevens, D. M.; Mickols, B.; V Funk, C., Asymmetric Reverse Osmosis Sulfonated Poly (Arylene Ether Sulfone) Copolymer Membranes. *Journal of Membrane Science* **2014,** *452*, 193-202.
154. Rose, J. B. Sulfonated Polyarylethersulphone Copolymers. EP8894A1, 1980.
155. Konáš, M.; Moy, T. M.; Rogers, M. E.; Shultz, A. R.; Ward, T. C.; Mcgrath, J. E., Molecular Weight Characterization of Soluble High Performance Polyimides. 2. Validity of

Universal Sec Calibration and Absolute Molecular Weight Calculation. *Journal of Polymer Science part B: Polymer Physics* **1995,** *33* (10), 1441-1448.
156. Konáš, M.; Moy, T. M.; Rogers, M. E.; Shultz, A. R.; Ward, T. C.; Mcgrath, J. E., Molecular Weight Characterization of Soluble High Performance Polyimides. 1. Polymer-Solvent-Stationary Phase Interactions in Size Exclusion Chromatography. *Journal of Polymer Science Part B: Polymer Physics* **1995,** *33* (10), 1429-1439.
157. Viswanathan, R.; Johnson, B. C.; McGrath, J. E., Synthesis, Kinetic Observations and Characteristics of Polyarylene Ether Sulphones Prepared Via a Potassium Carbonate Dmac Process. *Polymer* **1984,** *25* (12), 1827-1836.
158. Ravve, A., *Principles of Polymer Chemistry*. Springer New York: New York, 2012.